

A Macro-Finance Model with Sentiment*

Peter Maxted

Berkeley Haas

August 26, 2022

Abstract

This paper incorporates diagnostic expectations into a general equilibrium macroeconomic model with a financial intermediary sector. Diagnostic expectations are a forward-looking model of extrapolative expectations that overreact to recent news. Frictions in financial intermediation produce nonlinear spikes in risk premia and slumps in investment during periods of financial distress. The interaction of sentiment with financial frictions generates a short-run amplification effect followed by a long-run reversal effect, termed the feedback from behavioral frictions to financial frictions. The model features sentiment-driven financial crises characterized by low pre-crisis risk premia and neglected risk. The conflicting short-run and long-run effect of sentiment produces boom-bust investment cycles. The model also identifies a stabilizing role for diagnostic expectations. Under the baseline calibration, financial crises are less likely to occur when expectations are diagnostic than when they are rational.

*Haas School of Business, University of California, Berkeley. 545 Student Services Building #1900, Berkeley, CA 94720. Email: maxted@haas.berkeley.edu. I would like to thank Francesca Bastianello, Pedro Bordalo, John Campbell, William Diamond (discussant), Daniele d'Arienzo, Emmanuel Farhi, Paul Fontanier, Xavier Gabaix, Nicola Gennaioli, Thomas Graeber, Samuel Hanson, Zhiguo He (discussant), Arvind Krishnamurthy, Spencer Yongwook Kwon, David Laibson, Lu Liu, Matteo Maggiori, Andrei Shleifer, Jakob Ahm Sørensen, Jeremy Stein, Ludwig Straub, Yeji Sung (discussant), Stephen Terry, Emil Verner, and participants at the NBER Behavioral Finance Conference, the Western Finance Association Conference, the China Star Tour, and various institutions for helpful discussion and comments. I would like to thank the NBER Fellowship Program in Behavioral Macroeconomics for financial support.

1 Introduction

Models of financial frictions successfully replicate the eruption of financial crises and the broader the transmission of financial sector vulnerabilities into aggregate downturns. However, the rational expectations version of these models struggles to match the empirical pattern of low risk premia in the lead-up to crises. [Baron and Xiong \(2017\)](#) find that bank equity is repeatedly overvalued prior to financial crises due to overoptimistic beliefs. [Krishnamurthy and Muir \(2020\)](#) show that credit spreads are “too low” before financial crises, and that frothy financial markets predict future crises. This conclusion is strengthened in [Greenwood et al. \(2022\)](#), who document that the combination of rapid credit and asset price growth is highly predictive of future crises. All three papers conclude from this pre-crisis evidence that systemic crash risk is neglected during the buildup to financial crises.

These findings are not unique to crises, with patterns of excessive optimism preceding economic downturns appearing consistently ([Greenwood and Hanson, 2013](#), [López-Salido et al., 2017](#)). Furthermore, this channel of belief-driven economic fluctuations is supported by direct expectations data from experts and professional forecasters, which frequently displays cyclical overreaction to macro-financial trends (e.g., [Mian et al., 2017](#), [Bordalo et al., 2020a](#), [Bordalo et al., 2020b](#), [d’Arienzo, 2020](#), [Bordalo et al., 2021b](#)).

Collectively, this evidence points towards a model of financial crises that features *behavioral frictions* alongside financial frictions. This paper provides such a model by incorporating non-rational diagnostic expectations into a macroeconomic model with a financial intermediary sector. In this model, the role of financial frictions is to introduce systemic downside risks to both financial markets and the broader real economy that are caused by disruptions in financial intermediation. But, under rational expectations the model is devoid of triggering events and instead relies on a long sequence of negative shocks to set crises in motion. Alternatively, and in line with the evidence above, the role of diagnostic expectations is to provide a sentiment-driven trigger for financial crises. Together, the contribution of this paper is its characterization of the endogenous financial market and business cycle dynamics that are generated by the interaction of behavioral and financial frictions.

The macro-financial environment that I study is based on [He and Krishnamurthy \(2019\)](#).

The [He and Krishnamurthy \(2019\)](#) model is a continuous-time Real Business Cycle (RBC) model augmented with a financial intermediary sector that faces an occasionally binding equity issuance constraint. This model behaves similarly to a frictionless RBC model when intermediary constraints are slack. However, a sequence of poor returns moves intermediaries closer to their constraint and leads to financial distress. In distress periods the nonlinearities arising from financial frictions become quantitatively important. Financial crises erupt in the tail state where the constraint binds, causing risk premia to spike and asset prices to plummet.

Building on this rich macro-financial framework, I depart from rational expectations by incorporating behavioral frictions into this model of financial intermediary frictions. This paper develops a method for generalizing rational models with a continuous-time variant of diagnostic expectations. Diagnostic expectations are a forward-looking model of extrapolative expectations in which agents overweight future states that are representative of recent news ([Bordalo et al., 2018](#)). In addition to being psychologically grounded, diagnostic expectations are tractable and have been shown to provide a parsimonious account of financial experts' beliefs (e.g., [Bordalo et al., 2019](#), [Bordalo et al., 2020b](#)), thus making them a natural candidate for exploration in a model of financial intermediary frictions. In the model presented here, diagnostic expectations cause agents to be overoptimistic about future economic growth following a sequence of positive shocks, and overpessimistic following negative shocks. Importantly, diagnostic expectations do not add an independent source of shocks to the model. Instead, they alter the way that shocks drive the economy in equilibrium.

The interaction of diagnostic expectations with frictions in financial intermediation produces conflicting short-run and long-run dynamics. Consider a sequence of positive shocks, which alleviates financial frictions and increases asset prices and investment. In the short run, forward-looking diagnostic expectations amplify this boom because positive shocks create overoptimism about fundamentals, further elevating asset prices and investment. However, a direct consequence of this short-run amplification is that it sets in motion a long-run reversal. Beliefs act like a slingshot — the elevated sentiment that propels short-run amplification simultaneously induces a progressive erosion of intermediary risk-bearing capacity as expectations are disappointed, causing financial frictions to tighten in the long run. I refer

to this novel long-run reversal effect as the *feedback from behavioral frictions to financial frictions*.

I present three results arising from the interaction of behavioral and financial frictions. First, the model produces sentiment-driven financial crises. Overoptimism dislocates asset prices from fundamentals. The inflation of asset prices initiates a feedback from behavioral frictions to financial frictions that impairs the risk-bearing capacity of intermediaries and heightens financial fragility in the background of seemingly low-risk environments. Consistent with the empirical findings outlined above, sentiment-driven crises feature low pre-crisis risk premia and neglected crash risk.

Second, the interaction of behavioral and financial frictions causes boom-bust fluctuations in investment and output growth. These cyclical business cycle dynamics are driven by the conflicting short- and long-run effects of diagnostic expectations. Sentiment-driven amplification in the short run begets a financial-frictions-driven reversal in the long run.

Third, I identify a stabilizing effect in which diagnostic expectations can lower the probability of financial crises. This possibility sits in direct opposition to the typical narrative that extrapolative expectations create financial fragility (e.g., the Financial Instability Hypothesis of [Minsky \(1977\)](#)). Since sentiment tracks recent economic shocks, sentiment is typically depressed during periods of financial distress. Depressed sentiment increases intermediary returns relative to expectations, which repairs intermediary balance sheets and reduces the potential for financial distress to erupt into a full-blown crisis. However, diagnostic expectations only produce this financial sector recovery by dragging down investment and slowing economic growth, thereby generating a recovery on “Wall Street” that is dislocated from the recovery on “Main Street.”

By interacting sentiment and financial frictions, this paper identifies a novel long-run feedback from behavioral frictions to financial frictions that is a key driver of equilibrium dynamics. I explore three predictions to evaluate whether this feedback effect improves the model’s empirical fit. First, the feedback effect produces long-run reversals. I examine the persistence of financial distress, the price-dividend ratio, and the investment-output ratio. In all three cases, the shorter persistence produced by diagnostic expectations improves the model’s fit. Second, the feedback effect implies that elevated sentiment causes financial

market overheating that can trigger the emergence of financial fragility. Once this fragility has been triggered, however, it can persist even after sentiment has subsided. I use this prediction to identify a new fact about financial markets in the buildup to crises: the first eruption of a financial crisis is often preceded by frothy financial markets, but this is rarely the case for residual “double-dip” crises. Third, I evaluate the prediction of sentiment-driven financial crises by applying the model to the 2007-2008 Financial Crisis. This exercise suggests that overoptimism in the mid-2000s was critical for exacerbating financial market vulnerability prior to the failure of Lehman Brothers.

The analysis in this paper relies on two methodological contributions. First, this paper develops a method for applying diagnostic expectations to an endogenous economic growth process. I use this method to generalize the [He and Krishnamurthy \(2019\)](#) model with non-rational expectations. This allows for the study of beliefs without compromising the equilibrium dynamics on which sentiment can interact. Indeed, a key takeaway from this paper is that both behavioral and financial frictions are necessary for understanding the evolution of the economy around financial crises.

Relatedly, this paper highlights the benefits of using global solution methods to characterize the full equilibrium impact of beliefs on economic dynamics. The analysis of sentiment-driven expansions and slumps fundamentally requires evaluating the cyclical effects of expectations away from the steady state. This paper uses global solution methods to characterize the complete nonlinear dynamical system.

Related Literature. This paper builds on a large financial frictions literature. Seminal work includes [Kiyotaki and Moore \(1997\)](#) and [Bernanke et al. \(1999\)](#). Recent research often uses continuous-time methods to analyze global dynamics in nonlinear models. Examples include [Adrian and Boyarchenko \(2012\)](#), [He and Krishnamurthy \(2013, 2019\)](#), [Brunnermeier and Sannikov \(2014\)](#), [Di Tella \(2017\)](#), [Maggiore \(2017\)](#), and [Moreira and Savov \(2017\)](#).

There is a growing theoretical literature on credit cycles and the behavioral triggers of crises. [Bordalo et al. \(2018\)](#) develop the original model of diagnostic expectations. [Bordalo et al. \(2021b\)](#) quantify the business cycle implications of diagnostic expectations in a partial equilibrium heterogeneous-firm model, and [Bianchi et al. \(2021\)](#) and [L’Huillier et](#)

al. (2021) analyze diagnostic expectations in linear macroeconomic frameworks.¹ [Gennaioli and Shleifer \(2018\)](#) summarize the research on diagnostic expectations and present a belief-driven narrative of the 2007-2008 Financial Crisis. The authors identify understanding the interaction between beliefs and financial frictions as a key open problem, which this paper aims to address.

The contribution of this paper is the analysis of diagnostic expectations jointly with frictions in financial intermediation. This allows the model to characterize how sentiment shapes disruptions in financial intermediation, and how this propagates to the real economy. In more recent work, [Krishnamurthy and Li \(2021\)](#) extend the crisis model of [Li \(2020\)](#) with time-varying beliefs about the hidden risk of illiquidity shocks in order to quantitatively dissect the drivers of crises. [Krishnamurthy and Li \(2021\)](#) provide a distinct but complementary analysis to the current paper, as their model uses an additional set of financial-illiquidity shocks to generate exogenous neglected risk from hidden information. I focus instead on the direct extrapolation of economic fundamentals, a channel that is ruled in by the beliefs data discussed above. Taking this beliefs data as my starting point, I show that diagnostic expectations of economic fundamentals can generate the neglected risk that is critical for matching pre-crisis patterns. [Greenwood et al. \(2019\)](#), [Gertler et al. \(2020\)](#), and [Wachter and Kahana \(2020\)](#) also study the effect of beliefs on booms and busts in financial markets. [Barberis \(2018\)](#) surveys the field of extrapolative expectations in finance. While this paper contributes to a growing literature studying the behavioral drivers of financial crises, rational explanations have also been forwarded for certain pre-crisis patterns ([Gomes et al., 2018](#), [Diamond and Landvoigt, 2020](#), [Farboodi and Kondor, 2020](#), [Khorrami and Mendo, 2021](#)).

2 Macro-Finance Model

This paper embeds diagnostic expectations into the macro-finance model of [He and Krishnamurthy \(2019\)](#), henceforth HK). The HK model is one of the first quantitative papers in the continuous-time macro-finance literature, and it successfully replicates the downside risks precipitated by disruptions in financial intermediation. However, because the HK model fea-

¹More broadly, this paper adds to the literature on general equilibrium macroeconomic models featuring non-rational beliefs. A small set of recent examples includes [Fuster et al. \(2012\)](#), [Woodford \(2013\)](#), [Hirshleifer et al. \(2015\)](#), [Adam and Merkel \(2019\)](#), [Caballero and Simsek \(2020\)](#), and [Farhi and Werning \(2020\)](#).

tures rational expectations, risk premia in this model are always high when financial crises are likely, whereas in the data they are often low (e.g., [Baron and Xiong, 2017](#), [Krishnamurthy and Muir, 2020](#), [Greenwood et al., 2022](#)).

I extend the HK model in two ways. Most importantly, I generalize the model to allow for diagnostic expectations. I also introduce a simple labor income margin to improve the model’s quantitative fit. I adopt HK’s notation when possible.

2.1 Model Setup

Time is continuous, with t denoting the current period. Note that the purpose of continuous time is not to target high-frequency dynamics, but rather that continuous-time methods can be used to solve the model globally.² This advantage of continuous time is critical for the analysis in this paper. A global solution allows for a characterization of nonlinear financial crises, together with an examination of the role of beliefs in shaping the evolution of the economy in and out of these periods of financial distress.

The economy has two sectors: households and financial intermediaries. The economy has two types of assets in positive supply: productive capital K_t and housing H . The housing supply is fixed and normalized to $H \equiv 1$. The price of capital is denoted q_t , and the price of housing is denoted P_t . Asset prices are endogenous and will be determined in equilibrium.³

Only intermediaries can directly hold K_t and H .⁴ Accordingly, this is an intermediary asset pricing model because financial intermediaries will be responsible for determining the prices of these risky assets in equilibrium.

Intermediaries fund these purchases by issuing debt and equity to households. However, each intermediary faces an “equity capital constraint” that restricts its ability to raise equity funding. This is the key financial friction. When binding, intermediaries must replace their equity funding with additional debt funding.

²See [Brunnermeier and Sannikov \(2016\)](#) for an overview and discussion of the continuous-time approach to macro-finance models.

³[He and Krishnamurthy \(2019\)](#) use two assets to improve the model’s quantitative predictions. The assumption that housing is in fixed supply allows the model to generate additional volatility in financial markets relative to the volatility of the broader macroeconomy. As discussed in [Section 3.2](#) below, the calibrated model with two assets successfully fits both empirical investment volatility and the overall risk-return profile of intermediary equity. [Appendix B.2](#) provides further details on the role of housing.

⁴The model can be extended to allow households to directly hold a share of K_t and H , but [He and Krishnamurthy \(2019\)](#) conclude that the quantitative impact is negligible.

Output flow Y_t is produced according to an “AK” production technology

$$Y_t = AK_t. \tag{1}$$

Parameter A governs the productivity of capital. Capital evolves endogenously, as follows:

$$\frac{dK_t}{K_t} = (i_t - \delta)dt + \sigma dZ_t. \tag{2}$$

i_t is the endogenous rate of capital installation at time t , δ is the exogenous depreciation rate, and $\{Z_t\}$ is a standard Brownian motion. The term σdZ_t is a capital quality shock. Capital quality shocks are the only source of uncertainty in the model.

Investment in capital is subject to quadratic adjustment costs. For a gross capital installation of $i_t K_t$, the cost is given by $\Phi(i_t, K_t) = i_t K_t + \frac{\xi}{2}(i_t - \delta)^2 K_t$.

2.2 Diagnostic Expectations

Overview. All agents have diagnostic expectations about the log capital stock.⁵ Capital is the fundamental in this economy — capital alone determines output ($Y_t = AK_t$), and capital quality shocks are the only source of uncertainty.

Diagnostic expectations are based on Kahneman and Tversky’s representativeness heuristic, defined as follows: “an attribute is representative of a class if it is very diagnostic; that is, the relative frequency of this attribute is much higher in that class than in the relevant reference class” (Tversky and Kahneman, 1983, p. 296). In the context of expectations the reference class reflects the absence of new information, meaning that representative future states are those that become more likely to occur in light of incoming data. Judging by representativeness implies that diagnostic expectations are characterized by the “kernel of truth” property: beliefs are forward looking, but overreact to recent patterns in the data.

This paper features two innovations on the original diagnostic expectations model of Bordalo et al. (2018). First, diagnostic expectations are cast in continuous time so that they can be applied to the globally solved HK model. More importantly, the methodology developed here allows for agents to have diagnostic expectations about the *endogenous* capital

⁵Log capital evolves according to $dk_t = (i_t - \delta - \frac{\sigma^2}{2})dt + \sigma dZ_t$.

process.⁶ This key innovation enables the model to make predictions about the impact of sentiment on future economic growth, because it implies not only that recent economic performance affects expectations (a standard feature of extrapolative expectations), but also that expectations feed back into the dynamical system to alter the future evolution of the capital process on which expectations are formed.

Below I present a reduced-form specification of diagnostic expectations as applied to the macroeconomic model that I study. More broadly, this paper’s specification of diagnostic expectations is designed portably so that diagnostic expectations can be added to rational models using a single additional state variable. Even though I introduce a state variable to the HK model, I do not introduce any additional shocks. Capital quality shocks remain the sole driving shock. Appendix A.1 provides a microfoundation for my specification of diagnostic expectations and Appendix E provides additional details, including a discussion of how this paper’s specification relates to the original model of [Bordalo et al. \(2018\)](#).⁷

Expectations of Capital. The psychology of diagnostic expectations is as follows. Agents have in the back of their mind all necessary information to form correct expectations. However, limited and selective memory means that representative states come to mind more easily. Representative states are those that are diagnostic of incoming data, which in this model corresponds to recent capital quality shocks. This is formalized in the following measure of “recent information” at time t :

$$\mathcal{I}_t \equiv \int_0^t e^{-\kappa(t-s)} \sigma dZ_s. \quad (3)$$

\mathcal{I}_t is a weighted integral of past shocks to capital, where the weight decays at rate κ as shocks occur further in the past.⁸ $\mathcal{I}_t > 0$ when recent shocks have tended to be positive, and $\mathcal{I}_t < 0$ when recent shocks have tended to be negative. \mathcal{I}_t drifts back to 0 at rate κ in the absence

⁶The [Bordalo et al. \(2018\)](#) model only applies to exogenous AR(N) processes.

⁷Appendix E.1 builds a discrete-time version of this paper’s specification of diagnostic expectations, and shows that it provides a one-parameter generalization of the [Bordalo et al. \(2018\)](#) model when applied to AR(1) processes.

⁸ \mathcal{I}_t is an Ornstein-Uhlenbeck process. In discrete time, any individual shock can itself represent new information. In continuous time, I integrate over the past sequence of shocks because each individual shock σdZ_s has only an infinitesimal effect on the capital stock. My specification is similar to the definition of sentiment in [Barberis et al. \(2015\)](#).

of new shocks.

Throughout, I will use hat notation to denote the beliefs of diagnostic agents. The current period is t , and let $\tau \geq 0$ denote a prediction horizon. Diagnostic agents believe that capital in period $t + \tau$ evolves according to:

$$\frac{d\widehat{K}_{t+\tau}}{K_{t+\tau}} = (i_{t+\tau} - \delta + \theta\mathcal{I}_t e^{-\kappa\tau})dt + \sigma dZ_{t+\tau}. \quad (4)$$

Parameter θ governs the extent to which agents judge by representativeness. $\theta = 0$ recovers rationality. When $\theta > 0$, expectations of capital growth are biased toward states that are diagnostic of recent information. For this reason, information parameter \mathcal{I}_t will be referred to as “sentiment” henceforth.

Consider equation (4) when $\tau = 0$: $\frac{d\widehat{K}_t}{K_t} = (i_t - \delta + \theta\mathcal{I}_t)dt + \sigma dZ_t$. Diagnostic expectations bias the perceived growth rate of capital in the direction of recent information by $\theta\mathcal{I}_t$. At more distant horizons ($\tau > 0$), this bias dissipates at rate κ since information that is diagnostic of economic conditions at time t slowly dims as agents form expectations about the economy’s evolution in the more distant future.

The psychology of diagnostic expectations suggests that the reduced-form specification of beliefs in equation (4) should be interpreted as an “as if” process. Diagnostic agents do not consciously calculate the evolution of capital in a biased way. Agents have the true model in their memory database, but selective retrieval from memory leads to biased probability assessments (Bordalo et al., 2021a). Importantly, diagnostic agents are not consciously aware of information parameter \mathcal{I}_t . Rather, \mathcal{I}_t serves as a sufficient statistic for the modeling of beliefs, as it characterizes agents’ unconscious state of representativeness at time t .⁹

Forward-Looking Extrapolation. Bordalo et al. (2018) emphasize that a key advantage of diagnostic expectations relative to other commonly used models of beliefs is that

⁹ \mathcal{I}_t is defined in terms of objective information σdZ_s , meaning that diagnostic agents overreact to objective news despite having biased expectations. This choice follows the original specification of diagnostic expectations in Bordalo et al. (2018). As discussed in Bordalo et al. (2019) and Bordalo et al. (2020b), overreaction to objective information is consistent with the “kernel of truth” hypothesis, and it makes the model portable across domains (e.g., in addition to asset pricing and macroeconomic applications, the model has been used to study conjunction/disjunction fallacies (Gennaioli and Shleifer, 2010) and social stereotypes (Bordalo et al., 2016)). However, it is just as tractable to specify \mathcal{I}_t in terms of subjective information, $\sigma d\widehat{Z}_s = \frac{dY_s}{Y_s} - \widehat{\mathbb{E}}_s \frac{dY_s}{Y_s} = \sigma dZ_s - \theta\mathcal{I}_s dt$. This alternate specification is presented in Appendix E.3.

diagnostic expectations are forward looking. In contrast to mechanical extrapolation or adaptive expectations, forward-looking extrapolation is robust to the Lucas critique and has been found to provide an accurate description of survey data from professional forecasters (Bordalo et al., 2020b, d’Arienzo, 2020) and stock market analysts (Bordalo et al., 2019).

Equation (4) highlights the forward-looking dependence of beliefs on the underlying capital process. In particular, agents’ expectations of capital growth depend on the equilibrium investment rate i_t , which is both endogenous and time-varying. Reflecting standard notions of rationality, diagnostic agents correctly expect faster capital growth when i_t is high, and slower capital growth when i_t is low. Similarly, the extent to which agents revise their expectations following a shock depends not only on the shock itself, but also on the endogenous response of investment to that shock.

I highlight two main channels through which forward-looking beliefs are shaped by the endogenous response of investment, one driven by financial frictions and one driven by behavioral frictions. The first channel is the nonlinearity effect of financial frictions emphasized in HK. Investment rate i_t is both high and insensitive to shocks when intermediary balance sheets are strong, but i_t becomes sensitive to intermediary health as it deteriorates. This implies that diagnostic agents’ forward-looking beliefs about economic growth depend endogenously on the tightness of financial frictions.

Second, this paper identifies a novel channel in which economic growth is directly altered by agents’ beliefs about it. That is, not only do diagnostic expectations depend on investment rate i_t , diagnostic expectations actually change the investment process in equilibrium. Belief distortions alter agents’ perceptions about the return on capital (see equation (17)) and hence the equilibrium price of capital q_t , which then affects investment through a q -theory investment channel (see equation (12)). This novel channel only emerges because diagnostic expectations are applied to the endogenous capital process, which is one of this paper’s key methodological innovations. Importantly, this equilibrium reaction of investment to beliefs is what drives the short-run amplification effect of diagnostic expectations.

Decomposing Diagnostic Expectations. Diagnostic expectations reconcile dynamic, forward-looking, expectations with mechanical models of extrapolation. A decomposition of

the perceived capital process highlights this property:

$$\frac{d\widehat{K}_{t+\tau}}{K_{t+\tau}} = \underbrace{\frac{dK_{t+\tau}}{K_{t+\tau}}}_{\text{Actual}} + \underbrace{\theta \mathcal{I}_t e^{-\kappa\tau} dt}_{\text{Wedge}}. \quad (5)$$

As discussed above, diagnostic expectations are forward looking and depend on the actual (endogenous) growth rate of capital. Nonetheless, expectations are subject to persistent extrapolative errors because the “diagnostic wedge” is a backward-looking function of past shocks, with $\mathcal{I}_t \equiv \int_0^t e^{-\kappa(t-s)} \sigma dZ_s$.

A Simplified Illustration. Figure 1 provides an example of diagnostic expectations applied to an exogenous arithmetic Brownian motion (ABM).¹⁰ The blue line plots the realized path of the ABM up to time t . The dashed black line plots the rational prediction of the ABM’s future path, and the solid red line plots the diagnostic prediction. Because recent shocks have tended to be positive, diagnostic expectations are biased upward.

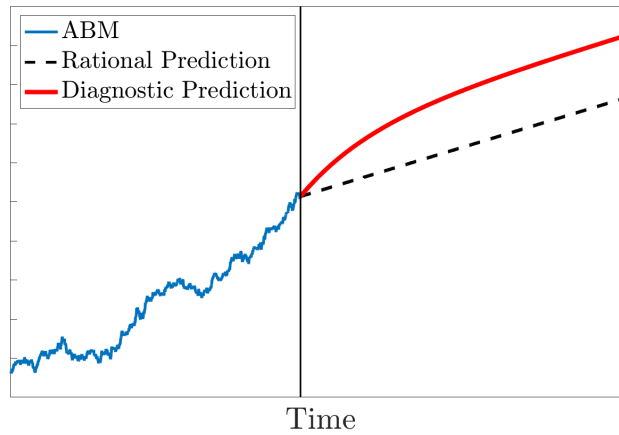


Figure 1: **Diagnostic expectations of arithmetic Brownian motion.** The blue line plots the sample path of an arithmetic Brownian motion (ABM). The solid red line plots diagnostic expectations of the ABM’s future evolution, and the dashed black line plots rational expectations. The calibration is illustrative.

2.3 The Financial Intermediary Sector

Individual Intermediaries. There is a continuum of financial intermediaries, each run by a single banker. Intermediaries raise funds from households by issuing risk-free (instantaneous) debt and risky equity. Equity issuance is subject to a constraint. Each intermediary

¹⁰Log capital k_t would follow arithmetic Brownian motion if i_t were constant.

can issue up to ϵ_t of equity, and constraint ϵ_t evolves as

$$\frac{d\epsilon_t}{\epsilon_t} = d\tilde{R}_t, \quad (6)$$

where $d\tilde{R}_t$ denotes the instantaneous return on the intermediary’s equity at time t . Following HK, constraint ϵ_t can be thought of as the intermediary’s “reputation.” Poor performance damages the intermediary’s reputation and reduces its capacity to issue equity in the future.¹¹

The banker does not consume. Instead, the banker has mean-variance preferences over their intermediary’s reputation:

$$\hat{\mathbb{E}}_t \left[\frac{d\epsilon_t}{\epsilon_t} \right] - \frac{\gamma}{2} \widehat{Var}_t \left[\frac{d\epsilon_t}{\epsilon_t} \right] = \hat{\mathbb{E}}_t \left[d\tilde{R}_t \right] - \frac{\gamma}{2} \widehat{Var}_t \left[d\tilde{R}_t \right]. \quad (7)$$

Hat-notation is used in equation (7) to indicate that the banker has diagnostic expectations about the return process $d\tilde{R}_t$.

This reputational constraint is designed to behave analogously to a standard net-worth constraint in which agency frictions imply that an intermediary’s ability to raise outside capital depends on its net worth (e.g., He and Krishnamurthy, 2012, 2013). As with a net-worth constraint, reputation ϵ_t evolves with past returns $d\tilde{R}_t$ such that external financing becomes more difficult to obtain following a sequence of poor performance. The benefit of the reputational constraint is quantitative, as it allows for a more conventional calibration of the HK model.¹²

¹¹As detailed below, this equity constraint implies that: (i) the market leverage of financial intermediaries is countercyclical, and (ii) financial distress is the result of a capital crunch. These predictions are supported by the empirical evidence in He et al. (2017) and Baron et al. (2021), respectively. An alternative modeling choice sometimes used in related papers is for intermediaries to face a debt constraint (e.g., Brunnermeier and Pedersen, 2009). As discussed in He et al. (2017), both types of constraints are likely at play during crises, and different types of constraints will be more or less relevant for different types of intermediaries (e.g., commercial banks versus hedge funds). Following He and Krishnamurthy (2019), my use of an equity constraint in isolation is a simplification. However, I focus mainly on the role of diagnostic expectations in the lead-up to crises, where constraints do not yet bind tightly. This suggests that the exact specification of constraints will not be critical for the model’s qualitative predictions about the effect of behavioral frictions. Further analysis is beyond the scope of this paper, but is an important area for future research.

¹²With the reputation-based constraint, bankers do not consume. This allows for households to consume all of the economy’s output, as is standard in macroeconomic models without financial frictions. For further details, see Section I.B of He and Krishnamurthy (2019).

The Aggregate Intermediary Sector. Let \mathcal{E}_t denote the maximum equity that can be raised by the aggregate intermediary sector. \mathcal{E}_t evolves as follows:

$$\frac{d\mathcal{E}_t}{\mathcal{E}_t} = d\tilde{R}_t - \eta dt + d\psi_t. \quad (8)$$

All intermediaries behave identically. The term $d\tilde{R}_t$ implies that the aggregate constraint evolves with the reputation of each individual intermediary. Parameter η governs the exogenous exit rate of intermediaries. Exit is needed to ensure that intermediaries do not escape their equity issuance constraint in equilibrium. The term $d\psi_t \geq 0$ reflects entry into the banking sector. Entry occurs deep in crisis times when reputation is sufficiently low, and establishes a boundary condition for the model. Details are provided in Appendix B.3.

2.4 The Household Sector

Consumption. There is a unit measure of households. Households consume the output good (c_t^y) and housing services (c_t^h). The output good is the numeraire. Since households do not hold housing directly, housing services are rented at price D_t .

Households maximize

$$\widehat{\mathbb{E}}_t \left[\int_t^\infty e^{-\rho(s-t)} \frac{C_s^{1-\gamma_h}}{1-\gamma_h} ds \right], \quad (9)$$

where C_t is a Cobb-Douglas consumption aggregator $C_t = (c_t^y)^{1-\phi}(c_t^h)^\phi$. Intratemporal maximization yields:

$$\frac{c_t^y}{c_t^h} = \frac{1-\phi}{\phi} D_t. \quad (10)$$

Labor Income. Households can supply up to one unit of labor, without disutility, at wage \mathcal{W}_t . In equilibrium, households earn share $1-\nu$ of output as labor income:

$$\mathcal{W}_t = (1-\nu)AK_t. \quad (11)$$

Here I take this wage equation as given. A microfoundation is provided in Appendix B.1. In addition to diagnostic expectations, this stylized labor income margin is where my model

differs from HK. The benefit of introducing labor income is that it produces realistic consumption and investment output shares (see Appendix B.1 for details).

Capital Production. Investment follows q -theory. There exists a capital producer who is responsible for investment. The capital producer solves $\max_{i_t} q_t i_t K_t - \Phi(i_t, K_t)$. All profits are passed on to households. This results in an investment rate of

$$i_t = \delta + \frac{q_t - 1}{\xi}. \quad (12)$$

Equation (12) highlights a key macro-financial linkage: the economy’s growth rate depends on investment rate i_t , which in turn depends on equilibrium capital price q_t . To the extent that both financial and behavioral frictions affect q_t , these frictions will propagate out of financial markets to affect the growth rate of the broader real economy.

2.5 Portfolio Choice and Asset Returns

Household Portfolio Choice. Let W_t denote aggregate household wealth. Households can invest in two assets: the debt and equity issued by intermediaries. Debt offers a risk-free return of r_t , and equity offers a stochastic return of $d\tilde{R}_t$. Reduced-form assumptions will now be made to ensure that households purchase at least λW_t of intermediary debt. Households are not the focal point of the model, and these simplifying assumptions allow the equilibrium leverage of the financial sector to be regulated by exogenous parameter λ .

Each household is split into a “debt member” and an “equity member.” The debt member can only invest in the risk-free debt of intermediaries. The equity member is free to purchase intermediary equity (but cannot make levered investments). At the start of each period, the debt member is given share λ of wealth and the equity member is given share $1 - \lambda$. Investments pay off at time $t + dt$, and returns are pooled before this process is repeated.

The model will be calibrated such that equity members collectively invest their allocated wealth of $(1 - \lambda)W_t$ in intermediary equity, subject to the restriction that they do not purchase more than \mathcal{E}_t .¹³ If the constraint binds, equity members place their remaining wealth in bonds. The total equity capital raised by the intermediary sector at time t is

¹³This condition is verified as part of the model solution. For details, see Appendix C.3.

therefore

$$E_t = \min\{\mathcal{E}_t, (1 - \lambda)W_t\}. \quad (13)$$

Households also pin down the risk-free rate r_t through their intertemporal optimization:

$$r_t dt = \rho dt + \zeta \widehat{\mathbb{E}}_t \left[\frac{dc_t^y}{c_t^y} \right] - \frac{\zeta(\zeta + 1)}{2} \widehat{Var}_t \left[\frac{dc_t^y}{c_t^y} \right]. \quad (14)$$

Parameter $\zeta = 1 - (1 - \phi)(1 - \gamma_h)$ can be interpreted as the inverse of the elasticity of intertemporal substitution (EIS). Equation (14) is the standard consumption-based risk-free rate formula in continuous time, except that households have diagnostic expectations of the consumption process.¹⁴ Households' diagnostic expectations therefore affect the risk-free rate, with parameter ζ governing the strength of this effect.

Intermediary Portfolio Choice. This is an intermediary asset pricing model, and intermediaries' portfolio choices determine the prices of K_t and H in equilibrium. Because intermediaries are diagnostic, they may not have correct beliefs about equilibrium asset returns when making their portfolio decisions.

I begin by postulating that intermediaries expect q_t and P_t to evolve according to:

$$\frac{\widehat{dq}_t}{q_t} = \widehat{\mu}_t^q dt + \widehat{\sigma}_t^q dZ_t, \text{ and} \quad (15)$$

$$\frac{\widehat{dP}_t}{P_t} = \widehat{\mu}_t^P dt + \widehat{\sigma}_t^P dZ_t. \quad (16)$$

These endogenous processes will be determined in equilibrium.

Using equation (15), the return on capital is perceived to be:

$$\widehat{dR}_t^k = \left(\frac{\nu A}{q_t} + \widehat{\mu}_t^q - \delta + \theta \mathcal{I}_t + \sigma \widehat{\sigma}_t^q \right) dt + \left(\sigma + \widehat{\sigma}_t^q \right) dZ_t. \quad (17)$$

The perceived return on capital consists of a dividend component $\left(\frac{\nu A}{q_t} dt \right)$ and a capital

¹⁴To generate equation (14), it is assumed that any marginal savings are given to the debt member. The benefit of this assumption is that it recovers the standard continuous-time risk-free rate formula. See footnote 5 of He and Krishnamurthy (2019) for details.

gains component $\left(\frac{d(\widehat{q_t K_t})}{\widehat{q_t K_t}} - i_t dt\right)$. Equation (17) illustrates how diagnosticity affects agents' expectations of capital returns. First, there is a direct effect: capital growth expectations are biased by $\theta \mathcal{I}_t$.¹⁵ Second, diagnostic agents misjudge how the economy evolves in equilibrium. This introduces an indirect effect in which diagnostic agents misperceive the endogenous drift and volatility of q_t .

Proceeding similarly, the perceived return on housing is:

$$\widehat{dR_t^h} = \left(\frac{D_t}{P_t} + \widehat{\mu_t^P}\right) dt + \widehat{\sigma_t^P} dZ_t. \quad (18)$$

The dividend on housing is rental income D_t . Since diagnosticity biases agents' expectations of economic growth, it also biases their expectations of housing rent growth. And since P_t is the present discounted value of these future rental dividends, diagnostic expectations produce non-rational expectations of price process P_t .

Let $\widehat{\pi_t^k} \equiv \left(\frac{\nu A}{q_t} + \widehat{\mu_t^q} - \delta + \theta \mathcal{I}_t + \sigma \widehat{\sigma_t^q}\right) - r_t$ denote the perceived risk premium on capital. Let $\widehat{\pi_t^h} \equiv \left(\frac{D_t}{P_t} + \widehat{\mu_t^P}\right) - r_t$ denote the perceived risk premium on housing. Equations (17) and (18) can be rewritten as follows:

$$\begin{aligned} \widehat{dR_t^k} &= \left(\widehat{\pi_t^k} + r_t\right) dt + \widehat{\sigma_t^k} dZ_t, \text{ and} \\ \widehat{dR_t^h} &= \left(\widehat{\pi_t^h} + r_t\right) dt + \widehat{\sigma_t^h} dZ_t, \end{aligned}$$

where $\widehat{\sigma_t^k} \equiv \sigma + \widehat{\sigma_t^q}$ and $\widehat{\sigma_t^h} \equiv \widehat{\sigma_t^P}$.

Let α_t^k and α_t^h denote the intermediary's portfolio share of capital and housing, respectively. The intermediary's perceived return on equity is:

$$\widehat{d\widetilde{R}_t} = \alpha_t^k \widehat{dR_t^k} + \alpha_t^h \widehat{dR_t^h} + (1 - \alpha_t^k - \alpha_t^h) r_t dt.$$

¹⁵For empirical evidence showing the extrapolation of fundamentals by financial market professionals, see e.g., Greenwood and Hanson (2013), Fahlenbrach et al. (2017), Bordalo et al. (2019, 2020a), Gulen et al. (2019), Bordalo et al. (2020b), Pflueger et al. (2020), and Nagel and Xu (2021, 2022).

From the objective in equation (7), the intermediary solves:

$$\max_{\alpha_t^k, \alpha_t^h} \left[r_t + \alpha_t^k \widehat{\pi}_t^k + \alpha_t^h \widehat{\pi}_t^h \right] - \frac{\gamma}{2} \left(\alpha_t^k \widehat{\sigma}_t^k + \alpha_t^h \widehat{\sigma}_t^h \right)^2. \quad (19)$$

This results in the optimality condition:

$$\frac{\widehat{\pi}_t^k}{\widehat{\sigma}_t^k} = \frac{\widehat{\pi}_t^h}{\widehat{\sigma}_t^h} = \gamma (\alpha_t^k \widehat{\sigma}_t^k + \alpha_t^h \widehat{\sigma}_t^h). \quad (20)$$

Equation (20) is the key asset pricing equation. It says that intermediaries choose portfolio shares in order to equate the perceived Sharpe ratio on each asset to their risk aversion times their perceived portfolio risk. Thus, when intermediaries are required to bear additional risk, they demand higher Sharpe ratios as compensation.

Financial Crises. Following HK, financial crises are defined as states in which the equity issuance constraint binds: $\mathcal{E}_t < (1 - \lambda)W_t$. When the constraint binds, the economy exhibits a dramatic increase in risk premia, a collapse in asset prices, and impaired economic growth. These crisis nonlinearities arise for two reasons. First, the binding equity issuance constraint forces intermediaries to increase leverage in order to fund asset purchases. Second, the binding constraint endogenously amplifies the sensitivity of asset prices to shocks because once the constraint already binds, negative shocks will cause the constraint to bind even more tightly in the future. Increased leverage is reflected in portfolio shares α_t^k and α_t^h , while the amplification of shocks is reflected in volatility coefficients $\widehat{\sigma}_t^k$ and $\widehat{\sigma}_t^h$. As equation (20) shows, the sudden onset of both effects when the equity issuance constraint binds will generate the spikes in risk premia that typify financial crises.

3 Equilibrium and Model Calibration

3.1 Equilibrium

Definition 1. Diagnostic Expectations Equilibrium (DEE). A diagnostic expectations equilibrium is a set of prices $\{q_t, P_t, D_t, r_t, \mathcal{W}_t\}$ and decisions $\{c_t^y, c_t^h, i_t, \alpha_t^k, \alpha_t^h\}$ such that:

1. Given prices, decisions as specified by (10), (12), (14), and (19) are optimal under

diagnostic expectations.

2. The goods market and housing rental market clear (using C^y and C^h to indicate aggregate household consumption):

$$Y_t = AK_t = C_t^y + \Phi(i_t, K_t), \text{ and} \quad (21)$$

$$C_t^h = H \equiv 1.$$

3. The equity issuance constraint is satisfied:

$$E_t = \min\{\mathcal{E}_t, (1 - \lambda)W_t\}.$$

4. Asset markets clear with intermediaries holding all capital and housing:

$$q_t K_t = \alpha_t^k E_t, \text{ and} \quad (22)$$

$$P_t = \alpha_t^h E_t. \quad (23)$$

5. The total value of assets equals total household wealth:

$$W_t = q_t K_t + P_t.$$

Diagnostic expectations generalize rational expectations. Rationality is recovered by setting $\theta = 0$. This is formalized in the following definition, which will serve as a benchmark for later comparison.

Definition 2. Rational Expectations Equilibrium (REE). A rational expectations equilibrium is a diagnostic expectations equilibrium for $\theta = 0$.

Solution Strategy. I consider Markov equilibria in state variables K_t , \mathcal{E}_t , and \mathcal{I}_t . K_t scales the size of the economy, \mathcal{E}_t is the financial sector's capital capacity, and \mathcal{I}_t characterizes sentiment. HK use K_t and \mathcal{E}_t as state variables in their rational model. The innovation of this paper is to capture behavioral frictions with state variable \mathcal{I}_t . When expectations are

extrapolative it is not enough to know the current state of the economy (K_t and \mathcal{E}_t). One must also know the path taken to get there, and \mathcal{I}_t is a sufficient statistic for characterizing that path.

The solution can be simplified further by scaling the economy by K_t . Define

$$e_t \equiv \frac{\mathcal{E}_t}{K_t}.$$

e_t captures the capital capacity of the intermediary sector relative to the size of the overall economy. I look for price functions of the form $p_t = \frac{P_t}{K_t} = p(e_t, \mathcal{I}_t)$ and $q_t = q(e_t, \mathcal{I}_t)$. The model is solved numerically as a function of e_t and \mathcal{I}_t : e_t characterizes financial frictions, and \mathcal{I}_t characterizes behavioral frictions. Full solution details are presented in Appendix C.

In the class of Markov equilibria considered here, each diagnostic expectations equilibrium nests its corresponding rational expectations equilibrium. When solving for a DEE, this means that a REE comes “for free.” Formally:

Proposition 1. *For any DEE that is Markov in $\{K, e, \mathcal{I}\}$, the price and policy functions for $\{K, e, \mathcal{I} = 0\}$ compose a REE that is Markov in $\{K, e\}$.*

Proof. Equation (4) specifies that when $\mathcal{I}_t = 0$, agents act as if $\mathcal{I} = 0$ in perpetuity. Decisions that are optimal when $\mathcal{I} = 0$ in perpetuity will also be optimal when $\theta = 0$ (REE). In both cases, \mathcal{I} is perceived to have no effect on the resulting equilibrium. \square

3.2 Calibration

The HK model is a standard RBC model augmented with a financial intermediary sector. The economy behaves like an RBC model when e_t is far from the constraint, but intermediary frictions become quantitatively important near the crisis region. I follow HK in defining $e_{distress}$ as the 33rd percentile value of e_t in the model’s stationary distribution. $e_{distress}$ separates “normal” periods from periods of financial distress.

Table 1 presents the baseline calibration. I use the parameters and/or calibration targets of He and Krishnamurthy (2019) when possible. Parameters that are marked with an asterisk in the Choice column are equivalent to the HK calibration. Asterisks in the Target column indicate parameters for which the value differs from HK, but the target is the same. The

only parameters for which neither the value nor the target aligns with HK are the three new parameters. These are expectations parameters θ and κ , and labor income parameter ν .

	Parameter	Choice	Target
Panel A: Intermediation Parameters			
γ	Banker Risk Aversion	2*	Mean Sharpe Ratio
λ	Debt Ratio	0.75*	Intermediary Leverage
η	Bank Exit Rate	0.126	Probability of Crisis*
\underline{e}	Lower Entry Barrier	0.080	Max Sharpe Ratio*
β	Entry Cost	2.8*	Land Price Volatility
Panel B: Technology Parameters			
σ	Capital Shock Volatility	3%*	C and I Volatility
δ	Depreciation Rate	10%*	Literature
ξ	Adjustment Cost	3*	Literature
A	Productivity	$\frac{1}{3}$	Consumption-Output Ratio*
ν	Capital Share	0.415	Investment-Capital Ratio
Panel C: Household Preference Parameters			
ρ	Time Discount Rate	2%*	Literature
$1/\zeta$	EIS	1.5	Interest Rate Volatility*
ϕ	Housing Expenditure Share	0.197	Housing-Wealth Ratio*
Panel D: Diagnostic Expectations Parameters			
κ	Decay of New Information	0.116	$\text{Corr}(e, \mathcal{I})$
θ	Diagnosticity	0.120	Bordalo et al. (2020b)
Unconditional Simulated Moments			
	Mean($\frac{\text{Investment}}{\text{Capital}}$)		10.05%
	Mean($\frac{\text{Consumption}}{\text{Output}}$)		69.86%
	Mean(Realized Sharpe Ratio)		0.47
	Mean(Realized Intermediary Risk Premium)		14.95%
	Probability of Crisis		3.13%
	Volatility(Land Price Growth)		11.03%
	Volatility(Interest Rate)		0.85%
	Corr(e, \mathcal{I})		0.71
Non-Distress Simulated Moments			
	Volatility(Investment Growth)		4.74%
	Volatility(Consumption Growth)		2.22%
	Volatility(Output Growth)		2.96%
	Mean($\frac{\text{Housing Wealth}}{\text{Total Wealth}}$)		45.45%

Table 1: **Baseline calibration.** Model-generated moments are calculated by simulating the model at a monthly frequency. Growth rates are computed as log changes from month $t - 6$ to month $t + 6$.

RBC Parameters. Discount rate ρ , depreciation rate δ , and adjustment cost ξ are relatively standard RBC parameters. My calibration follows HK.

Parameter σ governs the volatility of capital quality shocks. As in HK, I set $\sigma = 3\%$. HK report that from 1975 to 2015 the volatility of investment growth in non-distress periods was 5.79%, and the volatility of consumption growth was 1.24%. In the model, $\sigma = 3\%$

generates investment growth volatility of 4.74% and consumption growth volatility of 2.22% in non-distress periods. The model features too much consumption volatility and too little investment volatility, with $\sigma = 3\%$ balancing the two targets.

Parameters A and ν are calibrated jointly to target the average investment-capital ratio and consumption-output ratio. The targeted investment-capital ratio is 10% so that average investment matches depreciation. Since the dividend yield on capital is $\frac{\nu A}{q_t}$, ν and A are calibrated to generate a capital price q commensurate with a 10% investment-capital ratio. To separately identify A and ν , I also target an average consumption-output ratio of 70%. The consumption-output ratio equals $\frac{AK_t - \Phi(i_t, K_t)}{AK_t} \approx 1 - \frac{i_t}{A}$. An investment-capital ratio of 10% pins down $A = \frac{1}{3}$.

Intermediation Parameters. Parameter γ represents bankers' risk aversion. As in HK, I set $\gamma = 2$. This generates an average realized Sharpe ratio of 0.47, and an average realized intermediary risk premium of 14.95%. This aligns with [He et al. \(2017\)](#), who estimate an average Sharpe ratio of 0.48 and an average return of 13% for assets intermediated by the financial sector.

Intermediary leverage is governed by λ . Since intermediaries have assets of $P_t + q_t K_t = W_t$ and equity of E_t , equation (13) gives a market leverage value of $\frac{W_t}{E_t} = \frac{1}{1-\lambda}$ in non-crisis states. Again following HK, I set $\lambda = 0.75$. This generates a leverage ratio of 4 when the constraint does not bind.

Crisis Parameters. Crises are defined as states in which the equity issuance constraint binds. Bank exit rate η targets a 3% crisis probability.

Parameters \underline{e} and β control the lower boundary condition, represented by $d\psi_t$ in equation (8) (details in Appendix B.3). Parameter \underline{e} is the minimum level of capital capacity at which new entry occurs, and β is the cost of entry into the intermediary sector. HK set \underline{e} such that the Sharpe ratio at \underline{e} is 6.5 (i.e., \underline{e} is set low enough that entry occurs rarely). Here, I set \underline{e} such that the perceived Sharpe ratio at \underline{e} and $\mathcal{I} = 0$ is 6.5. Parameter β determines the slope of house price P_t at \underline{e} , which in turn affects the volatility of P_t throughout the distress region. As in HK, I set $\beta = 2.8$. HK estimate that the empirical volatility of land price growth from 1975 to 2015 was 11.9%. In the model, $\beta = 2.8$ generates land price growth

volatility of 11.03%.

Household Parameters. Parameter ϕ governs the relative value of housing services to the output good. This determines the rental rate D_t (see equation (10)). P_t is the discounted value of these rental payments. I set $\phi = 0.197$ to target a non-distress housing-wealth ratio of 45%. $\phi = 0.197$ also generates a housing services to total consumption expenditure ratio that is consistent with NIPA consumption data (Davis and Van Nieuwerburgh, 2015).

ζ is the inverse of the EIS, and determines the responsiveness of the risk-free rate to households' consumption expectations (see equation (14)). When household expectations are diagnostic, they misperceive the equilibrium consumption process. Thus, ζ governs the sensitivity of the risk-free rate to variation in household sentiment. When $\zeta = 1$, any bias in expectations of economic growth is passed one-for-one into r_t . An important implication is that when $\zeta = 1$, asset prices q_t and P_t are insensitive to \mathcal{I}_t , as all bias in cash-flow expectations is exactly offset by the risk-free rate. When $\zeta < 1$, r_t responds less than one-for-one to biased growth expectations. In this case, q_t and P_t are increasing in \mathcal{I}_t .

I set the EIS ($1/\zeta$) equal to 1.5. This is a standard choice in the finance literature (e.g., Bansal and Yaron, 2004), and, as in HK, generates real interest rate volatility of roughly 1%. Since $\zeta < 1$, asset prices are increasing in \mathcal{I}_t . This will be important for generating the boom-bust investment dynamics in Section 5.2.

Behavioral Parameters. θ governs the extent to which expectations are biased by representativeness. κ governs the persistence of sentiment. θ and κ are calibrated jointly using two targets. The first target aligns the magnitude of the expectations bias with the estimates of Bordalo et al. (2020b): one standard deviation in sentiment generates an output growth bias of 0.75 percentage points.¹⁶ The second target matches the model's unconditional correlation between state variables e_t and \mathcal{I}_t to the correlation between intermediary capital and sentiment estimated empirically. To estimate this correlation in the data, I measure e_t with the “Intermediary Capital Ratio” of He et al. (2017). \mathcal{I}_t can be calculated using beliefs data, given κ and θ . Full calibration details are provided in Appendix A.2.

These two calibration targets produce $\theta = 0.120$ and $\kappa = 0.116$. $\kappa = 0.116$ implies

¹⁶Note that $Var(\theta\mathcal{I}_t) = \frac{\theta^2\sigma^2}{2\kappa}$. This calibration target sets $\theta\frac{\sigma}{\sqrt{2\kappa}} = 0.0075$.

that sentiment is slow moving with a half-life of 6 years, therefore capturing the reaction of beliefs to prolonged periods of relatively positive or negative news rather than high-frequency volatility.¹⁷ Appendix B.7 examines robustness of the model’s main results to θ and κ .

Both calibration targets are based on expectations data from experts rather than households. This is consistent with the model, since sophisticated financial intermediaries drive the model’s dynamics.¹⁸ While this paper takes as its starting point the evidence that experts are not fully rational, it is natural to ask about the extent to which a diagnostic intermediary’s performance deviates from that of a hypothetical, fully rational, “arbitrageur” who understands the economy’s true laws of motion. I examine this question in Appendix B.5, and there are two main takeaways. First, since the calibrated level of θ is modest, the underperformance of diagnostic intermediaries is typically mild.¹⁹ Second, it is not uncommon for diagnostic intermediaries to outperform the arbitrageur, particularly when sentiment is elevated, because overoptimism encourages additional risk taking.²⁰

4 Global Solution: Financial and Behavioral Frictions

4.1 Prices, Policy Functions, and Forecast Errors

Select price and policy functions for the DEE are shown in Figure 2. The horizontal axis lists capital capacity $e = \frac{\mathcal{E}}{K}$, which characterizes the state of financial frictions. To jointly illustrate the effect of behavioral frictions, all panels plot three curves. The blue curve corresponds to depressed sentiment ($\mathcal{I} = -1.5SD$), the red curve corresponds to neutral sentiment ($\mathcal{I} = 0$), and the yellow curve corresponds to elevated sentiment ($\mathcal{I} = +1.5SD$).

I begin by describing the effect of financial frictions. The two leftmost panels of Figure 2 show asset prices $q(e, \mathcal{I})$ and $p(e, \mathcal{I})$. Financial frictions make asset prices sensitive to capital capacity e . In the crisis region (approximately $e < 0.4$), the binding constraint causes asset prices to plummet. Similarly, the Sharpe ratio panels illustrate the nonlinear spike in risk

¹⁷Using a different specification than this paper, [Bordalo et al. \(2019\)](#) estimate that the diagnostic expectations of stock market analysts incorporate the past three years of shocks. See also [Bordalo et al. \(2020a\)](#) and [Nagel and Xu \(2022\)](#) for similar evidence of slow-moving belief distortions.

¹⁸Though the beliefs of households are certainly important (e.g., [Chodorow-Reich et al., 2021](#)), the focus of this paper is on the beliefs of financial intermediaries.

¹⁹Diagnostic intermediaries underperform by an average of 87 basis points, compared to an average risk premium of 15%.

²⁰A full equilibrium analysis is beyond the scope of this paper, but this suggests that sentiment-driven mispricing may be difficult to correct during periods of overheating.

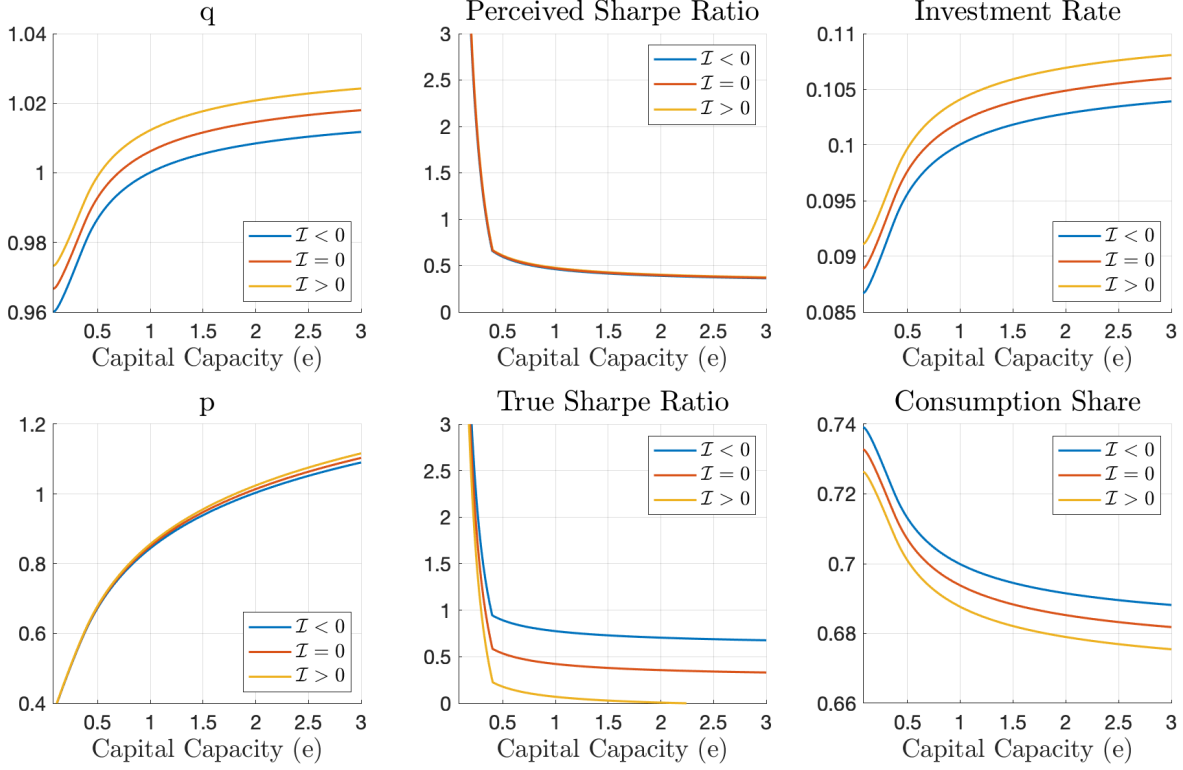


Figure 2: **Selected price and policy functions.** The horizontal axis lists capital capacity $e = \frac{\mathcal{E}}{K}$. Each panel plots three curves, corresponding to $\mathcal{I} = -1.5SD$ (blue), $\mathcal{I} = 0$ (red), and $\mathcal{I} = +1.5SD$ (yellow). See Appendix Figure 10 for more.

premia that characterizes crisis times. Moving right, asset prices rise and risk premia fall as intermediaries’ risk-bearing capacity improves. Asset prices eventually asymptote for high values of e as financial frictions dissipate.

Asset prices exhibit what HK refer to as “anticipation effects”: asset prices start to fall well before the equity issuance constraint binds. Anticipation effects arise in equilibrium because forward-looking intermediaries are unwilling to support elevated asset prices in the face of mounting systemic risk.²¹ Anticipation effects are captured by the “financial distress” region of the model, defined as e below its 33rd percentile, where the constraint does not necessarily bind but the effects of financial frictions are still present.²²

²¹Intermediaries perceive that risk premia are low when asset prices are high, and vice-versa. This goes against the findings of Greenwood and Shleifer (2014). However, Greenwood and Shleifer (2014) study total returns rather than excess returns, and focus predominantly on household expectations. In the model, it is the beliefs of financial intermediaries that are relevant for asset prices, and Adam et al. (2020) find that professional investors have excess return expectations that covary negatively with the price-dividend ratio.

²²Consistent with anticipation effects, Baron et al. (2021) document that bank equity declines predict output gaps, even when panics do not materialize.

Turning next to behavioral frictions, asset prices are increasing in \mathcal{I} because sentiment inflates expectations of cash-flow growth. [Bordalo et al. \(2020a\)](#) provide direct evidence of this effect, documenting that stock market analysts’ expectations of aggregate earnings are overoptimistic, and asset prices are inflated, following positive fundamental news. In the model, asset prices move so that sentiment gets “priced in” in equilibrium, consistent with the dynamics of subjective risk premia documented in [Nagel and Xu \(2021\)](#). This effect is illustrated by the Perceived Sharpe Ratio panel, which shows that perceived risk premia are insensitive to \mathcal{I} and are driven almost entirely by e . However, the True Sharpe Ratio panel highlights the consequences of pricing assets based on non-rational expectations of fundamentals. Risk premia are higher than expected when sentiment is depressed, but are dragged down when sentiment is elevated. The yellow curve in the True Sharpe Ratio panel even dips below zero for high e , indicating that diagnostic expectations produce negative risk premia when sentiment is highly elevated.²³

The investment and consumption panels show the propagation of financial and behavioral frictions to the real economy. From equation (12), investment rate i is high whenever either e or \mathcal{I} is high. The consumption share $\frac{C^y}{Y}$ moves in the opposite manner, which follows from output market clearing in equation (21).

Comparative Statics. I conduct comparative statics exercises in order to demonstrate the role of key model parameters. The main takeaways are discussed here, and details are presented in Appendix B.6.

Starting with beliefs, diagnosticity parameter θ governs the level of belief distortions at a point in time, and decay parameter κ governs the persistence of belief distortions. Since this is an intermediary asset pricing model, I also show that it is the beliefs of financial intermediaries, not households, that are critical for generating the mispricing shown in the Sharpe ratio panels of Figure 2.

Turning to financial intermediation, asset pricing equation (20) implies that equilibrium

²³[Baron and Xiong \(2017\)](#) estimate that excess returns on bank equity are significantly negative roughly 5-10% of the time. Though not targeted in the calibration of θ , the model is broadly consistent with this finding. In the model, risk premia are negative 4.1% of the time. [Greenwood and Hanson \(2013\)](#) also find periods of negative excess returns on high-yield bonds. Appendix Figure 11 provides a complete view of risk premia over the state space.

risk premia are increasing in intermediary risk aversion γ as well as in parameters λ , ϕ , and ξ , which affect the risk that intermediaries must bear.²⁴ I also examine crisis parameters β and \underline{e} . As discussed in the calibration section, β has some effect on the volatility of P_t , while \underline{e} is set low enough that risk premia are insensitive to variation in the entry barrier.

4.2 The Feedback from Behavioral Frictions to Financial Frictions

In order to illustrate how financial and behavioral frictions interact dynamically, Figure 3 plots the evolution of state variables e_t and \mathcal{I}_t . Each “x” marks a starting point and the blue curves plot the realized path of e_t and \mathcal{I}_t over the next 5 years, assuming no subsequent shocks. The different shades of blue correspond to different years, with the shading getting lighter as time progresses. For reference, the dotted gray line running diagonally through the figure marks where the drift of capital capacity e_t equals zero.

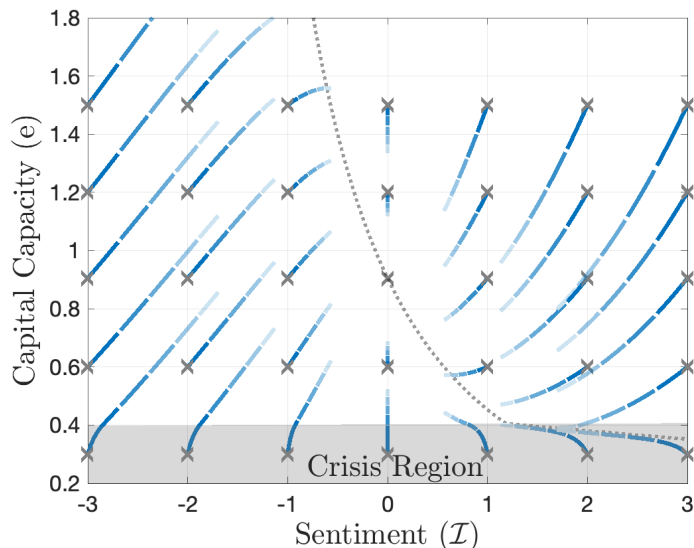


Figure 3: **5-year evolution of e_t and \mathcal{I}_t (no shocks)**. Each “x” is a starting point, and blue curves plot the realized evolution of e_t and \mathcal{I}_t over the next 5 years under the assumption of no capital quality shocks. The dotted gray line marks where the drift of e_t equals zero. Sentiment is reported in standard deviation units.

The evolution of sentiment \mathcal{I}_t in Figure 3 is straightforward, with sentiment steadily reverting toward zero in the absence of shocks. This reflects slow-moving belief distortions, consistent with analyst expectations of earnings growth in [Bordalo et al. \(2019, 2020a\)](#).

²⁴ λ controls intermediary leverage. ϕ and ξ impact asset volatility through their effects on the rigidity of asset supply. For ϕ , the housing asset is volatile because it is in fixed supply (see footnote 3), and increasing ϕ makes volatile housing a larger component of intermediary portfolios. Increasing adjustment cost parameter ξ has a similar effect by making capital more rigid.

The evolution of intermediary capital capacity e_t is more nuanced. Shutting down behavioral frictions to start, consider the drift of e_t when $\mathcal{I}_t = 0$. Following typical intermediary asset pricing dynamics, when e_t is low and intermediaries' risk-bearing capacity is impaired, e_t proceeds to drift up because intermediaries demand large risk premia to hold risky capital. When e_t is high, e_t drifts down because intermediaries demand only small risk premia.

The next step is to understand how behavioral frictions alter the evolution of financial frictions. Looking from left to right across different sentiment levels, Figure 3 highlights that sentiment plays a critical role in shaping the evolution of capital capacity. Relative to the evolution of e_t when $\mathcal{I}_t = 0$, depressed sentiment leads to an improvement of capital capacity while elevated sentiment leads to a deterioration. This finding that sentiment impacts the subsequent evolution of financial frictions will be a central mechanism for the paper's results. I refer to this effect as *the feedback from behavioral frictions to financial frictions*.

Intuitively, the intermediary sector's ability to raise capital evolves with realized returns $d\tilde{R}_t$. However, intermediaries price assets according to their beliefs. Paralleling the belief-driven return dynamics documented in [Bordalo et al. \(2020a\)](#), belief distortions drive a wedge between the true return process and the perceived return process by dislocating prices from fundamentals. In the case of elevated sentiment, intermediaries purchase assets at expensive valuations, which lowers realized returns and induces a gradual tightening of financial frictions. Alternatively, excessive pessimism gradually relaxes financial frictions because intermediaries purchase assets cheaply and earn higher returns than expected.

4.3 Stationary Distribution

Figure 4 plots the economy's stationary distribution over state variables e and \mathcal{I} . The ergodic distribution is solved numerically using a Kolmogorov forward equation. The economy is more likely to be in lighter-colored areas, while dark blue regions are rarely encountered. The dotted gray line marks the boundary of the crisis region.

The unconditional correlation between e_t and \mathcal{I}_t is 0.71. This tight correlation arises in equilibrium because e_t and \mathcal{I}_t both load positively on capital quality shocks. For example, a positive shock increases e_t by generating large intermediary returns, and also increases \mathcal{I}_t by making future high-growth states more representative.

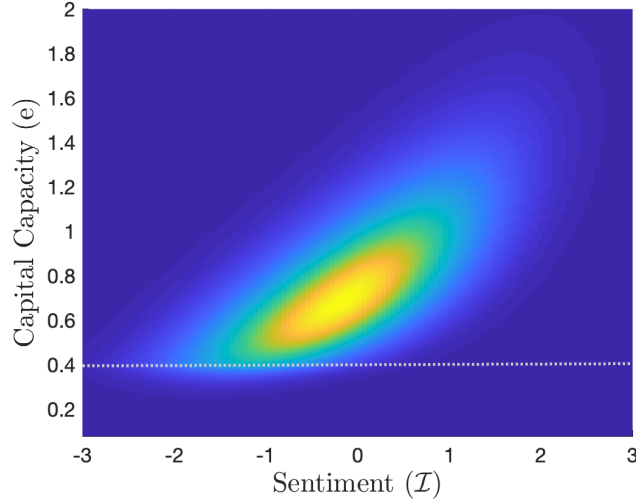


Figure 4: **Ergodic distribution.** Sentiment is reported in standard deviation units. The gray dotted line marks the boundary of the crisis region.

4.4 Discussion: The Role of Financial and Behavioral Frictions

A key contribution of this paper is that it characterizes how macro-financial dynamics are shaped by the interaction of diagnostic expectations and financial frictions. Having presented the calibrated model's solution, I now summarize the role that each friction plays.

Financial Frictions: Downside Risks and Financial Crises. Financial frictions allow the model to capture the downside risks to both financial markets and the broader real economy that are caused by disruptions in financial intermediation. Financial fragility is fundamentally asymmetric, an effect that is clearly evident in Figure 2. When intermediaries are well capitalized, valuations are both high and insensitive to small changes in capital capacity. But, low capital capacity impairs intermediaries' ability to bear risk. This drags down asset prices and investment, and also makes the economy highly sensitive to changes in capital capacity.

Behavioral frictions alone do not produce such asymmetries. As Figure 2 shows, when intermediaries are well capitalized the effect of sentiment is roughly symmetric. Overoptimism following good news temporarily raises asset prices, while overpessimism following bad news temporarily lowers them. Without financial frictions, behavioral frictions alone do not produce the severe financial crises that are a focus of this paper.

On the other hand, the model with only financial frictions has no path dependence. Under

rational expectations, all that matters is the current health of financial intermediaries, e_t . This lack of path dependence means that the only way to end up in a financial crisis is with a long sequence of negative shocks. As I will detail shortly, the addition of diagnostic expectations means that past economic performance shapes future equilibrium dynamics through agents' extrapolative beliefs. This path dependence is critical for generating the triggers – such as boom-bust cycles and neglected crash risk – that are needed to produce realistic crisis dynamics.

Short-Run Behavioral Frictions: Amplification. In the short run, diagnostic expectations amplify the effect of financial frictions on asset prices and investment. Consider a series of positive shocks. Positive shocks alleviate financial frictions, which raises asset prices and promotes investment (the reverse holds for negative shocks). Diagnostic expectations amplify the impact of shocks in the short run, since changes to sentiment cause further movements in asset prices and investment.

As discussed in Section 2.2, this short-run amplification effect is a key implication of this paper's novel application of diagnostic expectations to the endogenous capital growth process. By influencing the price of capital q_t , diagnostic beliefs about economic growth endogenously alter the path of future economic growth.

Long-Run Behavioral Frictions: Reversal. This paper also identifies a novel long-run effect of behavioral frictions that works in opposition to the short-run effect. As presented in Section 4.2, I call this reversal *the feedback from behavioral frictions to financial frictions*.

An important property of this long-run feedback effect is that it arises as an endogenous consequence of the short-run amplification effect. That is, short-run amplification sows the seeds of its own reversal. In a model with financial frictions, beliefs act like a slingshot for the business cycle. Beliefs amplify the short-run response of asset prices and investment, but this amplification has long-run repercussions for the health of financial intermediaries. Following a sequence of positive shocks, overoptimism amplifies the initial boom. But, since this amplification is driven by the elevation of asset prices above fundamentals, it erodes intermediary returns going forward. Following negative shocks, overpessimism amplifies the initial bust, but by increasing future returns it also promotes a faster recovery of capital

capacity. In this model with slow-moving beliefs, I show below in Section 5.2 that the short-run amplification effect dominates the investment response for roughly the first five years, and the long-run reversal effect takes over after that.

5 Results: Financial Market and Macroeconomic Dynamics

I now present three main results on the interaction of behavioral and financial frictions. I look first at how sentiment can trigger the buildup of crash risk, a pattern that I refer to as sentiment-driven financial crises. Second, I study how short-run amplification followed by a long-run reversal produces boom-bust fluctuations in investment and output growth. Third, I identify a stabilizing role for diagnostic expectations. For robustness, Appendix B.7 examines these three results under alternate calibrations of behavioral parameters θ and κ .

5.1 Sentiment-Driven Financial Crises

A critical shortcoming of rational models of financial crises is that they struggle to generate periods in which the probability of a crisis is high and yet risk premia are low. With diagnostic expectations, elevated sentiment can amplify financial fragility in the background of low risk premium environments.

To show this result, I use a Kolmogorov backward equation to calculate both the true and the diagnostically expected probability that the economy finds itself in a crisis at some point in the next three years. Figure 5 below plots contour lines corresponding to a 10%, 30%, and 50% crisis probability. The dashed lines plot the probability of a crisis that is perceived by agents with diagnostic expectations, and the solid lines plot the true probability. The solid gray area marks the crisis region.

Starting with agents' beliefs, the horizontal dashed lines indicate that sentiment has almost no impact on perceived crisis probabilities.²⁵ Intuitively, diagnostic expectations of fundamentals get incorporated into prices, so intermediaries perceive that crash risk is driven almost entirely by e_t . Perceived crash risk is high only near the crisis region, and intermediaries believe that fragility is quickly attenuated as capital capacity improves.

²⁵The dashed lines slope upward slightly. Recall that a crisis is defined as $e_t < (1 - \lambda)(p_t + q_t)$ (see equation (13)). Since the right-hand side of this inequality is increasing in sentiment, a given level of e_t is closer to the crisis region when \mathcal{I}_t is high.

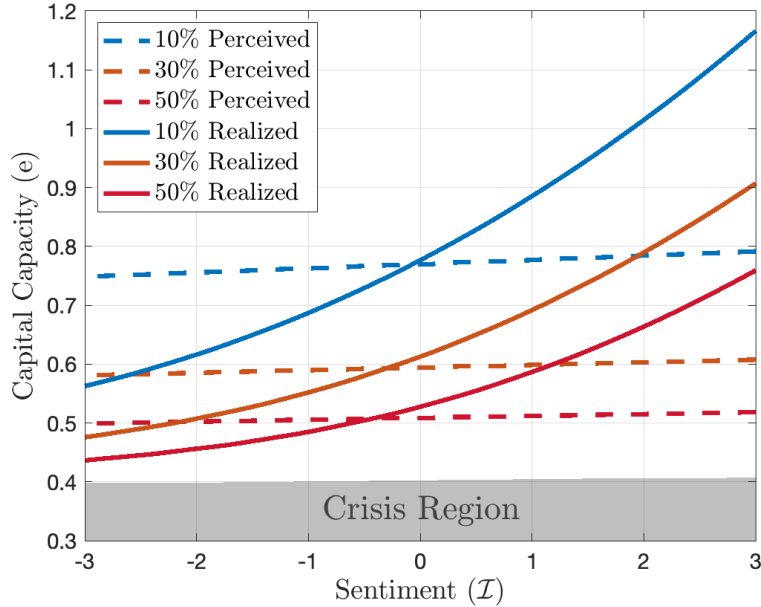


Figure 5: **Crisis hitting probabilities.** Each curve is a contour line corresponding to a 10%, 30%, or 50% probability that the economy enters a crisis in the next three years. Dashed lines report perceived crisis probabilities, and solid lines report true crisis probabilities. Sentiment is reported in standard deviation units.

Reality, however, does not always reflect beliefs. In particular, the tilting of the solid contour lines towards higher levels of capital capacity highlights the endogenous buildup of undetected crash risk that is triggered by overoptimism. Figure 3 above provides the intuition for why sentiment divorces perceptions of crash risk from reality. When $\mathcal{I}_t > 0$, intermediaries borrow at elevated interest rates and pay inflated prices to purchase capital and housing. As expectations disappoint, the feedback from behavioral frictions to financial frictions weakens intermediary balance sheets and moves the economy closer to the crisis region. Because this heightened fragility is an endogenous consequence of overoptimistic beliefs, it is neglected by intermediaries. Thus, diagnostic expectations allow the model to generate periods in which true crash risk is high and yet risk premia are low.

The reverse story explains why perceptions of crash risk are excessive when $\mathcal{I}_t < 0$. Now, the feedback effect works in the opposite direction and intermediaries quickly rebuild their capital capacity relative to expectations.

For policymakers, Figure 5 illustrates an important consequence of diagnostic expectations: when expectations are diagnostic, periods in which intermediary balance sheets appear to be strong can still be associated with heightened crisis risk. For example, when $\mathcal{I}_t = 0$ and

capital capacity e_t is at its median level, the three-year crisis probability is roughly 10%. This probability doubles to roughly 20% when sentiment is elevated by one standard deviation, and jumps to over 30% when sentiment is elevated by two standard deviations. This finding is consistent with the “procyclicality pitfall” of [Adrian and Brunnermeier \(2016\)](#), who document that contemporaneous measures of systemic risk are often inadequate because they fail to account for the stylized fact that risk builds up in the background of boom periods. As described earlier, [Baron and Xiong \(2017\)](#) also reach a similar conclusion.

This sentiment-driven crisis mechanism will be critical for the model’s ability to replicate the 2007-2008 Financial Crisis, as presented in Section 6.3 below. Additionally, the results in Figure 5 mirror the empirical findings of [Greenwood et al. \(2022\)](#), who estimate that the three-year probability of a crisis increases from 7% in normal times to 40% in periods where credit and asset prices are both growing rapidly. Consistent with Figure 5, the authors interpret such periods as the result of overheated financial markets, during which the combination of financial fragility (low e_t) and elevated sentiment (high \mathcal{I}_t) is highly predictive of future financial crises. [Greenwood et al. \(2022\)](#) also emphasize a timing dimension to crisis predictability, whereby crises are often slow to develop once financial markets start to overheat. The model shares this prediction, as Figure 3 shows that sentiment-driven crises take time to unfold. This prediction is fleshed out further below.

Behavioral Frictions Before Crises, Financial Frictions in Crises. Figure 6 explores the dynamic impact of behavioral and financial frictions around crises. Time 0 marks when the economy first enters a crisis. The blue curve plots the average realized (delevered) risk premium earned by intermediaries. The orange curve plots the average risk premium that intermediaries perceive they are demanding. For comparison, the horizontal line at 3.61% marks the unconditional mean realized (delevered) risk premium. Figure 6 reports delevered risk premia to control for the variation in intermediary leverage that occurs when the equity issuance constraint binds.

Elevated sentiment creates excessively low risk premia in the crisis buildup, consistent with the credit spread evidence of [Krishnamurthy and Muir \(2020\)](#). On average, realized risk premia are 17% below perceived risk premia at $t = -5$. Due to the feedback from behavioral

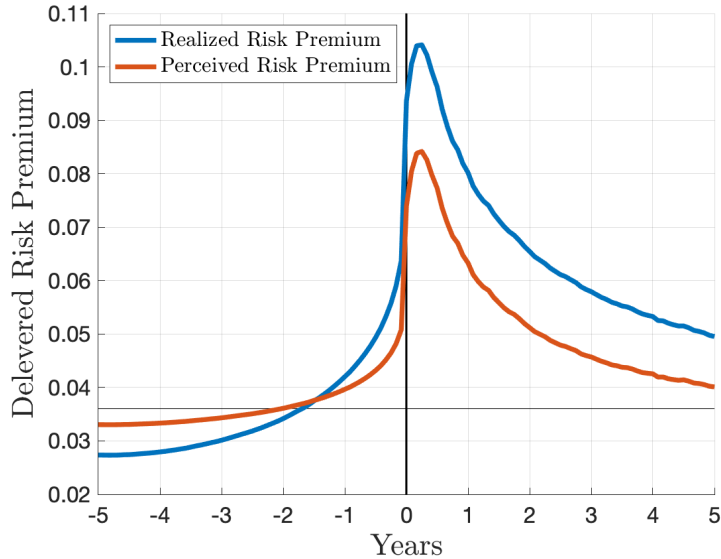


Figure 6: **Risk premia around crises.** Crises first occur at time 0. The blue line plots the average realized risk premium earned by financial intermediaries around crises. The orange line plots the average risk premium perceived by intermediaries. The unconditional mean realized risk premium is marked by the thin horizontal line. All reported risk premia are delevered. This analysis is inspired by [Krishnamurthy and Muir \(2020\)](#).

frictions to financial frictions, this overoptimism amplifies financial fragility by triggering the depletion of intermediary capital capacity.

Figure 6 also shows that sentiment-driven crises are generated by a persistently elevated *level* of sentiment, not a sudden and dramatic *change* of sentiment. In fact, realized risk premia catch up to perceived risk premia roughly 1.5 years before crises hit, a pattern also shown in [Krishnamurthy and Muir \(2020\)](#). More broadly, this aligns with the [Baron et al. \(2021\)](#) finding that crises are the result of a slow-building erosion bank capital.

The spike at $t = 0$ illustrates that both behavioral frictions and financial frictions are needed to replicate the full path of risk premia around crises. As discussed in Section 4.4, the interaction of the two frictions can be described with a “triggers-plus-vulnerabilities” framework ([López-Salido et al., 2017](#)). Elevated sentiment is a trigger. It produces low pre-crisis risk premia and neglected crash risk. However, slow-moving sentiment alone will not generate the sudden spikes in risk premia that flare up during crises. Vulnerability to systemic crashes is driven by financial frictions, with crises erupting when the constraints on financial intermediation bind.

The model’s post-crisis patterns reverse those of the pre-crisis period. The post-crisis

period is characterized by excessive pessimism, so risk premia sit above expectations in the aftermath of crises.

For a related analysis, Appendix Figure 12 compares the average path of investment around financial crises in the DEE and the REE. Investment is higher in the DEE during the pre-crisis period, indicating overoptimism in the crisis buildup. Financial frictions cause investment to crash when crises erupt, and diagnostic expectations amplify this crash as sentiment shifts from overoptimism to overpessimism. As above, the model’s post-crisis patterns reverse those of the pre-crisis period, with depressed sentiment dragging down investment in the aftermath of crises.

5.2 Boom-Bust Investment Cycles

I now turn to studying sentiment-driven macroeconomic fluctuations. Diagnostic expectations affect investment rate i_t , which in turn controls the growth rate of output: $\frac{dY_t}{Y_t} = (i_t - \delta)dt + \sigma dZ_t$.

I use impulse-response functions to study the response of investment to economic shocks. To capture periods of booms and malaise, I simulate the model at a monthly frequency and feed in a three-year sequence of either positive or negative shocks that result in a one standard deviation cumulative shock over three years.²⁶ Shocks are turned off thereafter.

The investment IRFs are provided in Figure 7.²⁷ The red curve plots the DEE and the dashed black curve plots the REE. For comparison, the dotted gray curve plots the investment IRF from a model with diagnostic expectations but without any intermediary capital constraints (i.e., $e \rightarrow \infty$). Together, these three curves show an economy with both financial and behavioral frictions (red), only financial frictions (dashed black), and only behavioral frictions (dotted gray). All economies start from their stochastic steady state at $t = -3$.²⁸

²⁶The monthly shock is set to $\pm \frac{\sigma\sqrt{3}}{12 \times 3}$. Summing gives a 3-year cumulative shock of $\pm\sigma\sqrt{3}$.

²⁷Note that these IRFs depend on the calibration of ζ . As discussed in Section 3.2, ζ governs the extent to which diagnostic expectations are incorporated into asset prices versus the risk-free rate. The baseline calibration sets $\zeta < 1$. This implies that q_t – and accordingly i_t – is increasing in \mathcal{I}_t .

²⁸By turning shocks off from $t = 0$ onward, the IRFs in Figure 7 plot the investment response under one specific sequence of shocks. An alternative is to calculate the expected future path of investment, $\mathbb{E}_0[i_\tau]$. In this nonlinear model these two alternatives are not equivalent. Appendix Figure 14 plots the corresponding IRFs for $\mathbb{E}_0[i_\tau]$ in the DEE and the REE, which are calculated using the Feynman-Kac formula.

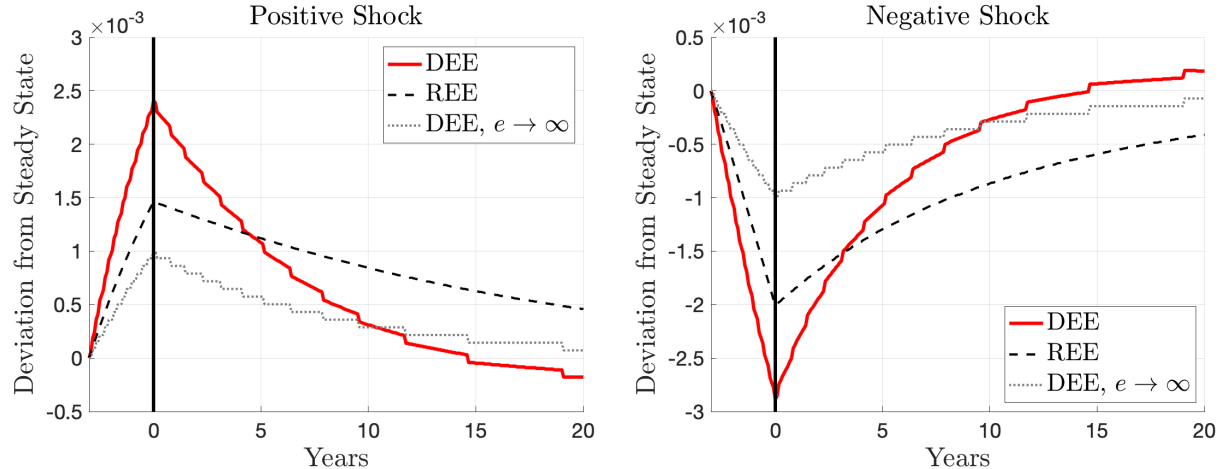


Figure 7: **Investment rate IRFs.** Starting from the stochastic steady state at $t = -3$, a sequence of positive/negative shocks is fed into the system until $t = 0$. The figure plots the response of i_t in the DEE (red), the REE (dashed black), and in a model with diagnostic expectations but without an intermediary capital constraint (dotted gray).

Comparing the DEE to the REE delineates the competing short- and long-run effects of sentiment. Diagnostic expectations promote boom-bust investment dynamics: short-run momentum is amplified, followed by steeper reversals. In the case of positive shocks, the sentiment-driven boom begets its own financial-frictions-driven bust. In the case of negative shocks, the sentiment-driven bust begets its own financial-frictions-driven boom.

First consider investment dynamics in the REE. For positive shocks, the boom from $t = -3$ to $t = 0$ increases e_t . This elevates capital price q_t and investment rate i_t . Since e_t and i_t are both above their steady-state levels when the shocks stop at $t = 0$, they proceed to drift slowly back to the steady state. The opposite holds for negative shocks.

Turning to the DEE, consider the boom-bust pattern of the positive shock case. Positive shocks from $t = -3$ to $t = 0$ now elevate \mathcal{I}_t in addition to e_t , which causes a sharper investment boom until roughly $t = 5$. However, the feedback from behavioral frictions to financial frictions implies that excessive optimism decreases the returns earned by intermediaries from $t = 0$ onward. Over time, this erodes intermediary balance sheets and drags down investment.

The negative shock case produces a bust-boom pattern in the DEE relative to the REE. Negative shocks depress sentiment, which amplifies the short-run drop in investment. But, the sentiment-driven bust also increases the future returns earned by intermediaries. As sentiment recovers, the economy is left with a stronger financial sector that is able to support

higher levels of investment.²⁹

Since the DEE features both financial and behavioral frictions, a natural question is whether the investment response in the DEE is merely the sum of: (i) the IRF from an economy with only financial frictions, plus (ii) the IRF from an economy with only behavioral frictions. Figure 7 shows that this is clearly not the case; the red curve does not equal the sum of the dashed black curve and the dotted gray curve. The difference highlights the interaction between the two frictions. In particular, the feedback from behavioral frictions to financial frictions produces much steeper reversals than either friction individually.

Recent empirical evidence supports the pattern of sentiment-driven boom-bust investment cycles. Gulen et al. (2019) find that overoptimism in year t correlates with a boom in corporate investment over the subsequent year, followed by a long-run contraction. López-Salido et al. (2017) estimate that elevated credit-market sentiment in year t predicts lower investment and GDP growth in year $t + 2$. The long-run feedback from behavioral frictions to financial frictions is also consistent with the observation of Greenwood et al. (2019) that financial fragility arises at the end of economic expansions. Finally, I show in Figure 9 below that these reversals allow the DEE to provide a better fit of empirical investment dynamics.

5.3 Financial Market Stability from Beliefs

This paper identifies a stabilizing role for extrapolative beliefs. Under the baseline calibration, financial crises are less likely to occur when expectations are diagnostic than when expectations are rational.

Figure 8 shows this result visually. The red and dashed black curves (right axis) plot the marginal CDF of state variable e_t in the DEE and the REE. The blue curve (left axis) plots the CDF of the DEE divided by the CDF of the REE. The dotted vertical line at $e \approx 0.4$ marks the boundary of the crisis region. The blue curve crosses 1 to the right of the crisis region. This indicates that the probability of being in a crisis is lower in the DEE than the REE. The blue curve remains above 1 for large values of e , meaning that the DEE also features fewer periods of pronounced financial sector strength.

The stabilizing effect of beliefs can be understood by superimposing the model dynamics

²⁹Figure 7 shows a mildly asymmetric response to positive versus negative shocks. Larger initial shocks produce larger asymmetries (see Appendix Figure 15 for details).

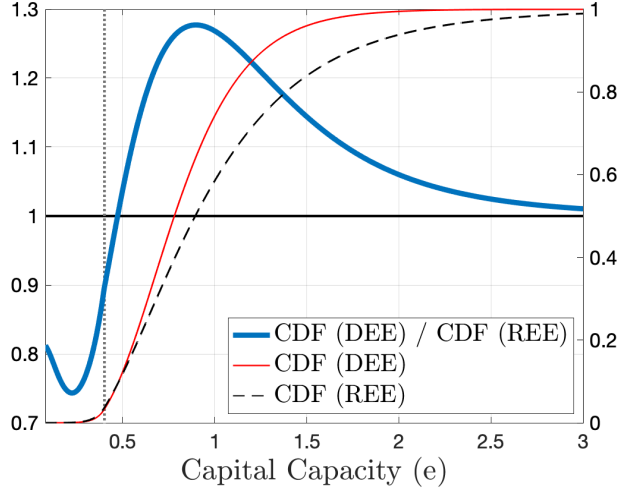


Figure 8: **Financial market stability from beliefs.** The solid red curve and the dashed black curve (right axis) plot the marginal CDF of capital capacity (e) in the DEE and the REE, respectively. The blue curve (left axis) divides the CDF of the DEE by the CDF of the REE. The dotted vertical line at $e \approx 0.4$ marks the boundary of the crisis region.

in Figure 3 onto the stationary distribution in Figure 4. The ergodic distribution shows that financial distress typically coincides with excessive pessimism. When sentiment is depressed, Figure 3 illustrates that the feedback from behavioral frictions to financial frictions safeguards intermediaries by increasing the drift of capital capacity. This limits the potential for initial distress to erupt into a full-blown financial crisis. While it is still the case that the combination of financial distress and elevated sentiment is highly predictive of future financial crises, the ergodic distribution shows that this precarious part of the state space is rarely encountered.

Discussion. Financial market stability may appear at odds with the earlier results of this paper. For example, Section 5.2 documents that diagnostic expectations amplify business cycles. The finding here is that diagnostic expectations stabilize financial markets. Though seemingly contradictory, these results are actually tightly linked: the way that the economy avoids a financial crisis is by going through a sentiment-driven recession. In the case of negative shocks, depressed sentiment amplifies the investment bust, but the feedback effect means that depressed sentiment simultaneously leads to a gradual improvement of capital capacity. Put differently, diagnosticity can produce a recovery on “Wall Street,” but does so by dragging down “Main Street.” This prediction is detailed further in Section 6.1 below.

This finding of financial market stability may also appear to contradict the earlier result

of sentiment-driven crises. Indeed, much of the empirical literature has found that elevated sentiment is predictive of financial market downturns, and concluded from this finding that extrapolative expectations promote financial instability. The model shows that such a conclusion does not necessarily follow from the evidence of sentiment-driven crises.

To reconcile sentiment-driven crises with financial market stability, note that the former is a conditional prediction while the latter is an unconditional prediction. The model's conditional prediction is that crash risk is amplified when financial distress and elevated sentiment occur jointly. However, it is rare for the economy to reach these fragile states. The model's unconditional prediction is that beliefs can stabilize the financial sector, because financial distress is correlated with depressed sentiment.

The goal of this section is not to assert that extrapolative expectations necessarily lower the probability of financial crises, but rather to show that this stabilizing effect of extrapolation is a legitimate theoretical possibility, and one that has been largely neglected to date.³⁰ The identification of a stabilizing role for beliefs highlights a benefit of globally solved economic models, which can be used to compare outcomes from different data generating processes (e.g., DEE versus REE). For the same reason, it is difficult to provide direct empirical evidence on financial market stability from beliefs. Nonetheless, expectations data is consistent with the channel of unanticipated reversals in financial conditions. [Bordalo et al. \(2018\)](#) analyze professional forecasts of the Baa-Treasury credit spread, finding that periods of financial distress reverse faster than forecasters expect. Similarly, [Pflueger et al. \(2020\)](#) document that market risk mean-reverts faster than analysts, options prices, and loan officers expect.

Finally, it is worth emphasizing that the crises that do erupt under diagnostic expectations often feature larger spikes in risk premia and collapses in investment. That is, despite the fact that diagnostic expectations lower the probability of financial crises, the crises that do occur can be more severe at their peak. This is because financial crises often coincide with sentiment turning more pessimistic. Consistent with the analysis of [Gennaioli and Shleifer \(2018\)](#) on the effect of beliefs following the collapse of Lehman Brothers, these negative

³⁰Though diagnostic expectations prevent financial crises under the baseline calibration, this result can be overturned under alternate calibrations, such as those in which the magnitude of perceptual error is increased (see [Appendix B.7](#) for details).

movements in sentiment can amplify the effect of financial frictions at the height of crises. For details, Appendix Figures 12 and 13 examine risk premia and investment around financial crises in the DEE and the REE, and illustrate that diagnostic expectations can lead to sharper crashes in the rare cases when crises do arrive.

6 Evaluating Diagnosticity: The Feedback Effect

The feedback from behavioral frictions to financial frictions is a key mechanism underlying the model’s equilibrium dynamics. This section tests three predictions that arise from this effect. First, the feedback effect produces long-run reversals in economic conditions, which implies that the economy exhibits less persistence under diagnostic expectations than under rational expectations. Second, I use the model’s prediction about how behavioral and financial frictions interact to identify a new fact about which crises are preceded by frothy financial markets. Third, I apply the model to the 2007-2008 Financial Crisis in order to assess the role of diagnostic expectations in shaping the evolution of the crisis.

6.1 Prediction 1: Long-Run Reversals and Economic Persistence

I start by comparing the persistence of macro-financial processes in the model and the data. Since the model’s calibration does not target measures of persistence explicitly, an indicator of success is the extent to which the long-run reversals channel of diagnostic expectations helps to align the model with empirical moments.

In the experiments below, the calibration of the REE is identical to the calibration of the DEE, except for $\theta = 0$. I choose not to recalibrate the REE in order to pinpoint the effect of θ . Results are essentially unchanged if the REE is recalibrated (see Appendix B.8).

The Persistence of Financial Fragility. I begin by studying the persistence of financial fragility in the aftermath of crises. The feedback from behavioral frictions to financial frictions implies that intermediaries’ capital capacity will recover more quickly under diagnostic expectations than under rational expectations, since sentiment is typically overpessimistic following crises.

This crisis-recovery effect is shown in Table 2. Starting from the time that the economy first enters a crisis, Table 2 lists the average number of years that it takes for capital capacity

e_t to recover to its X^{th} percentile.

e_t Percentile	DEE	REE
10	0.93	1.19
25	2.43	4.02
50	5.36	11.27
75	10.76	28.46

Table 2: **Average crisis recovery time (in years)**. The DEE and the REE are simulated at a monthly frequency. For both equilibria, this table lists the average time (in years) that it takes for e_t to recover from a financial crisis to its X^{th} percentile.

The key finding is that intermediaries recover more quickly under diagnostic expectations than under rational expectations. For example, in the DEE it takes an average of 5 years for intermediaries to recover from a crisis to their median level of capitalization, compared to 11 years in the REE. Though there is no direct empirical counterpart to this analysis, the available data is suggestive of recovery times that are consistent with the DEE. [Krishnamurthy and Muir \(2020\)](#) find that credit spreads recover to their mean value between 4 and 5 years after a financial crisis. Similarly, [Muir \(2017\)](#) shows that dividend yields typically recover within 5 years of a crisis.

Two additional points are worth emphasizing. First, economic recoveries from crises are still slow under diagnostic expectations, just not exceedingly slow. Second, faster recoveries for financial intermediaries do not necessarily translate into faster recoveries for the broader macroeconomy. Though excessive pessimism boosts the recovery of intermediaries, this pessimism simultaneously drags down investment and output growth in the aftermath of crises.³¹ As outlined in Section 5.3, diagnostic expectations therefore generate a recovery on “Wall Street” that is dislocated from the recovery on “Main Street.”

Macro-Financial Autocorrelations. The model focuses on financial crises, and abstracts from many macroeconomic considerations at the business cycle frequency. With this caveat in mind, the long-run reversal property can also be examined for broad macro-financial aggregates. I estimate the autocorrelation of the dividend-price ratio and the investment-output ratio using the Jordà-Schularick-Taylor Macrohistory Database for 17

³¹For details see Appendix Figure 12, which compares the average path of investment around financial crises in the DEE and the REE.

developed countries from 1950 – 2016 (Jordà et al., 2019).³² Each ratio is standardized at the country level and then pooled.³³

Figure 9 compares the estimated autocorrelation of the dividend-price ratio and the investment-output ratio (blue) to the corresponding autocorrelations in the DEE (red) and the REE (dashed black). For comparison, the dotted gray curve shows the autocorrelations for an economy with diagnostic expectations but without intermediary capital constraints (i.e., $e \rightarrow \infty$). The REE is too persistent, while the DEE is broadly consistent with the data. As the dotted gray curve shows, this improvement comes even though sentiment itself is highly persistent. Again, this highlights that the improved fit is due to the interaction of behavioral and financial frictions, which produces the long-run reversals needed to align the model with the data.

Bordalo et al. (2020a) provide additional evidence of belief-driven reversals in the dividend-price ratio, documenting that variation in the dividend-price ratio is driven by growth expectations that overreact to news. One may also wonder how diagnostic expectations affect the dynamics of consumption growth, a question that is related to the literature on long-run risks (e.g., Bansal and Yaron, 2004). Appendix Table 6 shows that diagnostic expectations increase the autocorrelation of consumption growth at first, due to short-run amplification, but this effect fades over longer horizons due to long-run reversals.

6.2 Prediction 2: Which Crises Are Preceded by Overheating?

Some crises erupt following periods of relatively robust financial activity (e.g., the 2007-2008 Financial Crisis), while other crises emerge after prolonged periods of financial distress (e.g., the 2011 Eurozone Crisis). In contrast to the REE, the DEE predicts that these two types of crises should be preceded by different levels of pre-crisis sentiment. Specifically, the feedback from behavioral frictions to financial frictions implies that the initial trigger of financial distress is often elevated sentiment and financial market overheating. However, once financial distress has been triggered, the economy can persist in this vulnerable state – sometimes leading to residual crises – even after sentiment has subsided.

³²These ratios are used because they are cointegrated. The concept of dividend-price cointegration is standard in financial economics. For the investment-output ratio, see Cochrane (1994). Post-WWII data is used to account for structural changes to the finance system (Schularick and Taylor, 2012).

³³For robustness, Appendix Figure 16 plots these autocorrelations using just U.S. data.

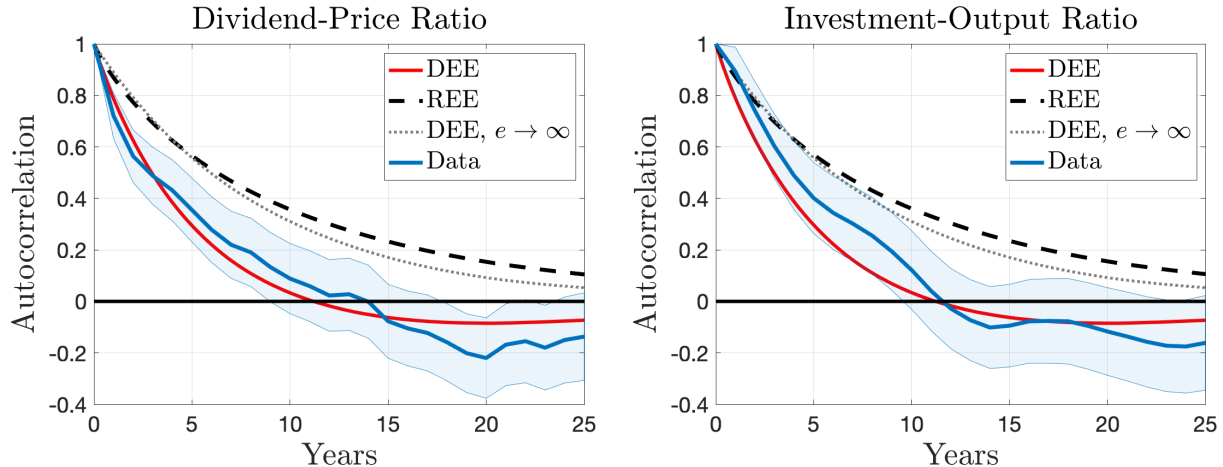


Figure 9: **Persistence: data and model.** The left-hand panel plots the empirical autocorrelation of the dividend-price ratio (blue) as well as the model-implied autocorrelation in the DEE (red), the REE (dashed black), and the model with diagnostic expectations but without an intermediary capital constraint (dotted gray). The right-hand panel conducts an equivalent analysis for the investment-output ratio. The shaded 95% confidence interval is calculated using Bartlett’s formula.

To formalize this prediction, I simulate the model and compare the path of sentiment prior to First Crises versus Residual Crises. I define a Residual Crisis, or double-dip, as a crisis that was preceded by an earlier crisis within the past five years. All other crises are First Crises. In the model, 59% of First Crises are preceded by elevated sentiment ($\mathcal{I} > 0$) in at least one of the three years leading up to the crisis. Alternatively, only 13% of Residual Crises are preceded by elevated sentiment.³⁴

I evaluate this prediction empirically using the Greenwood et al. (2022, henceforth GHSS) dataset, which includes annual financial data across 42 countries from 1950 – 2016. The GHSS dataset contains 33 First Crises and 11 Residual Crises. GHSS define “R-zones” as years in which credit growth is above its 80th percentile and asset price growth is above its 67th percentile, and interpret R-zones as periods of financial market overheating. Matching the DEE’s prediction about which crises are preceded by frothy financial markets, 73% of First Crises (24/33) are preceded by an R-zone in the prior three years, compared to only

³⁴For this analysis, I use the following crisis definition in order to align my model with the Greenwood et al. (2022) dataset that I analyze (details in the next paragraph). A crisis is defined as the equity issuance constraint binding for two consecutive months, and a crisis persists until e_t recovers beyond its 8th percentile. This recovery threshold is set such that when the simulated data is annualized the model produces the same unconditional crisis probability as in the Greenwood et al. (2022) data (4%). With this crisis definition, 66% of crises are First Crises in the model, compared to 75% in the GHSS data.

9% of Residual Crises (1/11).³⁵

This new fact about differential trends in financial markets prior to First versus Residual Crises highlights the importance of developing financial crisis models that include both behavioral and financial frictions. Behavioral frictions allow the model to capture R-zone periods in which sentiment-driven overheating triggers financial distress. But, not all crises are preceded by booms, and slow-moving financial frictions produce long periods of financial distress and occasional double-dips.

6.3 Prediction 3: Elevated Sentiment and the 2007-2008 Financial Crisis

This section applies the model to the 2007-2008 Financial Crisis in order to evaluate the channels through which sentiment influenced the evolution of the crisis.

Measuring Sentiment in the Data. An open question in the diagnostic expectations literature is how to measure sentiment in the data. Proposition 2 provides a simple model-based method. Sentiment can be constructed using forecast errors of economic growth.

Proposition 2. *Let $\sigma d\widehat{Z}_t = \frac{dY_t}{Y_t} - \widehat{\mathbb{E}}_t \frac{dY_t}{Y_t} = -\theta \mathcal{I}_t dt + \sigma dZ_t$ denote the economic growth forecast error at time t . Sentiment \mathcal{I}_t can be rewritten in terms of forecast errors as follows:*

$$\mathcal{I}_t = \int_0^t e^{(-\kappa+\theta)(t-s)} \sigma d\widehat{Z}_s. \quad (24)$$

Proof. See Appendix B.4. □

A feature of equation (24) is that it does not require strong assumptions about the data generating process for the economy. Given a calibration of κ and θ , all that equation (24) requires is forecast errors of output growth.

Figure 10 uses the Survey of Professional Forecasters (SPF) to calculate sentiment from 1970 through 2018. To initialize the calculation, I assume that sentiment equals zero in January 1970. Since SPF forecasts are collected at a quarterly frequency, Figure 10 is calculated using a discrete-time analogue of equation (24) (see Appendix A.2 for details).

³⁵GHSS define R-zones for both businesses and households, and in this analysis I define a crisis as preceded by an R-zone if it was preceded by either a business or a household R-zone. I drop crisis observations that do not have data coverage over the prior three years.

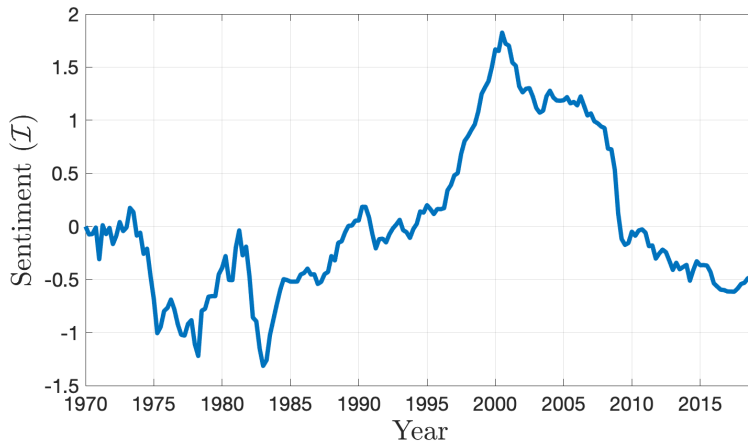


Figure 10: **SPF-measured sentiment**. Sentiment \mathcal{I}_t is measured using the median SPF forecast error from 1970 through 2018 under the model’s baseline calibration. Sentiment is reported in standard deviation units.

Sentiment in Figure 10 captures what [Kindleberger \(1978\)](#) refers to as “displacement”: financial crises are preceded by large positive shocks to economic fundamentals.³⁶ Sentiment builds rapidly during the 1990s economic boom. Though sentiment dips with the bursting of the dot-com bubble in the early 2000s, sentiment remains elevated until the financial crisis.

Simulating the Financial Crisis. I now use the model to evaluate the effect of elevated sentiment on the 2007-2008 Financial Crisis. To simulate the model, I need to choose initial conditions for state variables e_t and \mathcal{I}_t , and I need to choose a sequence of shocks to feed into the model. Typically, the modeler chooses the path of shocks that best aligns their model with the data. In this paper I take a more restrictive approach by calculating shocks externally from SPF forecast errors. That is, rather than asking whether any sequence of shocks can align the model with the data, I instead ask whether a specific sequence of shocks – one that is consistent with surveyed expectations – aligns the model with the data.

Given the measure of sentiment in Figure 10, capital quality shocks can be backed out of forecast errors: $\sigma dZ_t = \sigma \widehat{dZ}_t + \theta \mathcal{I}_t dt$. I use this procedure to calculate the shocks implied by SPF data for diagnostic expectations, and simulate the model conditional on these shocks. Forecast errors place empirical bounds on what can reasonably be considered a shock, and

³⁶[Cao and L’Huillier \(2018\)](#) observe that the three deepest recessions in developed countries all occurred roughly 10 years after periods of rapid technological innovation. [Gorton and Ordoñez \(2020\)](#) find that credit booms start with a positive productivity shock, persist for approximately ten years, and end in a bust when followed by negative productivity shocks.

this paper takes seriously the restrictions that expectations data provide (Manski, 2004).

I start the simulation at the trough of the tech bubble’s collapse in 2002Q4. I condition state variable e_t to $e_{distress}$ (the 33rd percentile of e_t) to broadly reflect the tightness of financial conditions at that time. \mathcal{I}_t is initialized to the 2002Q4 value shown in Figure 10. Proceeding from this initial condition using the shocks calculated from the SPF, the simulation is plotted in Figure 11.

Before presenting the results, I want to note that my initialization of the simulation in 2002Q4 points to a failure of the model. Using the shocks implied by SPF forecast errors, the model cannot jointly fit the 1990s boom and the 2007-2008 Financial Crisis, as the sequence of positive shocks realized during the boom places the financial sector too far above the crisis region for subsequent shocks to generate a crash in 2008. This failure is not surprising. The dot-com crash triggered significant turmoil in financial markets, but had relatively muted effects on the real economy. Because the model features only a single shock process, it cannot capture such differentiation between financial markets and the real economy. My initialization in 2002Q4 can be thought of as applying a single MIT shock to e_t in order to capture the differential effect of the dot-com crash on financial markets. It is also worth emphasizing that while the DEE cannot quite fit this full boom-bust cycle, the DEE still outperforms the REE over this period, as detailed in Appendix B.9.

Turning to the results, the top panel of Figure 11 shows the path of capital capacity e_t in the DEE (red, left axis) and the REE (dashed black, left axis). The gray area marks the crisis region. For comparison, the blue curve (right axis) plots the Intermediary Capital Ratio of He et al. (2017), which serves as an empirical counterpart to capital capacity e_t .

The key result from the simulation is that only the DEE produces a financial crisis. As shown in Section 5.1, elevated sentiment creates neglected crash risk in the background of low risk premium environments. In the simulation, these belief-driven dynamics allow the DEE to generate a financial crisis even though risk premia exhibit no signs of stress ex-ante and realized shocks are moderate. This is not to say that it is impossible to generate similar patterns in the REE, but, rather, that doing so would require a much larger sequence of negative shocks.³⁷ In particular, the divergence of the e_t profiles from 2002 through 2008 shows

³⁷He and Krishnamurthy (2019) reach a similar conclusion when applying their rational model to the 2007-

how a sentiment-driven crisis evolves. Realized shocks are mild over this period, so capital capacity in the REE recovers quickly from initial distress. In the DEE, elevated sentiment implies that risk premia are too low and balance-sheet vulnerability persists throughout the mid-2000s, leaving intermediaries exposed to the negative shocks that hit in 2008.

The middle panel evaluates the model’s ability to replicate patterns in risk premia. This panel plots the realized risk premium earned by intermediaries in the DEE (red, left axis) and the REE (dashed black, left axis), as well as the Baa – 10-year Treasury spread for comparison (blue, right axis). The DEE broadly reproduces the path of risk premia around the crisis. Pre-crisis risk premia are low. This is consistent with the narrow spreads observed prior to the crisis, which many argue were due to neglected risk (e.g., [Gennaioli and Shleifer, 2018](#)). Once the crisis hits, risk premia spike. Because the crisis de-biases expectations, post-crisis risk premia remain persistently higher than pre-crisis risk premia. Alternatively, because the REE never enters a crisis, it exhibits almost no variation in risk premia over the simulated period.

The bottom panel assesses how these movements in risk premia are reflected in beliefs. The red and dashed black curves plot forecast errors in the DEE and the REE, respectively (left axis). Specifically, this figure plots intermediary forecast errors of the delevered risk premium averaged over quarters $t + 1$ through $t + 4$. The blue curve (right axis) plots the corresponding forecast error of the Baa – Treasury spread reported in [Bordalo et al. \(2018\)](#).³⁸ As in the data, the DEE generates large positive forecast errors heading into the crisis, and large negative forecast errors exiting the crisis. The REE produces only modest forecast errors, since risk premia exhibit little variation away from the crisis region in the REE.

2008 Financial Crisis, and show that a “hidden leverage” mechanism can help to amplify financial fragility. My model with diagnostic expectations complements and builds on their conclusion by microfounding non-rational beliefs and systematizing the channels through which sentiment can endogenously trigger neglected risk in financial markets. My examination of a general beliefs mechanism is important, because the neglected risk observed prior to the 2007-2008 Financial Crisis is not unique to that period. Instead, as discussed in the introduction, neglected crash risk is a recurrent pattern in the buildup to financial crises. For further analysis, Appendix B.9 presents the corresponding crisis simulation for a model with “hidden leverage.”

³⁸This data was kindly provided by the authors.

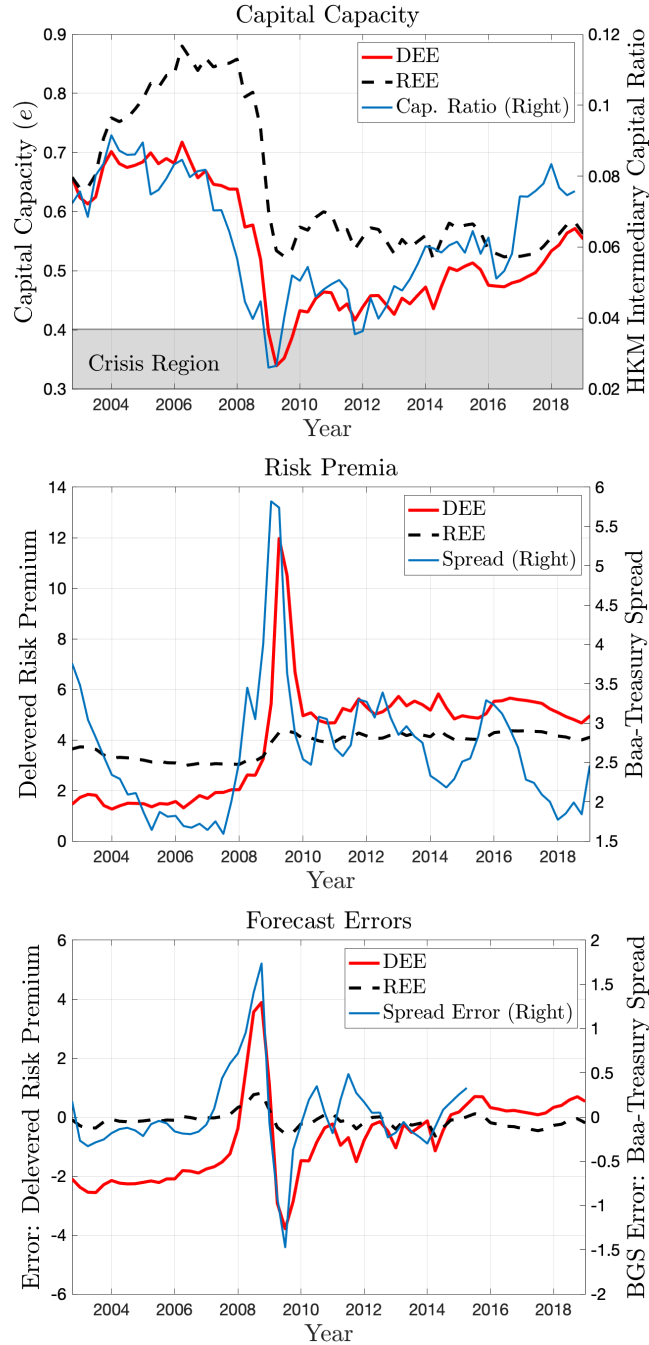


Figure 11: **Simulating the 2007-2008 Financial Crisis.** The sequence of shocks implied by SPF forecast errors is fed into the model from 2002Q4 through 2018Q4. The top panel plots the path of capital capacity e_t in the DEE and the REE (left axis), as well as the corresponding empirical measure from He et al. (2017) (right axis). The middle panel plots the intermediary risk premium in the DEE and the REE (left axis), and the Baa – 10-year Treasury spread (right axis). The bottom panel plots the forecast error of the risk premium averaged over quarters $t + 1$ through $t + 4$ in the DEE and the REE (left axis), and compares it to the credit spread forecast error reported in Bordalo et al. (2018) (right axis).

7 Conclusion

This paper develops a general equilibrium macroeconomic model that combines frictions in financial intermediation with diagnostic expectations. The model examines how the interplay of behavioral and financial frictions drives macro-financial dynamics. When the financial sector is distressed, elevated sentiment amplifies systemic risk and sets the stage for financial crises. For the broader macroeconomy, the conflicting short-run and long-run effect of diagnostic expectations generates endogenous boom-bust patterns in investment and output growth. Even with this business cycle amplification, the long-run reversal effect of diagnostic expectations can inhibit financial crises. Empirical tests support the feedback from behavioral frictions to financial frictions as a channel that improves the model’s fit of macro-financial dynamics.

This paper takes a first step toward integrating diagnostic expectations into models of financial frictions, and there are many interesting pathways for future research. First, the model lends itself to the study of policy interventions in financial markets with non-rational intermediaries.³⁹ Second, the discussion in footnote 11 suggests that extending this paper’s framework to capture key dimensions of heterogeneity in financial intermediation, potentially also allowing for heterogeneous beliefs (e.g., [Ma et al., 2021](#)), is a promising direction for future work. Third, it will be valuable to examine how more complex belief processes, such as one with both slow-moving and high-frequency components, affect economic dynamics.

References

- Adam, Klaus and Sebastian Merkel**, “Stock Price Cycles and Business Cycles,” *SSRN 3455237*, 2019.
- , **Dmitry Matveev, and Stefan Nagel**, “Do Survey Expectations of Stock Returns Reflect Risk Adjustments?,” *Journal of Monetary Economics*, 2020.
- Adrian, Tobias and Markus K. Brunnermeier**, “CoVaR,” *American Economic Review*, 2016, *106* (7), 1705–41.
- **and Nina Boyarchenko**, “Intermediary Leverage Cycles and Financial Stability,” *FRB of New York Staff Report*, 2012, (567).

³⁹See [Davila and Walther \(2021\)](#) and [Fontanier \(2021\)](#) for rich theoretical analyses in this regard.

- Bansal, Ravi and Amir Yaron**, “Risks for the Long Run: A Potential Resolution of Asset Pricing Puzzles,” *The Journal of Finance*, 2004, 59 (4), 1481–1509.
- Barberis, Nicholas**, “Psychology-Based Models of Asset Prices and Trading Volume,” *Handbook of Behavioral Economics-Foundations and Applications 1*, 2018, pp. 79–175.
- , **Robin Greenwood, Lawrence Jin, and Andrei Shleifer**, “X-CAPM: An Extrapolative Capital Asset Pricing Model,” *Journal of Financial Economics*, 2015, 115 (1), 1–24.
- Baron, Matthew and Wei Xiong**, “Credit Expansion and Neglected Crash Risk,” *The Quarterly Journal of Economics*, 2017, 132 (2), 713–764.
- , **Emil Verner, and Wei Xiong**, “Banking Crises Without Panics,” *The Quarterly Journal of Economics*, 2021, 136 (1), 51–113.
- Bernanke, Ben S., Mark Gertler, and Simon Gilchrist**, “The Financial Accelerator in a Quantitative Business Cycle Framework,” *Handbook of Macroeconomics*, 1999, 1, 1341–1393.
- Bianchi, Francesco, Cosmin L. Ilut, and Hikaru Saijo**, “Implications of Diagnostic Expectations: Theory and Applications,” *NBER w28604*, 2021.
- Bordalo, Pedro, Katherine Coffman, Nicola Gennaioli, and Andrei Shleifer**, “Stereotypes,” *The Quarterly Journal of Economics*, 2016, 131 (4), 1753–1794.
- , – , – , **Frederik Schwerter, and Andrei Shleifer**, “Memory and Representativeness,” *Psychological Review*, 2021, 128 (1), 71–85.
- , **Nicola Gennaioli, and Andrei Shleifer**, “Diagnostic Expectations and Credit Cycles,” *The Journal of Finance*, 2018, 73 (1), 199–227.
- , – , – , **and Stephen J. Terry**, “Real Credit Cycles,” *NBER w28416*, 2021.
- , – , **Rafael La Porta, and Andrei Shleifer**, “Diagnostic Expectations and Stock Returns,” *The Journal of Finance*, 2019, 74 (6), 2839–2874.
- , – , – , **and –**, “Expectations of Fundamentals and Stock Market Puzzles,” *NBER w27283*, 2020.
- , – , **Yueran Ma, and Andrei Shleifer**, “Overreaction in Macroeconomic Expectations,” *American Economic Review*, 2020, 110 (9), 2748–82.
- Brunnermeier, Markus K. and Lasse Heje Pedersen**, “Market Liquidity and Funding Liquidity,” *The Review of Financial Studies*, 2009, 22 (6), 2201–2238.

- **and Yuliy Sannikov**, “A Macroeconomic Model with a Financial Sector,” *American Economic Review*, February 2014, *104* (2), 379–421.
- **and –**, “Macro, Money, and Finance: A Continuous-Time Approach,” in “Handbook of Macroeconomics,” Vol. 2, Elsevier, 2016, pp. 1497–1545.
- Caballero, Ricardo J. and Alp Simsek**, “A Risk-Centric Model of Demand Recessions and Speculation,” *The Quarterly Journal of Economics*, 2020, *135* (3), 1493–1566.
- Cao, Dan and Jean-Paul L’Huillier**, “Technological Revolutions and the Three Great Slumps: A Medium-Run Analysis,” *Journal of Monetary Economics*, 2018, *96*, 93–108.
- Chodorow-Reich, Gabriel, Adam M. Guren, and Timothy J. McQuade**, “The 2000s Housing Cycle With 2020 Hindsight: A Neo-Kindlebergerian View,” *NBER w29140*, 2021.
- Cochrane, John H.**, “Permanent and Transitory Components of GNP and Stock Prices,” *The Quarterly Journal of Economics*, 1994, *109* (1), 241–265.
- d’Arienzo, Daniele**, “Maturity Increasing Over-reaction and Bond Market Puzzles,” *SSRN 3733056*, 2020.
- Davila, Eduardo and Ansgar Walther**, “Prudential Policy with Distorted Beliefs,” *SSRN 3694722*, 2021.
- Davis, Morris A. and Stijn Van Nieuwerburgh**, “Housing, Finance, and the Macroeconomy,” *Handbook of Regional and Urban Economics*, 2015, *5*, 753–811.
- Diamond, William and Tim Landvoigt**, “Credit Cycles with Market-Based Household Leverage,” *SSRN 3318481*, 2020.
- Fahlenbrach, Rüdiger, Robert Prilmeier, and René M. Stulz**, “Why Does Fast Loan Growth Predict Poor Performance for Banks?,” *The Review of Financial Studies*, 2017, *31* (3), 1014–1063.
- Farboodi, Maryam and Péter Kondor**, “Rational Sentiments and Economic Cycles,” *NBER w27472*, 2020.
- Farhi, Emmanuel and Iván Werning**, “Taming a Minsky Cycle,” *Mimeo*, 2020.
- Fontanier, Paul**, “Optimal Policy for Behavioral Financial Crises,” *Mimeo*, 2021.
- Fuster, Andreas, Benjamin Hebert, and David Laibson**, “Natural Expectations, Macroeconomic Dynamics, and Asset Pricing,” *NBER Macroeconomics Annual*, 2012, *26* (1), 1–48.

- Gennaioli, Nicola and Andrei Shleifer**, “What Comes to Mind,” *The Quarterly Journal of Economics*, 2010, *125* (4), 1399–1433.
- **and** – , *A Crisis of Beliefs: Investor Psychology and Financial Fragility*, Princeton University Press, 2018.
- Gertler, Mark, Nobuhiro Kiyotaki, and Andrea Prestipino**, “A Macroeconomic Model with Financial Panics,” *The Review of Economic Studies*, 2020, *87* (1), 240–288.
- Gomes, João F., Marco Grotteria, and Jessica Wachter**, “Foreseen Risks,” *NBER w25277*, 2018.
- Gorton, Gary and Guillermo Ordoñez**, “Good Booms, Bad Booms,” *Journal of the European Economic Association*, 2020, *18* (2), 618–665.
- Greenwood, Robin and Andrei Shleifer**, “Expectations of Returns and Expected Returns,” *The Review of Financial Studies*, 2014, *27* (3), 714–746.
- **and Samuel G. Hanson**, “Issuer Quality and Corporate Bond Returns,” *The Review of Financial Studies*, 2013, *26* (6), 1483–1525.
- , – , **and Lawrence J. Jin**, “Reflexivity in Credit Markets,” *NBER w25747*, 2019.
- , – , **Andrei Shleifer, and Jakob Ahm Sørensen**, “Predictable Financial Crises,” *The Journal of Finance*, 2022, *77* (2), 863–921.
- Gulen, Huseyin, Ion Mihai, and Stefano Rossi**, “Credit Cycles and Corporate Investment,” *SSRN 3369295*, 2019.
- He, Zhiguo and Arvind Krishnamurthy**, “A Model of Capital and Crises,” *The Review of Economic Studies*, 2012, *79* (2), 735–777.
- **and** – , “Intermediary Asset Pricing,” *American Economic Review*, 2013, *103* (2), 732–70.
- **and** – , “A Macroeconomic Framework for Quantifying Systemic Risk,” *American Economic Journal: Macroeconomics*, October 2019, *11* (4), 1–37.
- , **Bryan Kelly, and Asaf Manela**, “Intermediary Asset Pricing: New Evidence from Many Asset Classes,” *Journal of Financial Economics*, 2017, *126* (1), 1–35.
- Hirshleifer, David, Jun Li, and Jianfeng Yu**, “Asset Pricing in Production Economies with Extrapolative Expectations,” *Journal of Monetary Economics*, 2015, *76*, 87–106.
- Jordà, Òscar, Katharina Knoll, Dmitry Kuvshinov, Moritz Schularick, and Alan M. Taylor**, “The Rate of Return on Everything, 1870–2015,” *The Quarterly Journal of Economics*, 2019, *134* (3), 1225–1298.

- Khorrami, Paymon and Fernando Mendo**, “Rational Sentiments and Financial Frictions,” 2021.
- Kindleberger, Charles P.**, *Manias, Panics and Crashes: a History of Financial Crises*, Basic Books, 1978.
- Kiyotaki, Nobuhiro and John Moore**, “Credit Cycles,” *Journal of Political Economy*, 1997, 105 (2), 211–248.
- Krishnamurthy, Arvind and Tyler Muir**, “How Credit Cycles across a Financial Crisis,” *NBER w23850*, 2020.
- **and Wenhao Li**, “Dissecting Mechanisms of Financial Crises: Intermediation and Sentiment,” *NBER w27088*, 2021.
- Li, Wenhao**, “Public Liquidity and Financial Crises,” *SSRN 3175101*, 2020.
- López-Salido, David, Jeremy C. Stein, and Egon Zakrajšek**, “Credit-Market Sentiment and the Business Cycle,” *The Quarterly Journal of Economics*, 2017, 132 (3), 1373–1426.
- L’Huillier, Jean-Paul, Sanjay R. Singh, and Donghoon Yoo**, “Diagnostic Expectations and Macroeconomic Volatility,” *Mimeo*, 2021.
- Ma, Yueran, Teodora Paligorova, and José-Luis Peydro**, “Expectations and Bank Lending,” *Mimeo*, 2021.
- Maggiore, Matteo**, “Financial Intermediation, International Risk Sharing, and Reserve Currencies,” *American Economic Review*, 2017, 107 (10), 3038–71.
- Manski, Charles F.**, “Measuring Expectations,” *Econometrica*, 2004, 72 (5), 1329–1376.
- Mian, Atif, Amir Sufi, and Emil Verner**, “Household Debt and Business Cycles Worldwide,” *The Quarterly Journal of Economics*, 2017, 132 (4), 1755–1817.
- Minsky, Hyman P.**, “The Financial Instability Hypothesis: An Interpretation of Keynes and an Alternative to ‘Standard’ Theory,” *Challenge*, 1977, 20 (1), 20–27.
- Moreira, Alan and Alexi Savov**, “The Macroeconomics of Shadow Banking,” *The Journal of Finance*, 2017, 72 (6), 2381–2432.
- Muir, Tyler**, “Financial Crises and Risk Premia,” *The Quarterly Journal of Economics*, 2017, 132 (2), 765–809.
- Nagel, Stefan and Zhengyang Xu**, “Dynamics of Subjective Risk Premia,” *Mimeo*, 2021.

- and —, “Asset Pricing with Fading Memory,” *The Review of Financial Studies*, 2022, 35 (5), 2190–2245.
- Pflueger, Carolin, Emil Siriwardane, and Adi Sunderam**, “Financial Market Risk Perceptions and the Macroeconomy,” *The Quarterly Journal of Economics*, 2020, 135 (3), 1443–1491.
- Schularick, Moritz and Alan M. Taylor**, “Credit Booms Gone Bust: Monetary Policy, Leverage Cycles, and Financial Crises, 1870–2008,” *American Economic Review*, 2012, 102 (2), 1029–61.
- Tella, Sebastian Di**, “Uncertainty Shocks and Balance Sheet Recessions,” *Journal of Political Economy*, 2017, 125 (6), 2038–2081.
- Tversky, Amos and Daniel Kahneman**, “Extensional Versus Intuitive Reasoning: The Conjunction Fallacy in Probability Judgment,” *Psychological Review*, 1983, 90 (4), 293.
- Wachter, Jessica A. and Michael J. Kahana**, “A Retrieved-Context Theory of Financial Decisions,” *SSRN 3333248*, 2020.
- Woodford, Michael**, “Macroeconomic Analysis without the Rational Expectations Hypothesis,” *Annual Review of Economics*, 2013, 5 (1), 303–346.

Appendix

Appendix Contents. Appendix [A](#) presents the continuous-time specification of diagnostic expectations used in this paper. Appendix [B](#) provides model details, proofs, and additional results. Appendix [C](#) describes the equilibrium derivation, and Appendix [D](#) outlines the numerical methods used to solve the model. Appendix [E](#) gives additional details and extensions for this paper’s model of diagnostic expectations, including a discrete-time formulation.

A Diagnostic Expectations Appendix

A.1 Diagnostic Expectations in Continuous Time

This section provides a microfoundation for the reduced-form expectations process outlined in Section [2.2](#). A goal for this paper’s model of diagnostic expectations is to be a portable extension of existing models [“PEEMish”]([Rabin, 2013](#)), and it is designed such that rational models can be augmented with diagnostic expectations using a single additional state variable.

Diagnostic expectations are applied to the log of the capital stock. Log capital evolves according to $dk_t = (i_t - \delta - \frac{\sigma^2}{2})dt + \sigma dZ_t$. Diagnostic expectations are applied to log capital for two reasons. Psychologically, it is consistent with Weber’s Law that shocks are perceived as percentage changes rather than level changes. Mathematically, working with log capital ensures that \mathcal{I}_t is stationary because the diffusion coefficient for log capital is constant.

Step 1: Defining the Background Context. Following the terminology of [Bordalo et al. \(2018\)](#), henceforth BGS), the first step is to define the “background context” for capital. The background context is a counterfactual level of the log capital stock that forms the dynamic “reference class” used to characterize representativeness.

The background context reflects the absence of recent information. Equation [\(3\)](#) introduces $\mathcal{I}_t \equiv \int_0^t e^{-\kappa(t-s)} \sigma dZ_s$ as a measure of recent information. This implies the following definition of the background context.

Definition 3. Let G_t^- denote the background context of log capital at time t . G_t^- is defined

as follows:

$$G_t^- = k_t - \mathcal{I}_t.$$

Step 2: Modeling Expectations Given the Background Context. The next step is to specify how agents form expectations. The current period is t . Because time is continuous, expectations must be specified for all future periods $t + \tau$, where $\tau > 0$. Let $h(k_{t+\tau}|k_t, e_t, \mathcal{I}_t)$ denote the true distribution of log capital at time $t + \tau$ conditional on current state variables k_t , e_t , and \mathcal{I}_t . Let $h(k_{t+\tau}|G_t^-, e_t, \mathcal{I}_t)$ denote the true distribution of log capital at time $t + \tau$ conditional on state variables e_t and \mathcal{I}_t , but now using counterfactual log capital level G_t^- .

Let $k'_{t+\tau}$ denote one possible realization of log capital at time $t + \tau$. Following BGS and Gennaioli and Shleifer (2010), the “representativeness” of future state $k'_{t+\tau}$ is given by the following likelihood ratio:

$$\frac{h(k'_{t+\tau}|k_t, e_t, \mathcal{I}_t)}{h(k'_{t+\tau}|G_t^-, e_t, \mathcal{I}_t)}. \quad (25)$$

The most representative states are the ones exhibiting the largest increase in likelihood based on recent information.

One difficulty with equation (25) is that little is known about distributions $h(k'_{t+\tau}|k_t, e_t, \mathcal{I}_t)$ and $h(k'_{t+\tau}|G_t^-, e_t, \mathcal{I}_t)$ because k_t is an endogenous process.⁴⁰ This difficulty is overcome by using an instantaneous prediction horizon of $\tau = dt$. Because k_t is an Itô process it is instantaneously Gaussian. Taking $\tau \rightarrow dt$, $h(k'_{t+dt}|k_t, e_t, \mathcal{I}_t) = \mathcal{N}\left(k_t + \left[i_t - \delta - \frac{\sigma^2}{2}\right] dt, \sigma^2 dt\right)$ and $h(k'_{t+dt}|G_t^-, e_t, \mathcal{I}_t) = \mathcal{N}\left(G_t^- + \left[i_t - \delta - \frac{\sigma^2}{2}\right] dt, \sigma^2 dt\right)$. I now define diagnostic expectations over prediction horizon $\tau = dt$. The prediction horizon will be extended iteratively in Step 3.

Diagnostic expectations overweight states that are representative of recent news. This is formalized by assuming that agents evaluate future levels of log capital “as if” capital follows

⁴⁰This is in contrast to BGS, where expectations are only specified for exogenous AR(N) processes.

the distorted density:

$$h_t^\theta(k'_{t+dt}|k_t, e_t, \mathcal{I}_t) = h(k'_{t+dt}|k_t, e_t, \mathcal{I}_t) \cdot \left[\frac{h(k'_{t+dt}|k_t, e_t, \mathcal{I}_t)}{h(k'_{t+dt}|G_t^-, e_t, \mathcal{I}_t)} \right]^{\theta dt} \frac{1}{Z}. \quad (26)$$

Equation (26) modifies a similar formula in BGS. The key adjustment for continuous time is that equation (26) defines expectations at $t + dt$, while the discrete-time formulation of BGS defines expectations at $t + 1$.

In equation (26), the true conditional probability $h(k'_{t+dt}|k_t, e_t, \mathcal{I}_t)$ is distorted by the representativeness term in brackets. The extent to which representativeness distorts expectations is governed by parameter θ . θ is scaled by the prediction horizon dt because representativeness should impose only an infinitesimal distortion on the perceived distribution of capital over an infinitesimally short horizon. Otherwise, the agent would expect that k_t jumps discontinuously between t and $t + dt$.

Using equation (26), the following proposition illustrates that judging by representativeness biases the perceived growth rate of capital by $\theta \mathcal{I}_t$.

Proposition 3. *A diagnostic agent perceives that capital evolves according to:*

$$\frac{d\widehat{K}_t}{K_t} = (i_t - \delta)dt + \theta \mathcal{I}_t dt + \sigma dZ_t. \quad (27)$$

Proof. See Appendix B.4. □

Step 3: The Evolution of Beliefs. Step 1 defines the background context G_t^- and Step 2 specifies diagnostic expectations of \widehat{dK}_t . Step 3 models the dynamics of expectations over longer horizons. Because capital is endogenous, future expectations are defined iteratively. In particular, repeated applications of the instantaneous Gaussian properties of k_t can be used to define expectations of the economy at $t + dt$, then $t + 2dt$, then $t + 3dt$, etc. This iterative procedure imposes that the law of iterated expectations holds with respect to distorted expectations, consistent with the BGS model.

Diagnostic agents form expectations by simulating the economy forward state-by-state. As the diagnostic agent simulates the economy forward from time t , the internal representa-

tiveness parameter at simulated future time $t + \tau$ is given by:

$$\begin{aligned}\mathcal{I}_{t+\tau}^S &\equiv \int_0^t e^{-\kappa(t+\tau-s)} \sigma dZ_s, \text{ or equivalently} \\ &= e^{-\kappa\tau} \mathcal{I}_t.\end{aligned}\tag{28}$$

The superscript S , for simulated, is used to signify that $\mathcal{I}_{t+\tau}^S$ is the agent's unconscious internal representativeness state as the agent forms expectations of the economy in period $t + \tau$. Information that is representative about time t decays at rate κ as the perceived economy is simulated forward in time.

Let $k'_{t+\tau}$ and $e'_{t+\tau}$ denote one possible realization of log capital and capital capacity at time $t + \tau$. Using equation (28), the simulated background context at $t + \tau$ can now be defined in an analogous fashion to Definition 3.

Definition 4. Let $k'_{t+\tau}$ denote some simulated level of log capital at future time $t + \tau$. Given $k'_{t+\tau}$, the simulated background context at time $t + \tau$ is defined as follows:

$$G'_{t+\tau} = k'_{t+\tau} - \mathcal{I}_{t+\tau}^S.$$

As above, the simulated future background context reflects the absence of recent information.

Again proceeding in an analogous fashion to Step 2, at time $t + \tau$ the agent iteratively forms expectations about $t + \tau + dt$ “as if” capital follows:

$$h_t^\theta(k'_{t+\tau+dt} | k'_{t+\tau}, e'_{t+\tau}, \mathcal{I}_{t+\tau}^S) = h(k'_{t+\tau+dt} | k'_{t+\tau}, e'_{t+\tau}, \mathcal{I}_{t+\tau}^S) \cdot \left[\frac{h(k'_{t+\tau+dt} | k'_{t+\tau}, e'_{t+\tau}, \mathcal{I}_{t+\tau}^S)}{h(k'_{t+\tau+dt} | G'_{t+\tau}, e'_{t+\tau}, \mathcal{I}_{t+\tau}^S)} \right]^{\theta dt} \frac{1}{Z}.\tag{29}$$

It follows that the diagnostic agent perceives that capital evolves according to:

$$\widehat{\frac{dK'_{t+\tau}}{K'_{t+\tau}}} = (i_{t+\tau} - \delta)dt + \theta \mathcal{I}_{t+\tau}^S dt + \sigma dZ_{t+\tau}.\tag{30}$$

The expectations in equation (30) should be contrasted with those of a rational agent who correctly believes that capital evolves according to $\frac{dK'_{t+\tau}}{K'_{t+\tau}} = (i_{t+\tau} - \delta)dt + \sigma dZ_{t+\tau}$. Since

$\mathcal{I}_{t+\tau}^S = e^{-\kappa\tau}\mathcal{I}_t$, equation (30) specifies that the effect of diagnostic expectations on the perceived growth rate of capital fades at rate κ as the agent simulates the evolution of the economy further into the future. This is because diagnostic expectations capture the overweighting of states that are representative of current economic conditions. As the agent looks further temporally ahead, information that is diagnostic of economic conditions at time t steadily dims.

It is worth noting that equation (30) only stipulates that the effect of sentiment on the perceived drift of $k_{t+\tau}$ fades as τ grows. Since the drift has a cumulative effect on the level of $k_{t+\tau}$, diagnostic expectations of the level of $k_{t+\tau}$ can diverge increasingly from rational expectations as τ increases (e.g., Figure 1).

Summary. This completes the microfoundation of the reduced-form beliefs process presented in Section 2.2. Extensions are given in Appendix E.3. Appendices E.1 and E.2 discuss how this paper’s expectations model relates to the original BGS model.

To summarize, expectations of the endogenous capital process are formed iteratively in order to make repeated use of the instantaneous Gaussian properties of $dk_{t+\tau}$. Step 2 defines how \mathcal{I}_t affects the expected evolution of the economy from t to $t+dt$. Step 3 then defines how $\mathcal{I}_{t+\tau}^S$ evolves as expectations are simulated forward. In detail, Step 2 takes k_t, e_t, \mathcal{I}_t as given and provides a perceived mapping into \widehat{k}_{t+dt} and \widehat{e}_{t+dt} given shock dZ_t . The hat-notation indicates that agents may not properly understand the evolution of these state variables. Step 3 takes \mathcal{I}_t as given and provides \mathcal{I}_{t+dt}^S . Then, Step 2 is applied again (now taking $\widehat{k}_{t+dt}, \widehat{e}_{t+dt}$, and \mathcal{I}_{t+dt}^S as given) to calculate \widehat{k}_{t+2dt} and \widehat{e}_{t+2dt} given shocks dZ_t and dZ_{t+dt} . Applying Step 3 again gives \mathcal{I}_{t+2dt}^S . This process is repeated to generate expectations at time $t + \tau$, for all $\tau > 0$.

Diagnostic agents make two mistakes when $\theta > 0$. First, they hold incorrect beliefs about the drift of capital. Second, they have incorrect expectations about their own future expectations because they do not understand that they are diagnostic. In particular, a comparison of equations (3) and (28) shows that diagnostic agents do not perceive that future capital quality shocks will alter the bias of their own future expectations.⁴¹

⁴¹Put differently, the realized future information parameter $\mathcal{I}_{t+\tau}$ is a random variable at time t whereas $\mathcal{I}_{t+\tau}^S$ is deterministic at time t .

I end by discussing why this paper’s model of diagnostic expectations can serve as a portable extension of existing rational models. First, equations (27) and (30) illustrate that state variable \mathcal{I}_t alone is sufficient to characterize the state of expectations relative to rationality. Second, the evolution of \mathcal{I}_t is self-contained. \mathcal{I}_t can be expressed in differential form as $d\mathcal{I}_t = -\kappa\mathcal{I}_t dt + \sigma dZ_t$. Thus, state variable \mathcal{I}_t plus the shock σdZ_t are sufficient to calculate $d\mathcal{I}_t$. It is these two attributes that make this paper’s formulation of diagnostic expectations portable: \mathcal{I}_t alone characterizes expectations relative to rationality, and \mathcal{I}_t is sufficient for its own evolution.

A.2 Diagnostic Expectations Calibration and Application

θ Calibration. The baseline calibration sets θ such that one standard deviation in \mathcal{I} corresponds to an output growth bias of 0.75 percentage points. The magnitude of this bias aligns with the estimates in Bordalo et al. (2018, henceforth BGS), Bordalo et al. (2019, BGLS), Bordalo et al. (2020, BGMS), Bordalo et al. (2021, BGST), and d’Arienzo (2020).

Using data from 1968Q4 through 2016Q4, BGMS assume that the realized annual growth rate of real GDP follows an AR(1) process: $x_t = \rho x_{t-1} + u_t$. BGMS estimate $\rho = 0.87$ and $\sigma_u = 1.10$. Let θ_D denote the representativeness parameter for the discrete-time specification of diagnostic expectations developed in BGS. The BGS model of diagnostic expectations applied to an AR(1) process predicts that in period t , the forecast of x_{t+1} is biased by $\theta_D \rho u_t$ (see BGS). Using the BGMS estimates of ρ and σ_u , a one standard deviation output growth bias of 0.75 percentage points corresponds to $\theta_D = 0.78$.⁴² This is consistent with the estimates of θ_D provided in BGS ($\theta_D = 0.91$), BGMS (estimates vary, with a single collective estimate of $\theta_D = 0.50$), BGLS ($\theta_D = 0.90$), BGST ($\theta_D = 0.99$), and d’Arienzo (2020) (two estimates: $\theta_D = 0.73$ and $\theta_D = 1.05$).

Calculating Sentiment with Expectations Data. This section details how to construct an empirical measure of sentiment given a calibration of κ and θ . This construction is used to calibrate κ , to calculate the empirical measure of sentiment shown in Figure 10, and to calculate the SPF-implied shocks used in Figure 11.

Sentiment is constructed using the median forecast of real GDP growth from the Survey

⁴²Setting $0.75 = \theta \times 0.87 \times 1.1$ yields the desired result.

of Professional Forecasters (SPF).⁴³ Let FE_t^{SPF} denote the SPF forecast error in quarter t . I define the forecast error in quarter t as the realized GDP growth rate in quarter t minus the median quarter $t - 2$ forecast of the GDP growth rate in quarter t . The forecast error is defined with a two-quarter lagged prediction to account for the slow incorporation of shocks into GDP statistics (e.g., Lehman Brothers declared bankruptcy near the end of 2008Q3, and U.S. GDP collapsed in 2008Q4).

Proposition 2 provides a method for calculating sentiment using subjective shocks to economic growth. SPF forecast data is collected quarterly while equation (24) is written in continuous time. Equation (24) can be discretized at a quarterly frequency as follows:

$$\mathcal{I}_t = \sum_{j=0}^{t-1} \left(\mathcal{K} + \frac{\theta}{4} \right)^j FE_{t-1-j}^{SPF}, \quad (31)$$

where $\mathcal{K} = e^{-\kappa/4}$. A derivation of equation (31) is provided below.

Equation (31) needs to be initialized with a “period 0.” I assume that sentiment is equal to 0 in 1970Q1. Starting from this initial condition, equation (31) provides a method for constructing sentiment using quarterly SPF forecast errors. These forecast errors, along with the measure of sentiment in Figure 10, are also used to calculate the shocks simulated in Figure 11.

κ Calibration. Sentiment persistence parameter κ is calibrated to align the model-implied correlation between e_t and \mathcal{I}_t with the data. Equation (31) provides a technique for calculating sentiment from SPF forecast data given a calibration of κ and θ . He et al. (2017) provide an empirical measure corresponding to e_t over the period 1970Q1 to 2018Q3. For any given κ and θ , this means that I can calculate the correlation between e_t and \mathcal{I}_t in both the data and the model. This analysis is presented in Figure 1 below, which suggests that sentiment should have a half-life of approximately 6 years.⁴⁴

Discretization of the Model: Derivation of Equation (31). I partially rewrite the model in discrete time. The discrete-time model is written at a quarterly frequency for

⁴³Expert forecasts are used for consistency with the model.

⁴⁴As κ is varied, θ is always set to $\frac{(\sqrt{2\kappa})^{0.0075}}{\sigma}$. This maintains the other calibration target that one standard deviation in \mathcal{I} corresponds to an output growth bias of 0.75 percentage points.

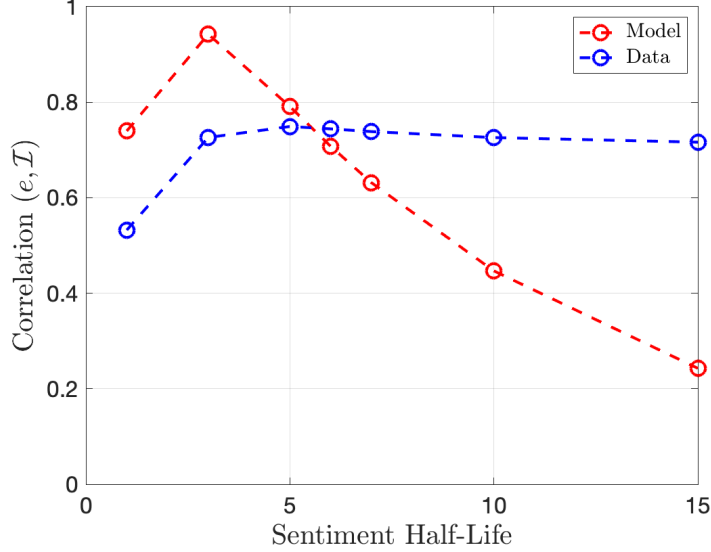


Figure 1: **Calibration of κ .** The red curve plots the correlation between e_t and \mathcal{I}_t in the model as a function of κ . The blue curve plots the empirical correlation between e_t (from He et al. (2017)) and \mathcal{I}_t (calculated from SPF forecast errors given κ and θ).

consistency with SPF data. Subscript t 's denote model periods, such that period $t + 1$ occurs one quarter after period t .

Define the capital law of motion as $K_{t+1} = K_t \exp(v_t + \sigma\epsilon_{t+1})$, where $\sigma\epsilon_t$ are quarterly capital quality shocks, v_t captures investment and depreciation, and $\epsilon_t \sim \mathcal{N}(0, \frac{1}{4})$.

Next, I introduce the analogous discrete-time definition of sentiment:

$$\mathcal{I}_t = \sum_{j=0}^{t-1} \mathcal{K}^j \sigma\epsilon_{t-j}, \quad (32)$$

where $\mathcal{K} = e^{-\kappa/4}$. Let k_t and y_t denote the log of capital and output, respectively. Under

diagnostic expectations, agents expect that output (or capital) evolves as follows:⁴⁵

$$\widehat{\mathbb{E}}_t [y_{t+1} - y_t] = \mathbb{E}_t [y_{t+1} - y_t] + \frac{\theta \mathcal{I}_t}{4}.$$

Analogous to equation (5), diagnostic expectations of GDP growth consist of an actual component plus a diagnostic wedge. The dt factor in equation (5) becomes $\frac{1}{4}$ here since the model is discretized at a quarterly frequency.

At a quarterly frequency, subjective shocks are defined as

$$\sigma \widehat{\epsilon}_{t+1} \equiv [y_{t+1} - y_t] - \widehat{\mathbb{E}}_t [y_{t+1} - y_t],$$

i.e., the difference between the true and the (diagnostically) expected growth rate of GDP. Unlike objective shocks $\sigma \epsilon_t$, these subjective shocks are directly observable with expectations data. Moreover, the above equations imply:

$$\sigma \widehat{\epsilon}_{t+1} = \sigma \epsilon_{t+1} - \frac{\theta \mathcal{I}_t}{4}.$$

Equation (32) can now be redefined in terms of subjective shocks. It follows from equation (32) that $\mathcal{I}_t = \mathcal{K} \mathcal{I}_{t-1} + \sigma \epsilon_t$. Plugging in the definition of subjective shocks gives

$$\mathcal{I}_t = \left(\mathcal{K} + \frac{\theta}{4} \right) \mathcal{I}_{t-1} + \sigma \widehat{\epsilon}_t.$$

⁴⁵In logs, the law of motion for capital is $k_{t+1} = k_t + v_t + \sigma \epsilon_{t+1}$. Let $G_t^- = k_t - \mathcal{I}_t$. In discrete time, equation (26) becomes:

$$h_t^\theta(k'_{t+1} | k_t, e_t, \mathcal{I}_t) = h(k'_{t+1} | k_t, e_t, \mathcal{I}_t) \cdot \left[\frac{h(k'_{t+1} | k_t, e_t, \mathcal{I}_t)}{h(k'_{t+1} | G_t^-, e_t, \mathcal{I}_t)} \right]^{\frac{\theta}{4}} \frac{1}{Z}.$$

The main difference relative to equation (26) is that the power term of θdt becomes $\frac{\theta}{4}$ here, since the model is specified at a quarterly frequency. Since $k_{t+1} | k_t, e_t, \mathcal{I}_t \sim \mathcal{N}\left(k_t + v_t, \frac{\sigma^2}{4}\right)$ and $k_{t+1} | G_t^-, e_t, \mathcal{I}_t \sim \mathcal{N}\left(G_t^- + v_t, \frac{\sigma^2}{4}\right)$, a similar argument to that of Appendix B.4 gives $\widehat{\mathbb{E}}_t [k_{t+1} - k_t] = v_t + \frac{\theta \mathcal{I}_t}{4}$.

Iterating backward and using the initial condition that $\mathcal{I}_0 = 0$ yields:

$$\mathcal{I}_t = \sum_{j=0}^{t-1} \left(\mathcal{K} + \frac{\theta}{4} \right)^j \sigma_{\hat{\epsilon}_{t-j}}.$$

Equation (31) is recovered by noting that $\sigma_{\hat{\epsilon}_t} = FE_{t-1}$. The difference in timing follows since $\sigma_{\hat{\epsilon}_t}$ is the forecast error realized from the start of period $t - 1$ to the start of period t .⁴⁶

⁴⁶In other words, $\sigma_{\hat{\epsilon}_t}$ is the forecast error that is realized over quarter $t - 1$.

B Model Details

B.1 Labor Income

Labor Income Microfoundation. The treatment here of Frankel (1962) follows from Aghion and Howitt (2008, Chapter 2). Each individual producer faces decreasing returns to capital, but decreasing returns at the producer level are offset at the aggregate level through knowledge externalities.

At time t , there exists a measure \mathbb{J}_t of intermediaries.⁴⁷ Each intermediary j operates $K_{j,t}$ units of capital and hires $L_{j,t}$ units of labor at time t . The intermediary faces the production function:

$$Y_{j,t} = \bar{A}_t K_{j,t}^\nu L_{j,t}^{1-\nu}, \quad (33)$$

where \bar{A}_t is an endogenous aggregate productivity level. Due to knowledge spillovers, \bar{A}_t depends on the total amount of capital in the economy:

$$\bar{A}_t = A \left(\int_j K_{j,t} dj \right)^\varsigma. \quad (34)$$

Parameter $\varsigma \in [0, 1]$ controls the level of knowledge externalities.

Let \mathcal{W}_t denote the wage rate. Intermediaries hire labor as follows:

$$L_{j,t} = \operatorname{argmax}_\ell \bar{A}_t K_{j,t}^\nu \ell^{1-\nu} - \mathcal{W}_t \ell.$$

The optimal labor choice is:

$$L_{j,t} = K_{j,t} \left(\frac{\bar{A}_t (1-\nu)}{\mathcal{W}_t} \right)^{\frac{1}{\nu}}. \quad (35)$$

The next step is to impose market clearing. Specifically, $\int_j K_{j,t} dj = K_t$ and $\int_j L_{j,t} dj = 1$. Since all intermediaries are identical, $K_{j,t} = \frac{K_t}{\mathbb{J}_t}$ and $L_{j,t} = \frac{1}{\mathbb{J}_t}$. Imposing market clearing

⁴⁷In the model, there is always a unit measure of households. The size of the financial intermediary sector can vary over time due to banker entry and exit.

gives:

$$\begin{aligned}
\bar{A}_t &= AK_t^\varsigma, \text{ and} \\
Y_t &= \int_j Y_{j,t} dj = AK_t^\varsigma \int_j K_{j,t}^\nu L_{j,t}^{1-\nu} dj \\
&= AK_t^\varsigma \mathbb{J}_t \left(\frac{K_t}{\mathbb{J}_t} \right)^\nu \left(\frac{1}{\mathbb{J}_t} \right)^{1-\nu} \\
&= AK_t^{\varsigma+\nu}.
\end{aligned}$$

The following parameter restriction generates aggregate linearity:

$$\varsigma + \nu = 1. \tag{36}$$

Assumption (36) recovers an “AK” economy with a linear aggregate production function $Y_t = AK_t$, as in the main text.

The final step is to use the market clearing conditions to solve for the wage rate. Plugging these into equation (35):

$$\begin{aligned}
\frac{1}{\mathbb{J}_t} &= \frac{K_t}{\mathbb{J}_t} \left(\frac{AK_t^\varsigma (1-\nu)}{\mathcal{W}_t} \right)^{\frac{1}{\nu}} \\
\mathcal{W}_t &= AK_t^{\varsigma+\nu} (1-\nu) \\
\mathcal{W}_t &= (1-\nu) AK_t,
\end{aligned} \tag{37}$$

where the last line follows from (36). The knowledge externalities model built here provides a simple microfoundation for equation (11) in the main text. The benefits of introducing a labor income margin are discussed below.

Quantitative Benefits of the Labor Income Margin. This model’s benchmark calibration sets $A = \frac{1}{3}$ and $\nu = 0.4$. The original HK model, which does not feature labor income, sets $A = 0.133$.⁴⁸ Since the average investment rate is roughly 10%, $A = 0.133$ implies that investment typically accounts for more than $\frac{2}{3}$ of the economy’s output in the

⁴⁸The labor income channel in this model can be shut down by setting $\nu = 1$.

original HK model. Consumption accounts for less than $\frac{1}{3}$ of output. Though some parsimony of the original HK model is lost, the upside of introducing a simple labor income margin is that it allows for a more realistic consumption-output share.

Generating a realistic consumption-output ratio yields two benefits. First, it allows for a more standard calibration of EIS parameter ζ . In the HK model, consumption accounts for only a small share of output. This implies that changes to the investment rate will cause consumption growth to swing wildly. This is particularly true in periods of financial distress, when the investment rate is sensitive to e_t . HK calibrate $\zeta = 0.13$ (EIS > 7) in order to prevent these swings in consumption from generating excessive interest rate volatility.

Second, the labor income extension generates a more realistic ratio of housing expenditures to total consumption. Recall that aggregate consumption is a Cobb-Douglas aggregator over the output good and housing services: $C_t = (c_t^y)^{1-\phi}(c_t^h)^\phi$. Parameter ϕ governs the ratio of housing expenditures to total consumption. To match the housing-wealth ratio of 45%, HK set $\phi = 0.6$. This implies that housing services compose 60% of expenditures. In order to match the same housing-wealth ratio of 45% in this paper, I calibrate $\phi = 0.2$.⁴⁹ Note that $\phi = 0.2$ is more consistent with the ratio of housing expenditures to total consumption of roughly 20% that is observed empirically.⁵⁰

B.2 Why Two Assets?

At first glance it is puzzling that the model includes two assets, K_t and H , since these assets are perfectly conditionally correlated. The model attempts to jointly match key macroeconomic and financial market data. As a macroeconomic model it aims to generate empirically plausible levels of investment volatility. As a finance model, enough asset price volatility is needed to produce quantitatively significant nonlinearities during periods of financial distress. These two goals present a well-known problem. Market values of capital are much more volatile than investment, both across firms and over time. In a standard q -theory model where investment is closely linked with asset prices, these two facts can only be reconciled

⁴⁹Matching the same housing-wealth ratio requires the equilibrium value of rental payments (D_t) to remain similar to the original HK model. Due to the labor income extension, my model features a larger share of output goods relative to housing services (i.e., $A \uparrow$). From equation (10), more output goods implies that a lower calibration of ϕ is needed in order to maintain D_t .

⁵⁰See [Davis and Van Nieuwerburgh \(2015\)](#) for details.

with unreasonably high adjustment costs (see e.g. the discussion in [Campbell, 2017](#), Ch. 7).

By introducing two assets, HK circumvent this issue. The two leftmost panels of [Figure 2](#) show that p_t is more sensitive to e_t than q_t . This is because the supply of houses is fixed while K_t is procyclical.⁵¹ Investment i_t is a function of q_t , so the lower variance of q_t allows the model to match empirical investment volatility under reasonable adjustment costs. But, since the intermediary holds both types of assets, the additional volatility provided by p_t generates an intermediary pricing kernel that is volatile enough to produce significant nonlinearities in financial intermediation. As [Section 3.2](#) highlights, the two-asset model does a good job of overcoming the problem outlined above, and successfully matches both empirical investment volatility as well as the overall risk-return profile of intermediary equity.

⁵¹In particular, recall that P_t is the present discounted value of perceived future rental payments. When e_t is low, investment rate i_t is also expected to be low for a long period of time. This implies that the growth rate of output – and therefore rental payments – is expected to be low, too. Through this investment channel, the growth rate of rental payments is highly correlated with e_t . Hence, housing price p_t is sensitive to e_t .

B.3 Boundary Conditions

Boundary conditions are needed to solve for price functions $q(e, \mathcal{I})$ and $p(e, \mathcal{I})$. As $e \rightarrow \infty$ the equity issuance constraint ceases to affect the equilibrium price and policy functions.

This implies $\lim_{e \rightarrow \infty} q_e(e, \mathcal{I}) = \lim_{e \rightarrow \infty} p_e(e, \mathcal{I}) = 0$.

A lower reflecting boundary is imposed by assuming entry into the intermediary sector deep in crisis times (term $d\psi_t$ in equation (8)). There exists an exogenous minimum reputation level \underline{e} such that new intermediaries enter the economy whenever e_t hits \underline{e} .⁵² Entry is costly because new intermediaries must acquire the skills to operate capital. Specifically, the economy must destroy $\beta > 0$ units of capital in order for entry to increase aggregate reputation \mathcal{E}_t by one unit.⁵³ The assumption of a reflecting barrier at \underline{e} implies that prices q and P must have a zero derivative with respect to e at \underline{e} . If this were not the case, an arbitrageur could bet on a unidirectional change in asset prices at the reflecting barrier. This implies $q_e(\underline{e}, \mathcal{I}) = 0$ and $p_e(\underline{e}, \mathcal{I}) = \frac{p(\underline{e}, \mathcal{I})\beta}{1+\underline{e}\beta}$.

To derive the lower boundary condition for p , start at the boundary with an aggregate reputation of $\underline{\mathcal{E}} = \underline{e}K$. Consider a further shock to reputation of z which sends reputation to $\underline{\mathcal{E}} - z < \underline{e}K$. After this shock, the reflecting boundary implies that capital will immediately be converted into reputation to restore \underline{e} . Specifically, let x denote the amount of new reputation required to restore \underline{e} . x is given by:⁵⁴

$$x = \frac{z}{1 + \underline{e}\beta}.$$

Shock z requires the destruction of βx capital to restore reputation to \underline{e} .

This capital destruction equation can be used to derive the boundary condition for price function p . The condition that $P_e = 0$ implies that $p = \frac{P}{K}$ will have a non-zero slope at \underline{e} .⁵⁵ Consider the above reputation shock of z . Immediately after this shock, the price of housing is $P = p\left(\underline{e} - \frac{z}{K}, \mathcal{I}'\right) K$. This must equal the price of housing immediately after capital is

⁵²Loosely, this captures (unmodeled) government intervention deep in crises.

⁵³Equations (2) and (4) are altered at \underline{e} to include this form of capital destruction.

⁵⁴ x is defined implicitly by $\underline{e} = \frac{\underline{\mathcal{E}} - z + x}{K - \beta x}$. The numerator of this equation is the level of initial reputation minus the shock and plus x of new reputation. The denominator is the initial level of capital minus the βx of capital destroyed to produce x reputation. Capital will be destroyed until \underline{e} (the minimum level of $e = \mathcal{E}/K$) is restored.

⁵⁵This is due to capital destruction, which makes the denominator of $\frac{P}{K}$ change at the entry boundary.

spent to rebuild reputation, given by $P = p(\underline{e}, \mathcal{I}') (K - \beta x)$. In the continuous-time limit with arbitrarily small shocks, $p(\underline{e} - \frac{z}{K}, \mathcal{I}') K$ can be rewritten as $p(\underline{e}, \mathcal{I}') K - p_e(\underline{e}, \mathcal{I}') z$. Combining:

$$p(\underline{e}, \mathcal{I}') K - p_e(\underline{e}, \mathcal{I}') z = p(\underline{e}, \mathcal{I}') \left(K - \beta \frac{z}{1 + \underline{e}\beta} \right)$$

$$p_e(\underline{e}, \mathcal{I}') = \frac{p(\underline{e}, \mathcal{I}')\beta}{1 + \underline{e}\beta}.$$

This gives the boundary condition for p at \underline{e} . Details on how the boundary conditions are imposed numerically are provided in [Appendix D](#).

B.4 Proofs

Proof of Proposition 2. By definition, $\mathcal{I}_t \equiv \int_0^t e^{-\kappa(t-s)} \sigma dZ_s$. Subjective shocks are defined as $\sigma d\widehat{Z}_t = -\theta \mathcal{I}_t dt + \sigma dZ_t$. The law of motion for \mathcal{I}_t is given by $d\mathcal{I}_t = -\kappa \mathcal{I}_t dt + \sigma dZ_t$. Plugging in the definition of subjective shocks gives

$$d\mathcal{I}_t = (-\kappa + \theta) \mathcal{I}_t dt + \sigma d\widehat{Z}_t.$$

Let $f(\mathcal{I}_t, t) = \mathcal{I}_t e^{(\kappa-\theta)t}$. Using Itô's lemma:

$$\begin{aligned} df(\mathcal{I}_t, t) &= e^{(\kappa-\theta)t} (d\mathcal{I}_t) + (\kappa - \theta) \mathcal{I}_t e^{(\kappa-\theta)t} dt \\ &= e^{(\kappa-\theta)t} \left((-\kappa + \theta) \mathcal{I}_t dt + \sigma d\widehat{Z}_t \right) + (\kappa - \theta) \mathcal{I}_t e^{(\kappa-\theta)t} dt \\ &= e^{(\kappa-\theta)t} \sigma d\widehat{Z}_t. \end{aligned}$$

Given an initial condition of $f(\mathcal{I}_0, 0) = 0$, integrating gives:

$$\begin{aligned} f(\mathcal{I}_t, t) &= \int_0^t df(\mathcal{I}_s, s) \\ \mathcal{I}_t e^{(\kappa-\theta)t} &= \int_0^t e^{(\kappa-\theta)s} \sigma d\widehat{Z}_s \\ \mathcal{I}_t &= \int_0^t e^{(-\kappa+\theta)(t-s)} \sigma d\widehat{Z}_s. \end{aligned}$$

This completes the proof.

Proof of Proposition 3 (in Appendix A.1). Consider the evolution of log capital k_t over a horizon of $\tau > 0$, holding investment fixed at $\bar{i} = i_t$. With fixed investment:

$$\begin{aligned} k_{t+\tau} &= k_t + \int_t^{t+\tau} \left(\bar{i} - \delta - \frac{\sigma^2}{2} \right) ds + \int_t^{t+\tau} \sigma dZ_s \\ &= k_t + \tau \left(\bar{i} - \delta - \frac{\sigma^2}{2} \right) + \sigma (Z_{t+\tau} - Z_t). \end{aligned}$$

Since $\{Z_t\}$ is a standard Brownian motion, $k_{t+\tau} \sim \mathcal{N} \left(k_t + \tau \left(\bar{i} - \delta - \frac{\sigma^2}{2} \right), \sigma^2 \tau \right)$.

For the arbitrary prediction horizon of τ , one can rewrite equation (26) as:

$$h_t^\theta(k'_{t+\tau} | k_t, e_t, \mathcal{I}_t) = h(k'_{t+\tau} | k_t, e_t, \mathcal{I}_t) \cdot \left[\frac{h(k'_{t+\tau} | k_t, e_t, \mathcal{I}_t)}{h(k'_{t+\tau} | G_t^-, e_t, \mathcal{I}_t)} \right]^{\theta \tau} \frac{1}{Z}.$$

Given a fixed investment level of \bar{i} , this implies:

$$h_t^\theta(k'_{t+\tau} | k_t, e_t, \mathcal{I}_t) = \mathcal{N} \left(k_t + \tau \left(\bar{i} - \delta - \frac{\sigma^2}{2} \right) + \theta(k_t - G_t^-) \tau, \sigma^2 \tau \right).$$

The [Bordalo et al. \(2018\)](#) Appendix provides algebraic details for this step. Equivalently, the agent perceives that

$$\widehat{k}_{t+\tau} - k_t = \int_t^{t+\tau} \left(\bar{i} - \delta - \frac{\sigma^2}{2} \right) ds + \int_t^{t+\tau} \theta(k_t - G_t^-) ds + \int_t^{t+\tau} \sigma dZ_s.$$

In the limit as $\tau \rightarrow dt$:

$$\widehat{dk}_t = \left(i_t - \delta - \frac{\sigma^2}{2} \right) dt + \theta(k_t - G_t^-) dt + \sigma dZ_t.$$

Definition 3 gives $\mathcal{I}_t = k_t - G_t^-$. Applying Itô's lemma to $K_t = \exp(k_t)$ yields:

$$\frac{d\widehat{K}_t}{K_t} = (i_t - \delta) dt + \theta \mathcal{I}_t dt + \sigma dZ_t.$$

This completes the proof.

B.5 Evaluating the Impact of Diagnosticity on Intermediary Returns

Diagnostic expectations cause assets to be mispriced by financial intermediaries. One way to evaluate the extent of this mispricing is to compare a diagnostic intermediary to a fully rational “arbitrageur” who understands the DEE’s true equilibrium laws of motion. Note that this arbitrageur is assumed to possess a very high level of knowledge about the economy, because the arbitrageur understands not only the true growth rate of capital, but also the dynamics of diagnostic expectations and the effect of agents’ beliefs on endogenous economic outcomes.

To conduct this analysis, I assume that the arbitrageur has the same mean-variance preferences as diagnostic intermediaries (see equation (7)), and the same risk aversion γ . The rational arbitrageur can borrow and save at the risk-free rate r_t , and can gain access to risky assets by purchasing intermediary equity.⁵⁶ Let $\tilde{\alpha}_t$ denote the arbitrageur’s portfolio share invested in intermediary equity, which earns return $d\tilde{R}_t$. Share $1 - \tilde{\alpha}_t$ is invested in risk-free bonds. The arbitrageur is assumed to have infinitesimal wealth, meaning that the arbitrageur does not influence equilibrium prices. A full equilibrium analysis that allows for interactions between rational and diagnostic agents – or agents with heterogeneous beliefs more generally – is beyond the scope of this paper but worthy of future exploration.

The rational arbitrageur solves:

$$\max_{\tilde{\alpha}_t} [r_t + \tilde{\alpha}_t \tilde{\pi}_t] - \frac{\gamma}{2} (\tilde{\alpha}_t \tilde{\sigma}_t)^2,$$

where $\tilde{\pi}_t = \alpha_t^k \pi_t^k + \alpha_t^h \pi_t^h$ denotes the risk premium on intermediary equity, and $\tilde{\sigma}_t = \alpha_t^k \sigma_t^k + \alpha_t^h \sigma_t^h$ denotes the volatility of intermediary equity. Unlike equation (19), hats are no longer used because the arbitrageur understands the DEE. This results in the portfolio-choice

⁵⁶I assume that the arbitrageur invests in intermediary equity, rather than having direct access to the risky capital and housing, in order to hold the relative portfolio shares of capital and housing constant. Diagnostic expectations can produce small differences in the realized Sharpe ratios of the two assets in equilibrium, and since capital and housing are perfectly conditionally correlated this can lead to arbitrage opportunities if an agent understands the true equilibrium. This is a downside of the model’s stylized single-shock, two-asset, structure (the benefits of which are detailed in Appendix B.2).

condition:

$$\tilde{\alpha}_t = \frac{\tilde{\pi}_t}{\gamma \tilde{\sigma}_t^2}.$$

Appendix Figure 2 details the performance of the arbitrageur under the baseline calibration. Because the arbitrageur has the same preferences as diagnostic intermediaries, the arbitrageur would set $\tilde{\alpha}_t = 1$ for all t if they also had the same beliefs. Thus, any difference in performance is due to mispricing by the diagnostic intermediaries.

The left-hand panel plots the arbitrageur’s risky portfolio share $\tilde{\alpha}_t$ as a function of sentiment (holding e at its median value). When sentiment is negative, the arbitrageur levers up because they know that capital is underpriced. As sentiment turns mildly positive, the arbitrageur downweights intermediary equity and invests more of their portfolio in risk-free bonds. Importantly, even when capital is moderately overvalued the arbitrageur is willing to invest a positive amount in intermediary equity because the risk premium is still positive. The arbitrageur does not actually short intermediary equity ($\tilde{\alpha}_t < 0$) until $\mathcal{I} > 2SD$, at which point the risk premium on intermediary equity turns negative.⁵⁷

The right-hand panel of Appendix Figure 2 plots the relative performance of \$1 invested by a diagnostic intermediary compared to \$1 invested by the arbitrageur. The economy is simulated at a monthly frequency for 50 years, starting from $\mathcal{I}_0 = -1.5SD$, $\mathcal{I}_0 = 0SD$, and $\mathcal{I}_0 = 1.5SD$.⁵⁸ The solid lines plot the median relative performance of the diagnostic intermediary. To illustrate the variation in performance, the dotted lines indicate the 25th and 75th percentiles of relative performance.

Starting from neutral sentiment ($\mathcal{I}_0 = 0$), after 50 years the median performance of the diagnostic intermediary is about 45% worse than the arbitrageur. This suggests a typical underperformance of roughly 1.2% per year in this simulation, which is modest in comparison to the average return earned by intermediaries (see Table 1). Moreover, the dotted lines show that diagnostic intermediaries frequently outperform the rational arbitrageur, particularly when sentiment is elevated. The intuition is similar to that of De Long et al. (1990) in that elevated sentiment causes the rational arbitrageur to take less risk than diagnostic

⁵⁷Appendix Figure 11 plots the intermediary risk premium over the state space.

⁵⁸Capital capacity e_0 is initialized to its median value in all cases.

intermediaries. Instead, where the arbitrageur typically earns their highest returns is when sentiment is initially depressed. As the left-hand panel shows, when sentiment is depressed the arbitrageur levers up in order to earn the high returns offered by underpriced assets.

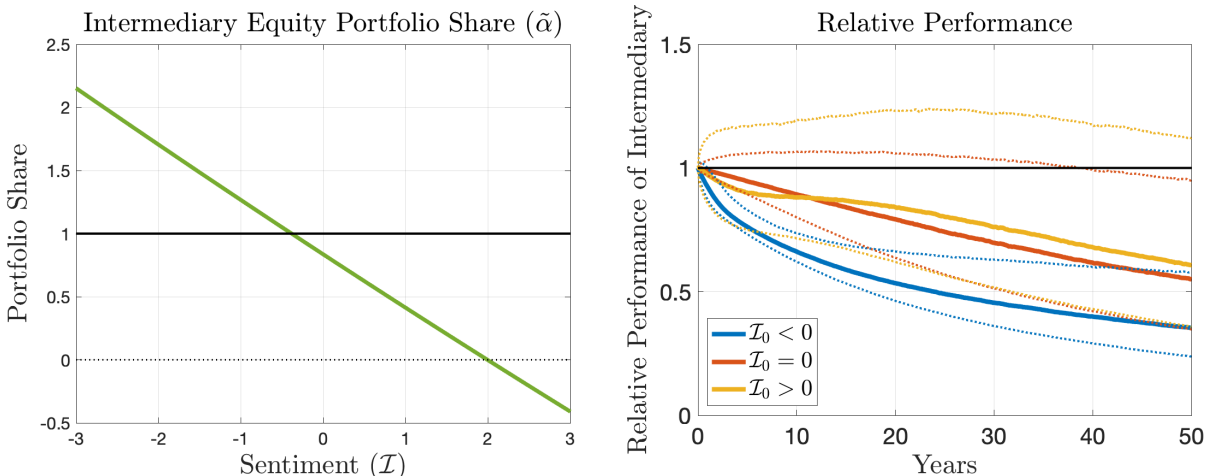


Figure 2: **Performance of rational arbitrageur.** The left-hand panel shows the portfolio share that the arbitrageur invests in intermediary equity, $\tilde{\alpha}$, as a function of sentiment (holding e at its median value). The right-hand panel shows the typical performance of a diagnostic intermediary relative to the rational arbitrageur. See text for details.

Dependence on θ and κ . I also outline how the arbitrageur’s relative performance depends on behavioral parameters θ and κ . As θ increases, intermediaries become more diagnostic. This causes the slope of the green line in the left-hand panel of Appendix Figure 2 to become steeper, meaning that the arbitrageur will lever up more when $\mathcal{I} < 0$ and will be more likely to take a short position when $\mathcal{I} > 0$. Parameter κ governs how long intermediaries’ beliefs remain dislocated from reality. Holding fixed the magnitude of belief distortions, as beliefs become more persistent the sentiment-driven performance differences shown in the right-hand panel of Appendix Figure 2 continue for longer.

B.6 Comparative Statics

This section examines the model equilibrium under selected parameter perturbations in order to highlight how the model depends on certain key parameters. These alternate calibrations are not intended to be realistic, but rather to demonstrate the workings of the model.

To investigate behavioral frictions I consider the following three perturbations: (a) diagnosticity θ is twice as large, (b) beliefs are twice as persistent, and (c) intermediaries are 50% less diagnostic than households. To investigate financial frictions I consider the following six perturbations: (d) intermediary risk aversion $\gamma = 3$, (e) intermediary leverage parameter $\lambda = 0.8$, (f) entry barrier \underline{e} is four times larger than baseline, (g) entry cost β is 50% larger than baseline, (h) housing value parameter $\phi = 0$, and (i) adjustment cost $\xi = 10$. Besides the parameter being perturbed, all other parameters are kept at their baseline value in Table 1.⁵⁹

Figure 3 below plots the realized (delevered) risk premium across these perturbations. For reference, the transparent lines in the background show the risk premium under the baseline calibration. I plot the realized risk premium because this one metric provides a simple way to evaluate both financial and behavioral frictions. The effect of financial frictions is characterized by the variation in risk premia over e , while the effect of behavioral frictions is characterized by the difference between realized risk premia when $\mathcal{I} < 0$, $\mathcal{I} = 0$, and $\mathcal{I} > 0$.

Starting with the three behavioral perturbations, perturbation (a) doubles the value of θ . This increases the effect of sentiment on the realized risk premium, meaning that intermediaries make larger asset pricing errors than in the baseline calibration when sentiment is either elevated or depressed.

Perturbation (b) doubles the half-life of sentiment from 6 years to 12 years. This perturbation has little effect on realized risk premia at a given point in the state space. However, the increased half-life of sentiment can still affect the model's dynamics by making intermediaries' asset pricing errors more persistent (see Appendix B.7 for more).

Perturbation (c) introduces belief heterogeneity by assuming that financial intermediaries are less diagnostic than households. Specifically, households have the same θ as in the

⁵⁹The one exception is perturbation (b). In order to isolate the effect of belief persistence, as I perturb κ I also change θ accordingly to ensure that $\theta \times SD(\mathcal{I})$ remains equal to 0.75%.

baseline calibration, but I halve the θ of intermediaries. Households and intermediaries now “agree to disagree,” with households’ beliefs exhibiting larger extrapolative errors than intermediaries’ beliefs. The main effect of reducing intermediaries’ diagnosticity is that it suppresses the impact of sentiment on risk premia because intermediaries make smaller asset pricing errors than in the baseline calibration. The key takeaway from this perturbation is that it is diagnostic expectations on the part of financial intermediaries that are critical for generating the interactions between behavioral and financial frictions that this paper highlights.⁶⁰

Turning next to the parameters governing macro-financial dynamics, perturbation (d) increases the risk aversion of financial intermediaries. This leads directly to higher equilibrium risk premia in order to compensate intermediaries for bearing risk on their balance sheets (see equation (20)).

Perturbation (e) increases the level of bank debt demanded by households, which also increases intermediary leverage in non-crisis states.⁶¹ Because intermediaries take on more leverage than in the baseline calibration, they demand higher risk premia. Additionally, the crisis region shifts slightly to the left. This follows directly from equation (13). Since households demand less equity, intermediary capital capacity must be lower for the equity issuance constraint to bind.

Perturbation (f) increases the entry barrier \underline{e} by a factor of four in order to confirm that the model’s crisis nonlinearities are not driven by assumptions about the ease of bank entry at the lower boundary. The main effect of this updated entry barrier is that the capital capacity state variable is truncated at $\underline{e} = 0.32$ rather than $\underline{e} = 0.08$. Crisis nonlinearities are slightly muted under this alternate calibration, because forward-looking intermediaries anticipate that the worst-case scenario is not as severe. Nonetheless, the model still produces significant nonlinearities over the truncated crisis region. Moreover, the model’s asset pricing predictions in the non-crisis region are insensitive to assumptions about \underline{e} .

Similarly, perturbation (g) increases the entry cost β by a factor of 1.5. This effectively makes housing a riskier asset near the crisis region, and increases risk premia accordingly.

⁶⁰While household expectations are certainly an important driver of macro-financial dynamics, they are not the focus of the analysis in this paper.

⁶¹In non-crisis states, market leverage is given by $\frac{1}{1-\lambda}$.

Because β governs the lower boundary condition, the effect of this perturbation diminishes as e increases.

Perturbation (h) sets $\phi = 0$, which effectively removes housing from the model. As discussed in Section V of [He and Krishnamurthy \(2019\)](#) and detailed in Appendix B.2 of the current paper, setting $\phi = 0$ significantly reduces the financial risk that intermediaries must bear. This causes risk premia to drop, and considerably reduces crisis nonlinearities. It is worth emphasizing that setting $\phi = 0$ only suppresses financial frictions, not behavioral frictions. Specifically, panel (h) shows that diagnostic expectations still generate belief-driven mispricing of a similar magnitude to the baseline calibration.⁶²

Finally, perturbation (i) increases the adjustment cost parameter ξ from 3 to 10. This perturbation makes the capital stock more difficult to adjust, which makes the price of capital more volatile (similar to housing price P that is in fixed supply). This effect is particularly large near the crisis region, and fades away as e rises and asset prices asymptote to their value in a model without financial frictions.

⁶²This is because diagnostic expectations continue to directly bias the perceived growth rate of capital by $\theta\mathcal{I}_t$ (see e.g. equation (17)).

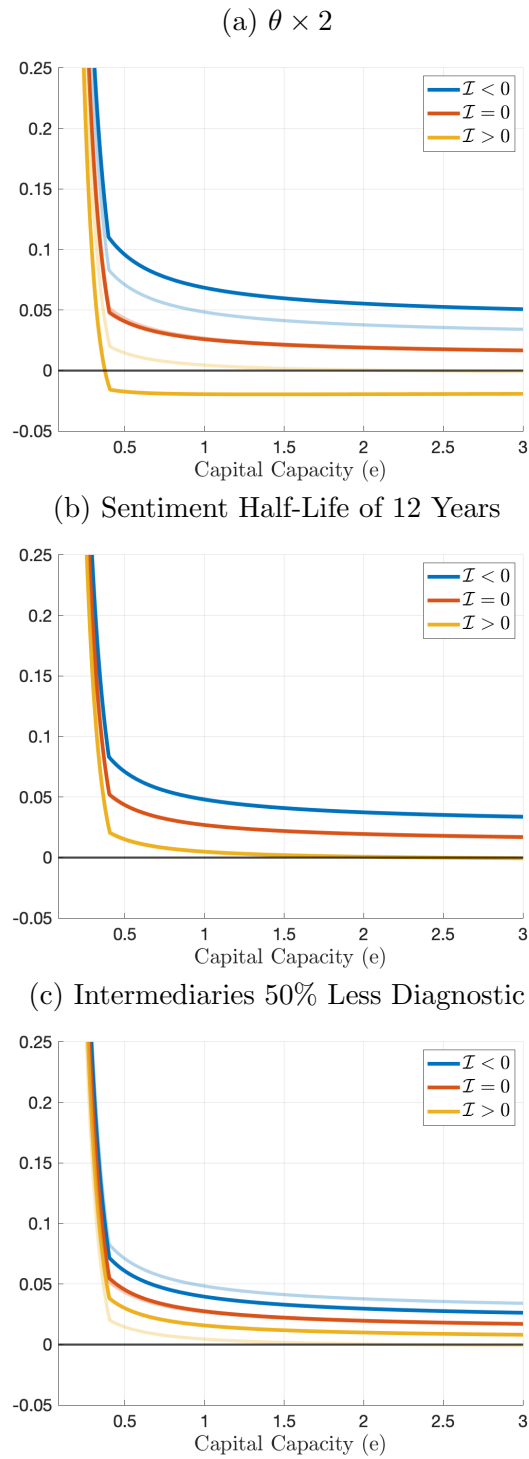


Figure 3: **Behavioral Frictions: realized risk premia across parameter perturbations.** The horizontal axis lists capital capacity $e = \frac{\mathcal{E}}{K}$, and curves correspond to $\mathcal{I} = -1.5SD$ (blue), $\mathcal{I} = 0SD$ (red), and $\mathcal{I} = +1.5SD$ (yellow). Solid lines show the perturbed calibration, and transparent lines show the baseline calibration. The order from top to bottom follows the order of the discussion in the text.

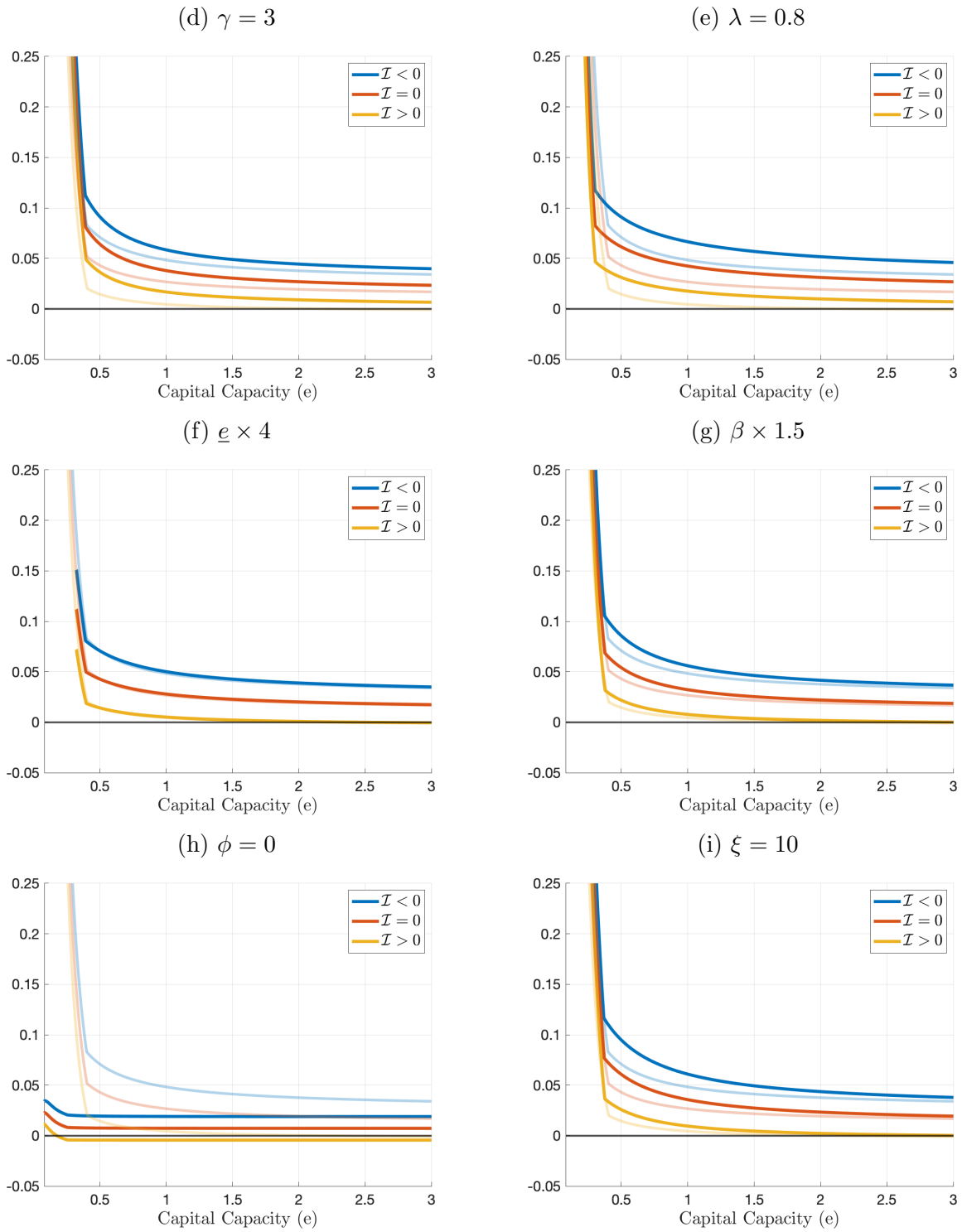


Figure 3: **Financial Frictions: realized risk premia across parameter perturbations.** The horizontal axis lists capital capacity $e = \frac{\xi}{K}$, and curves correspond to $\mathcal{I} = -1.5SD$ (blue), $\mathcal{I} = 0SD$ (red), and $\mathcal{I} = +1.5SD$ (yellow). Solid lines show the perturbed calibration, and transparent lines show the baseline calibration. The order from left to right, top to bottom follows the order of the discussion in the text.

B.7 Robustness

This section examines how the results in Section 5 depend on behavioral parameters θ and κ . The baseline calibration sets $\theta \times SD(\mathcal{I}) = 0.75\%$ and the half-life of \mathcal{I} to 6 years. Here I analyze the following four perturbations: (a) $\theta \times SD(\mathcal{I}) = 1.5\%$, (b) $\theta \times SD(\mathcal{I}) = \frac{0.75\%}{2}$, (c) 12 year sentiment half-life, and (d) 1 year sentiment half-life.

For perturbations to θ , all other parameters are kept at their baseline calibration in Table 1. For perturbations to persistence parameter κ , I change θ accordingly to ensure that $\theta \times SD(\mathcal{I})$ remains equal to 0.75%. This isolates the effect of persistence.

Sentiment-Driven Financial Crises.

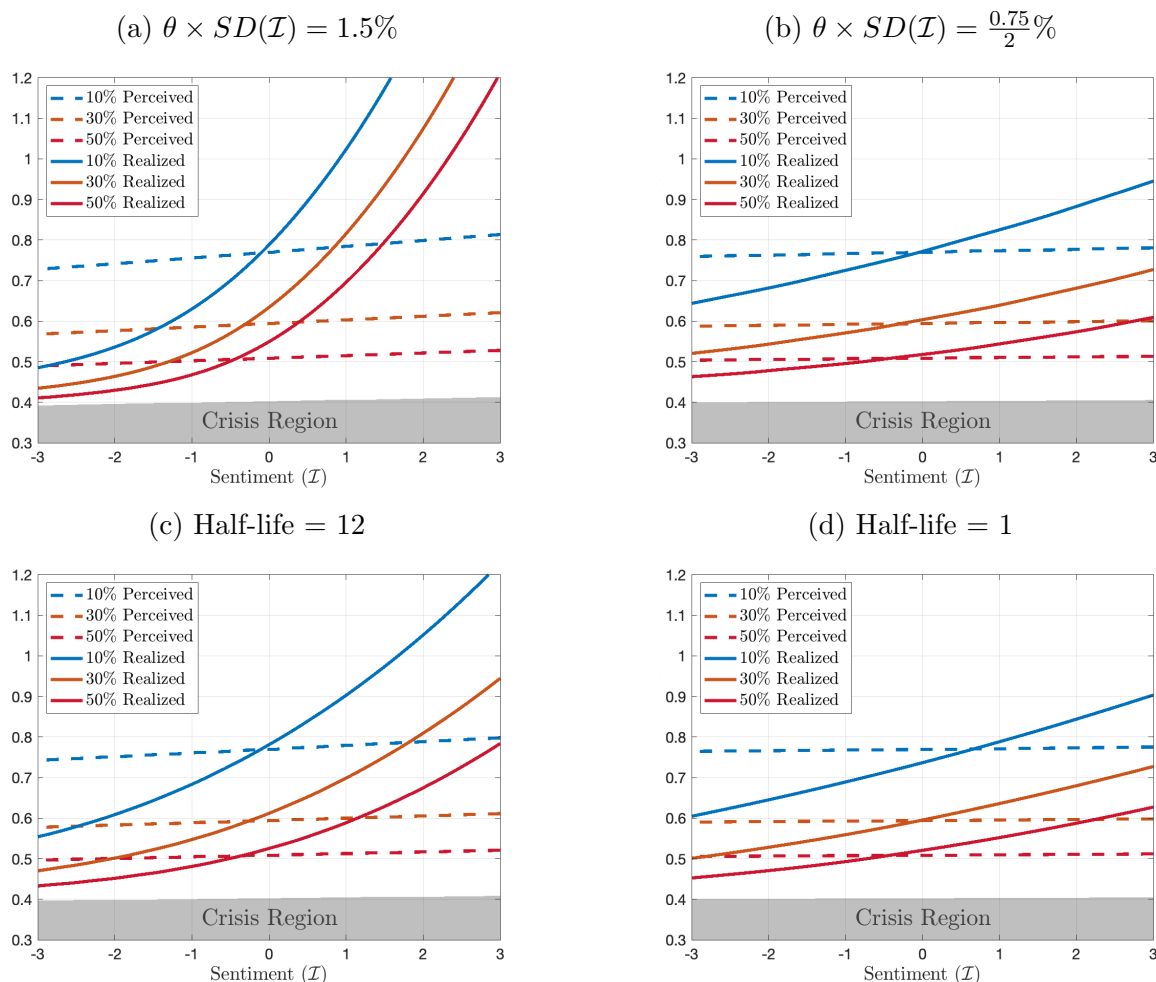
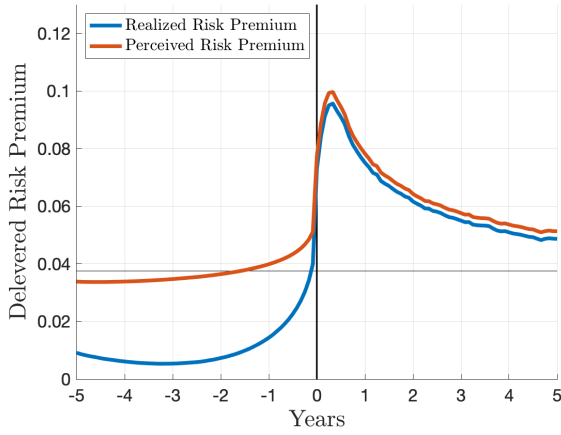
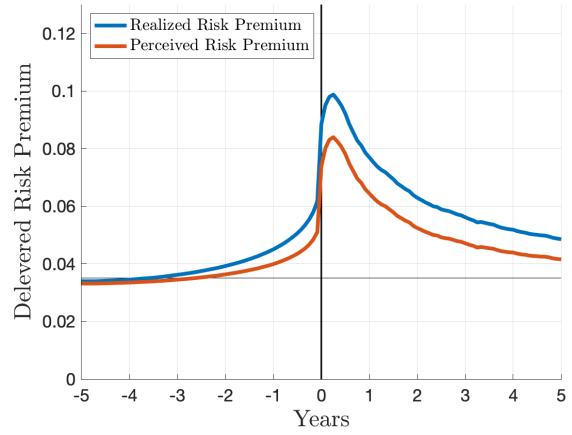


Figure 4: **Crisis hitting probabilities.** See Figure 5 for a description.

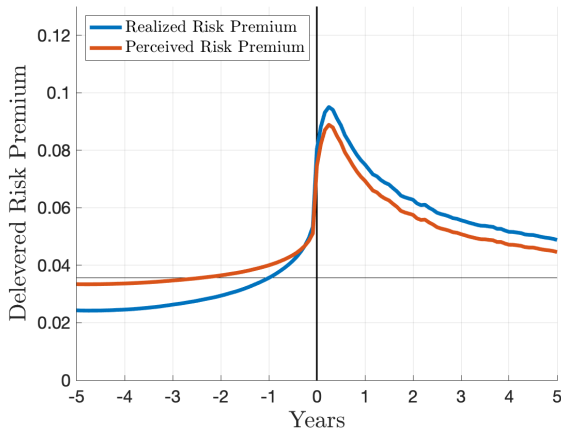
(a) $\theta \times SD(\mathcal{I}) = 1.5\%$



(b) $\theta \times SD(\mathcal{I}) = \frac{0.75}{2}\%$



(c) Half-life = 12



(d) Half-life = 1

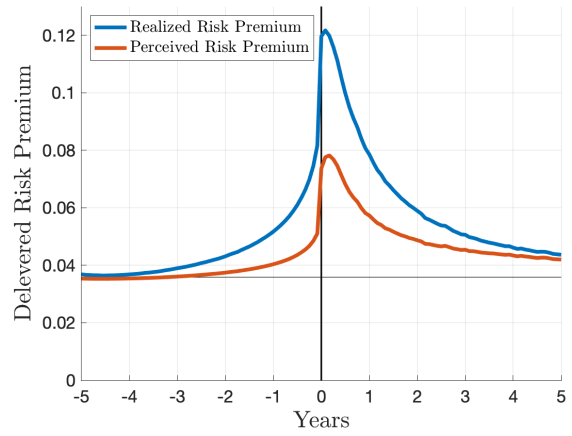


Figure 5: Risk premia around crises. See Figure 6 for a description.

Boom-Bust Investment Cycles (Positive Shock).

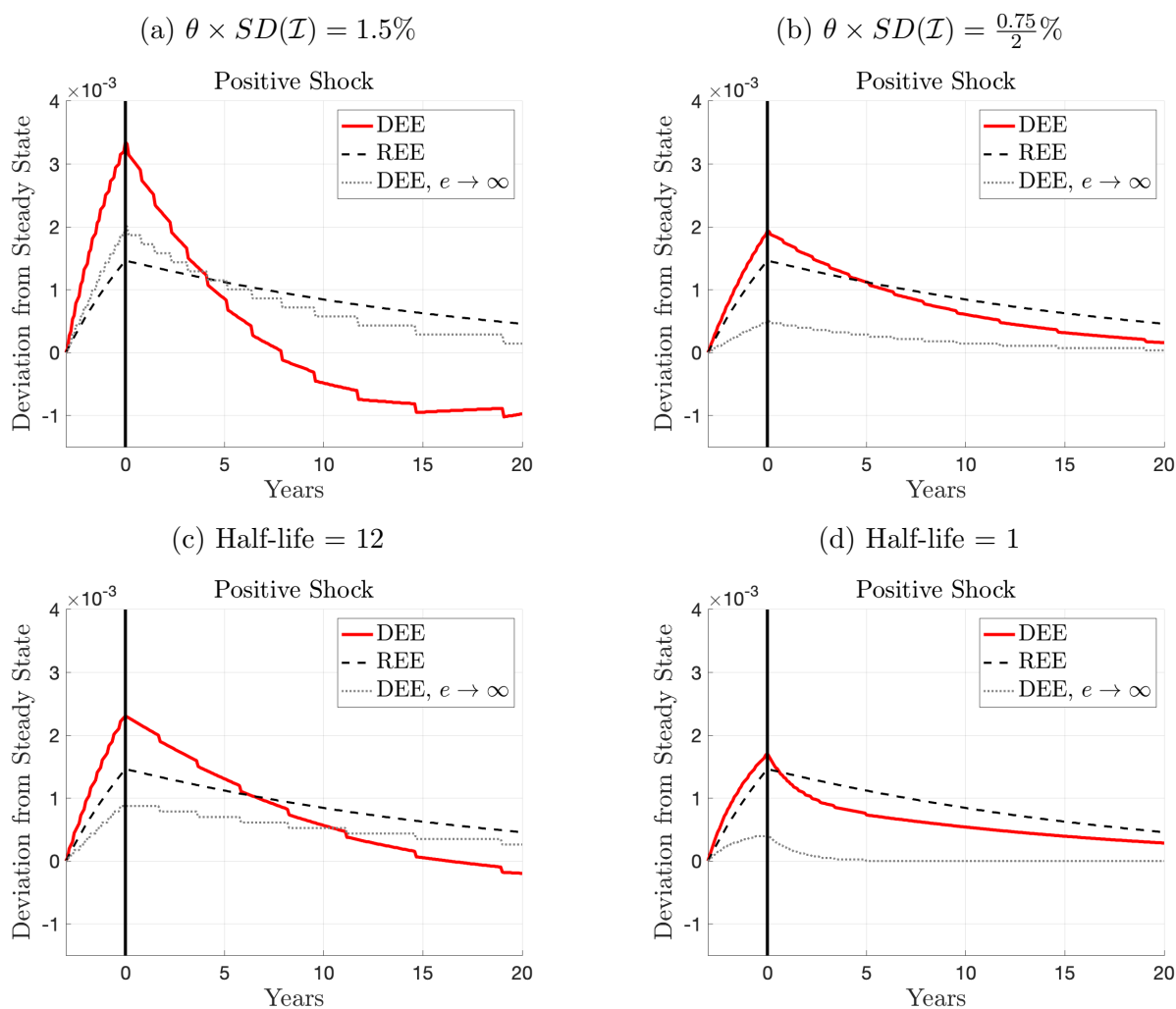


Figure 6: **Investment rate IRFs.** See Figure 7 for a description. Here I show just the positive shock case, but the negative shock case is similar.

Financial Market Stability from Beliefs.

	DEE Prob(Crisis)	REE Prob(Crisis)	$\frac{\text{DEE Prob(Crisis)}}{\text{REE Prob(Crisis)}}$
Baseline	3.13 %	3.57 %	0.88
$\theta \times SD(\mathcal{I}) = 1.5\%$	6.53 %	3.57 %	1.83
$\theta \times SD(\mathcal{I}) = \frac{0.75\%}{2}$	2.89 %	3.57 %	0.81
Half-life = 12	3.93 %	3.57 %	1.10
Half-life = 1	2.54 %	3.57 %	0.71

Table 3: **Financial market stability from beliefs: robustness.** This table lists crisis probabilities in the DEE and the REE for the four alternate beliefs calibrations.

B.8 Empirical Tests in the Recalibrated REE

In Section 6.1 the calibration of the REE is identical to the calibration of the DEE, except for $\theta = 0$. Here, I recalibrate parameters η , \underline{e} , β , and ϕ so that the REE is comparable with the DEE calibration in Table 1 (see Appendix Table 4 below). Then, I repeat the analysis of Section 6.1 using the recalibrated REE.

Parameter	Choice	Target
Updated Parameters		
η Bank Exit Rate	0.139	Probability of Crisis
\underline{e} Lower Entry Barrier	0.087	Max Sharpe Ratio
β Entry Cost	3.8	Land Price Volatility
ϕ Housing Expenditure Share	0.201	Housing-Wealth Ratio
Unconditional Simulated Moments		
Mean($\frac{\text{Investment}}{\text{Capital}}$)	10.01%	10.12%
Mean($\frac{\text{Consumption}}{\text{Output}}$)	69.97%	69.64%
Mean(Realized Sharpe Ratio)	0.54	0.51
Mean(Realized Intermediary Risk Premium)	15.99%	14.27%
Probability of Crisis	3.06%	3.57%
Volatility(Land Price Growth)	11.16%	9.93%
Volatility(Interest Rate)	0.42%	0.40%
Non-Distress Simulated Moments		
Volatility(Investment Growth)	4.03%	3.91%
Volatility(Consumption Growth)	2.53%	2.58%
Volatility(Output Growth)	2.98%	2.98%
Mean($\frac{\text{Housing Wealth}}{\text{Total Wealth}}$)	44.56%	46.81%

Table 4: **REE updated calibration.** See Table 1 for a description. Column REE (New) lists the simulated moments for the recalibrated REE used here. Column REE (Old) lists the simulated moments for the REE calibration used in the main text.

The Persistence of Financial Fragility. Appendix Table 5 uses the recalibrated REE to reproduce Table 2 of the main text. The recalibrated REE features a slightly lower persistence of financial distress, but results are similar.

e_t Percentile	REE (New)	REE (Old)
10	1.15	1.19
25	3.67	4.02
50	9.98	11.27
75	24.67	28.46

Table 5: **Average crisis recovery time (in years).** See Table 2 for a description. This table compares the persistence of financial fragility in the two REE calibrations.

Macro-Financial Autocorrelations. Appendix Figure 7 uses the recalibrated REE to reproduce Figure 9 of the main text. Autocorrelations in the recalibrated REE are presented with solid black lines. The two calibrations produce similar results.

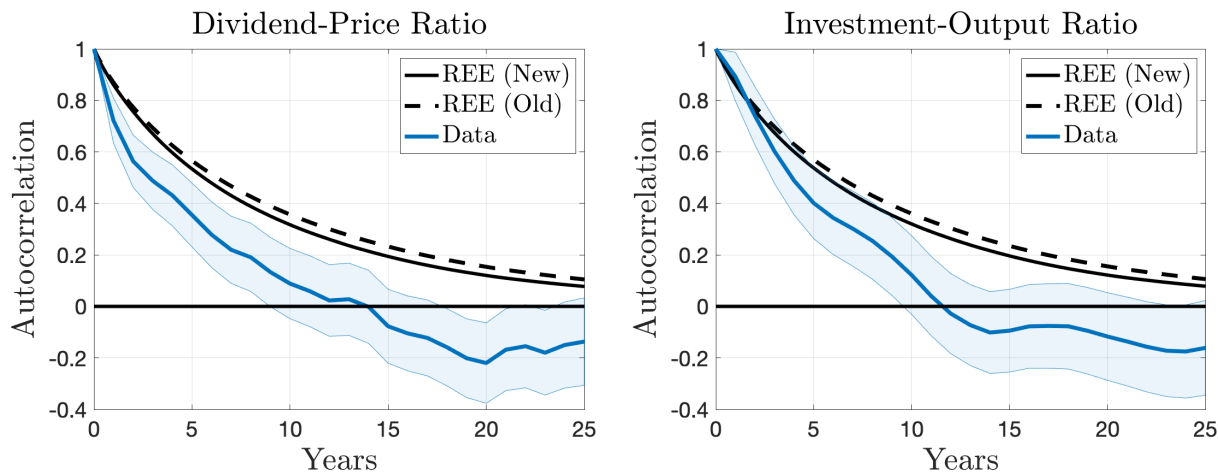


Figure 7: **Persistence: data and model.** See Figure 9 for a description. This figure compares the persistence of macro-financial aggregates in the two REE calibrations.

B.9 Simulating the 2007-2008 Financial Crisis: Additional Analysis

Alternate Crisis Initialization: Starting from 1992Q1. Here I present an alternate simulation that begins in 1992Q1, right as the U.S. is emerging from a minor financial crisis.⁶³ This initialization takes a very long-run view of the 2007-2008 Financial Crisis in order to understand the full effect of the 1990s boom on the subsequent crisis. I initialize e_t at the boundary of the crisis region, and \mathcal{I}_t at the 1992Q1 value shown in Figure 10. See Section 6.3 for details on how the model is simulated.

The long-run simulation from 1992 through 2018 is shown in Appendix Figure 8. I compare the simulated level of capital capacity e_t to the data using the He et al. (2017) Intermediary Capital Ratio. In this single-shock model with shocks taken externally from SPF forecast errors, the correlation between e_t and the Intermediary Capital Ratio is 0.77 in the DEE. Using the same set of shocks, the correlation is only 0.41 in the REE. The difference in fit is driven by a divergence between the DEE and the REE over the mid-2000s. In the DEE, elevated sentiment from the 1990s boom leads to an erosion of capital capacity prior to 2007. In the REE, the financial sector remains counterfactually well-capitalized throughout the mid-2000s.

As discussed in Section 6.3, though diagnostic expectations allow the model to qualitatively replicate the empirical profile of intermediary capitalization over this boom-bust period, this long-run simulation points to a failure of the model. Using the shocks implied by SPF forecast errors, the DEE cannot jointly fit the 1990s boom and the 2007-2008 Financial Crisis because the sequence of positive shocks realized throughout the 1990s places the financial sector too far above the crisis region for the negative shocks in 2007 and 2008 to generate a full-blown crisis. However, Appendix Figure 8 still highlights that diagnostic expectations are important, as the DEE outperforms the REE over this period.

⁶³See, for example, the crisis dating of Romer and Romer (2017) and Baron et al. (2021).

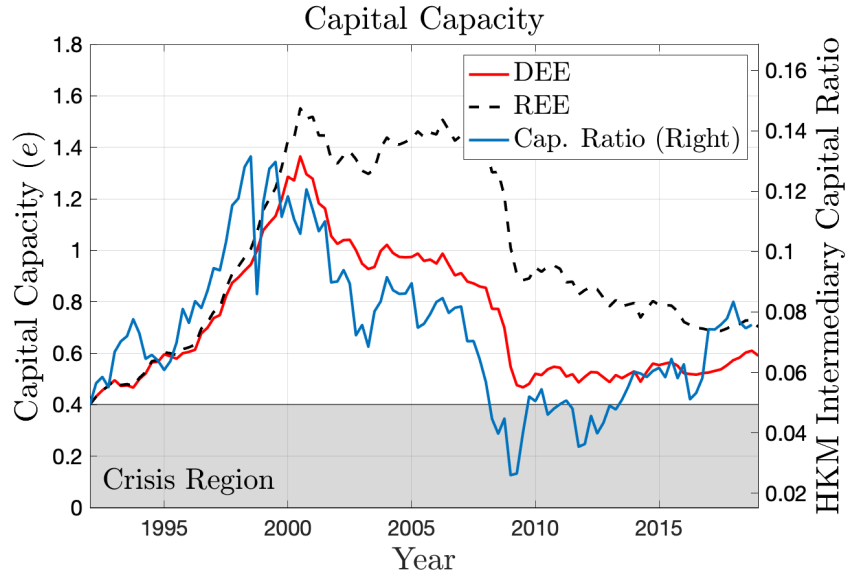


Figure 8: **A long-run analysis of the 2007-2008 Financial Crisis.** See Section 6.3 for a description. For the alternate simulation that begins in 1992Q1, this figure plots the path of capital capacity e_t in the DEE and the REE (left axis), as well as the corresponding empirical measure from He et al. (2017) (right axis).

Analysis of “Hidden Leverage.” Appendix Figure 9 provides a “hidden leverage” simulation following [He and Krishnamurthy \(2019\)](#) (see Appendix IV of HK for details). This hidden leverage scenario starts from the REE, but assumes that intermediaries hold additional leverage that is “hidden.” Intermediaries make decisions as if $\lambda = 0.75$, but in reality $\lambda = 0.772$. I follow HK by assuming that asset prices are calculated under $\lambda = 0.75$, but higher realized leverage makes e_t more sensitive to shocks. I also assume, somewhat arbitrarily, that hidden leverage starts in 2006 and persists until the end of 2009, at which point agents are likely aware of the risks that were previously hidden.⁶⁴ The dotted green curve plots the path of capital capacity e_t in this alternate scenario. For the shock sequence considered here, hidden leverage brings the REE closer to the data but still does not generate a crisis. Note too that by increasing λ , the crisis region for the hidden leverage case drops from $e \leq 0.4$ to $e \leq 0.36$. One important difference between the DEE and hidden leverage is that the feedback from behavioral frictions to financial frictions affects the drift of e_t , while hidden leverage affects the volatility of e_t . The drift effect is more powerful in this simulation because I study a shock sequence with shocks that are relatively small in magnitude.

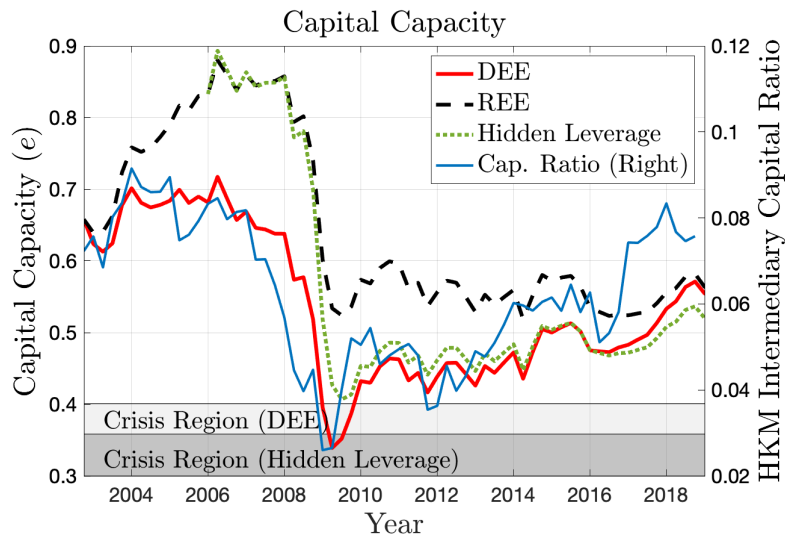


Figure 9: **Simulating the 2007-2008 Financial Crisis: hidden leverage.** See Figure 11 for a description. This figure adds an additional “hidden leverage” simulation following [He and Krishnamurthy \(2019\)](#).

⁶⁴I choose to start the hidden leverage scenario in 2006 to improve its fit. Starting earlier than 2006 would amplify the initial increase in e_t , thereby worsening the hidden leverage model’s fit.

B.10 Additional Tables and Figures

Prices, Policy Functions, and Forecast Errors.

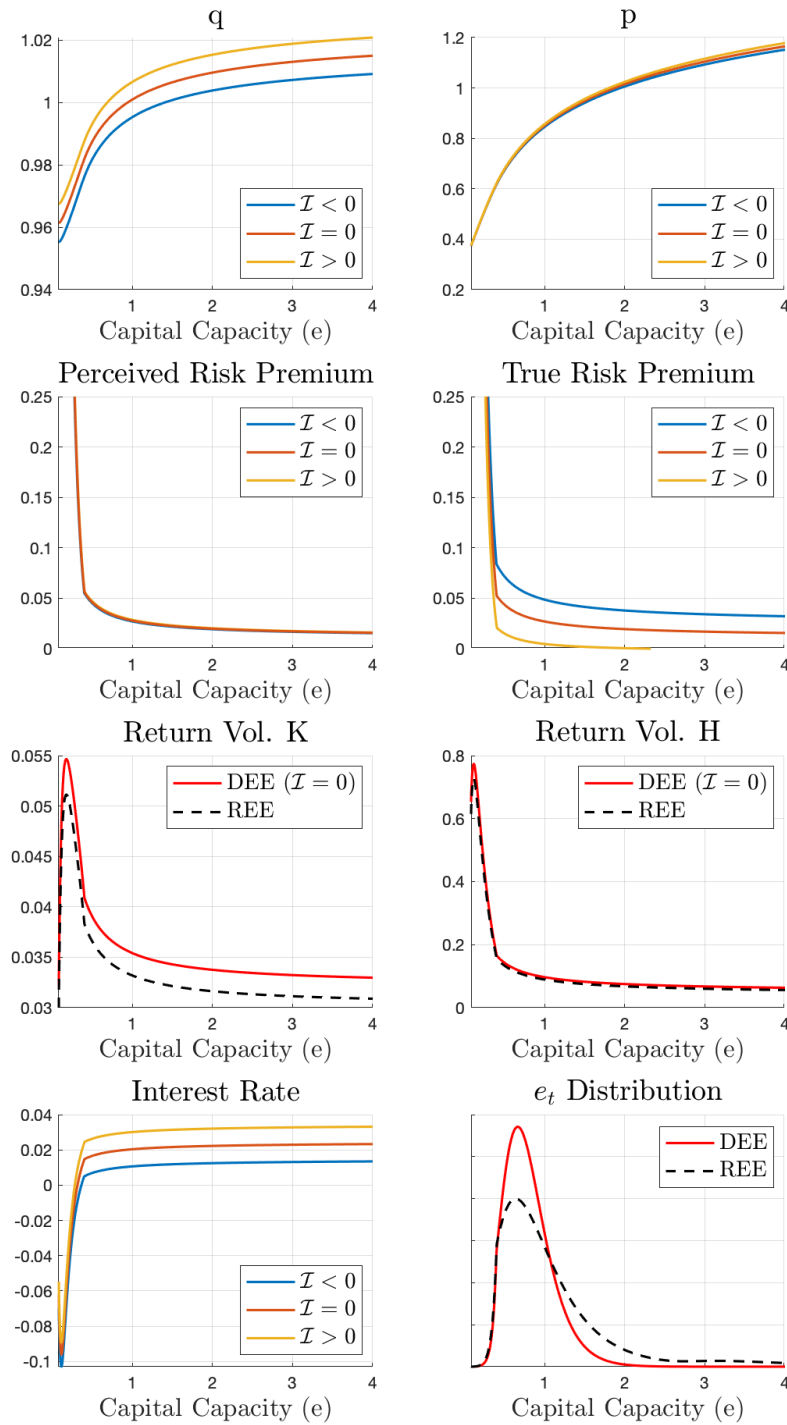


Figure 10: **Additional price and policy functions.** See Figure 2 for a description. This figure also contains information about delevered risk premia, asset volatilities (σ^k and σ^h), and interest rate r_t .

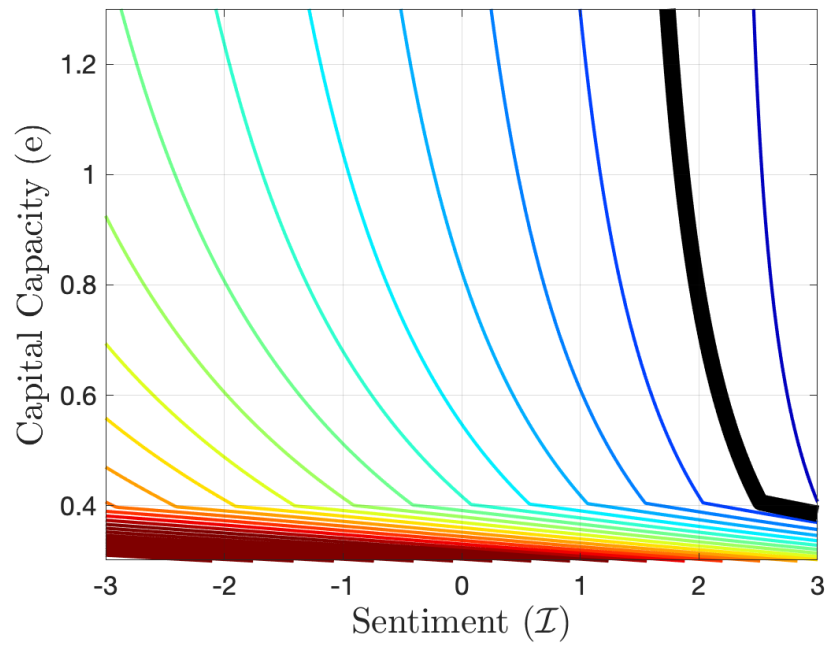


Figure 11: **Delevered risk premium contour plot.** Each contour line plots a 1% increment in the delevered risk premium earned by financial intermediaries. The thickened black line marks where intermediaries earn a 0% risk premium, such that risk premia are *negative* to the right of that line. Crisis nonlinearities are illustrated by the kinks in the contour lines that arise at a capital capacity level of roughly 0.4.

Sentiment-Driven Financial Crises.

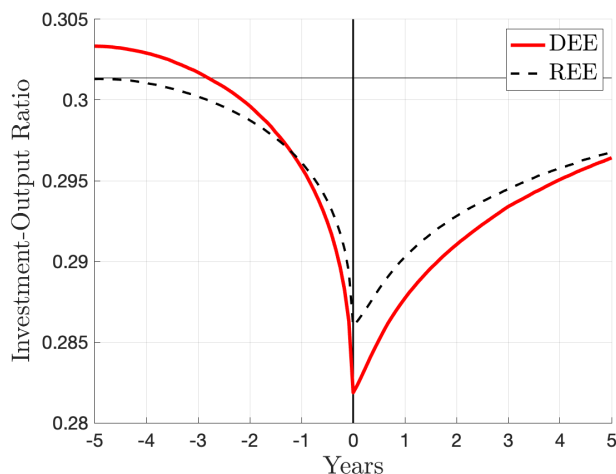


Figure 12: **Investment around crises.** This figure is similar to Figure 6, but plots the average path of the investment-output ratio $\frac{i_t}{A}$ around financial crises. The solid red line plots the DEE, and the dashed black line plots the REE. The unconditional mean investment-output ratio in the DEE is marked by the thin horizontal line. Comparing the two equilibria, pre-crisis investment is higher in the DEE, indicating elevated sentiment in the buildup to crises. Investment in the DEE subsequently drops further and is slower to recover because depressed sentiment drags down growth in the aftermath of crises. This holds even though capital capacity e_t recovers more quickly in the DEE than in the REE (see Table 2). This illustrates that diagnostic expectations dislocate the recovery on “Wall Street” from the recovery on “Main Street.”

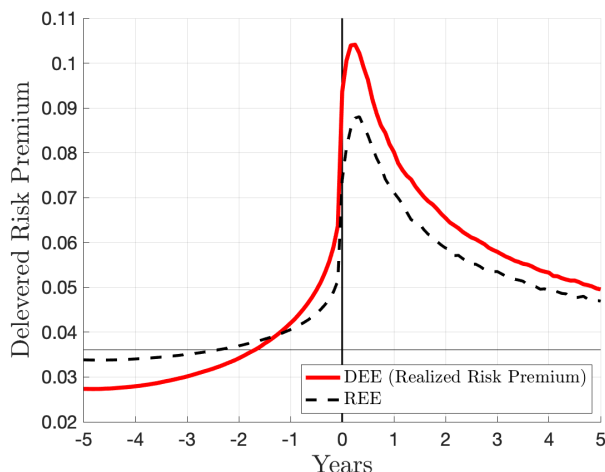


Figure 13: **Risk premia around crises.** This figure is similar to Figure 6, but compares crisis risk premia in the DEE to the REE. The solid red line plots the DEE, and the dashed black line plots the REE. Comparing the two equilibria, pre-crisis risk premia are lower in the DEE, indicating elevated sentiment in the buildup to crises. Risk premia in the DEE subsequently spike higher because depressed sentiment drags down asset prices in the aftermath of crises.

Boom-Bust Investment Cycles.

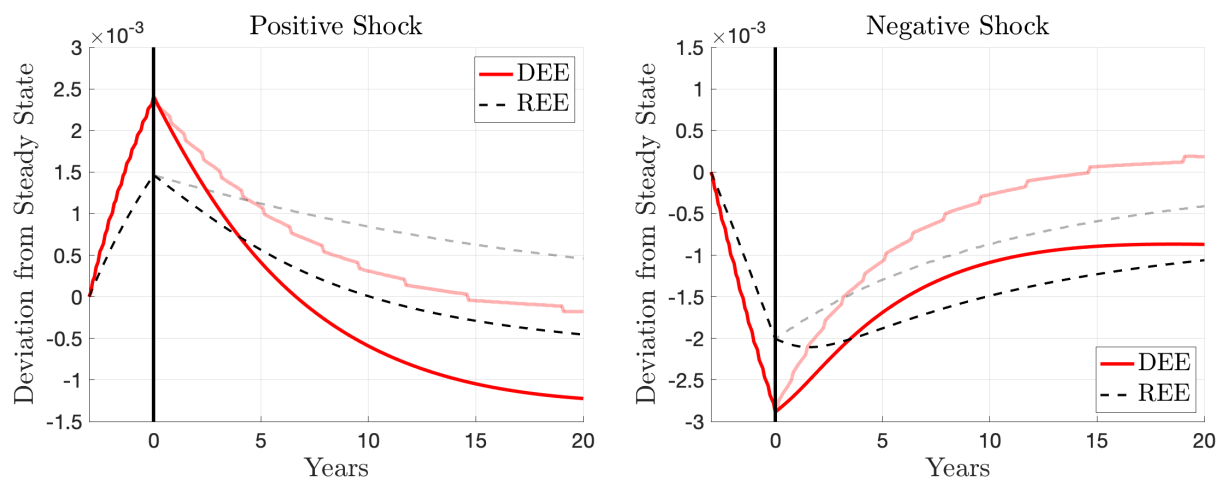


Figure 14: **Investment rate IRFs: $\mathbb{E}_0[i_\tau]$.** The baseline analysis in Figure 7 sets shocks to 0 for all $\tau \geq 0$ (shown here with transparent lines for reference). This figure instead plots the expected future investment rate $\mathbb{E}_0[i_\tau]$. These two approaches are not equivalent in this nonlinear model. In particular, asymmetric financial frictions mean that the long-run expected investment rate is less than the investment rate in the stochastic steady state. The expected investment rate is calculated using the Feynman-Kac formula (see Appendix D.3 for numerical details).

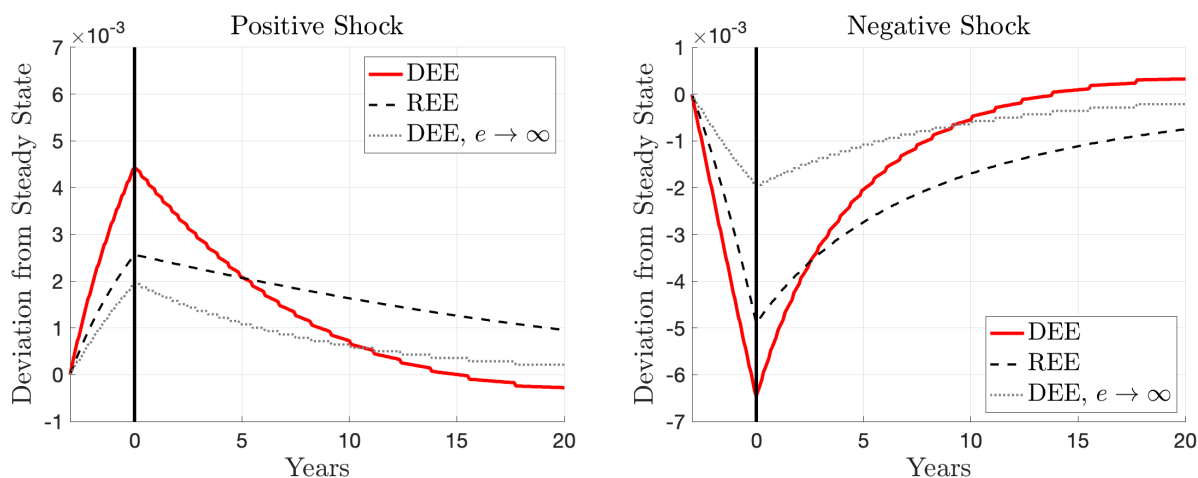


Figure 15: **Investment rate IRFs: 2SD shock.** See Figure 7 for a description. This figure replicates the investment rate IRF analysis, but doubles the size of the initial impulse. Due to the model's nonlinearity, the larger shock sequence produces a starker asymmetry between the positive and negative shock cases.

Macro-Financial Autocorrelations.

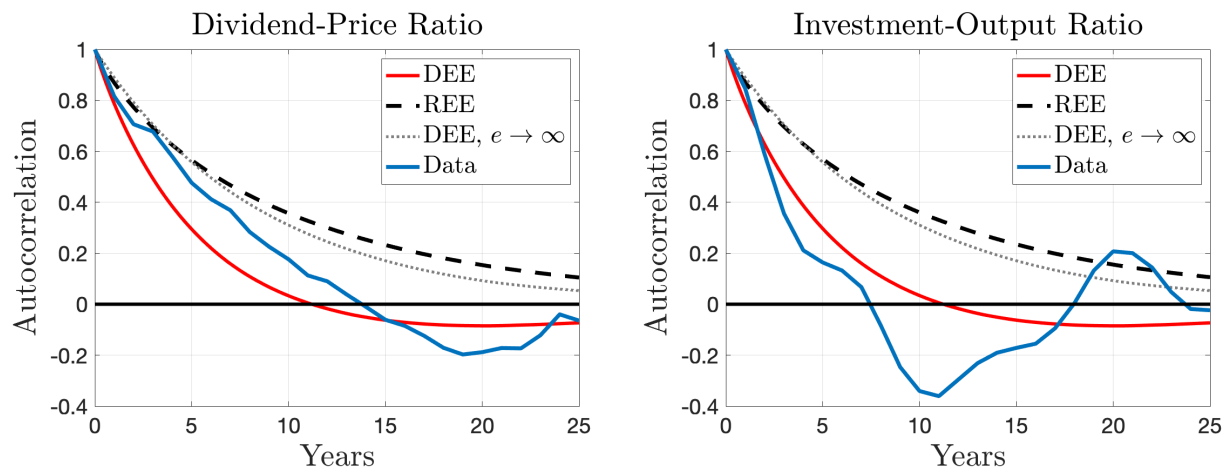


Figure 16: **Persistence: data and model.** This figure replicates Figure 9 using only U.S. data from 1950 – 2016.

	DEE	REE	Bansal-Yaron (S.E.)
AC(1)	0.19	0.09	0.49 (0.14)
AC(2)	0.15	0.07	0.15 (0.22)
AC(5)	0.08	0.05	-0.08 (0.10)
AC(10)	0.02	0.03	0.05 (0.09)
AC(20)	-0.01	0.01	-
VR(2)	1.19	1.09	1.61 (0.34)
VR(5)	1.62	1.29	2.01 (1.23)
VR(10)	2.05	1.54	1.57 (2.07)

Table 6: **Consumption growth autocorrelations.** This table reports (annual) autocorrelations and variance ratios for consumption growth. For reference I provide the empirical estimates from [Bansal and Yaron \(2004\)](#). In this exercise, both the DEE and the REE are broadly consistent with the data. However, the difference between the DEE and the REE is informative about the role of beliefs. The DEE features larger autocorrelations at first, which is evidence of the short-run amplification effect of beliefs. Over longer horizons the feedback from behavioral frictions to financial frictions implies that the initial amplification does not persist, which is why the autocorrelations also decay more quickly in the DEE.

C Equilibrium Solution Details

Here I detail how to solve for a Diagnostic Expectations Equilibrium (DEE) that is Markov in state variables e_t, \mathcal{I}_t , and K_t . Brunnermeier and Sannikov (2016) provide an excellent treatment of the techniques used here.

C.1 The Diagnostic Expectations Equilibrium

I postulate that agents perceive that q_t and p_t evolve as follows:

$$\frac{\widehat{dq}_t}{q_t} = \widehat{\mu}_t^q dt + \widehat{\sigma}_t^q dZ_t \quad (38)$$

$$\frac{\widehat{dp}_t}{p_t} = \widehat{\mu}_t^p dt + \widehat{\sigma}_t^p dZ_t. \quad (39)$$

Using these postulated price processes, the perceived laws of motion for the three state variables are:

$$\frac{\widehat{dK}_t}{K_t} = (i_t - \delta)dt + \theta \mathcal{I}_t dt + \sigma dZ_t \quad (40)$$

$$\begin{aligned} \frac{\widehat{de}_t}{e_t} = & \left(r_t + \alpha_t^h \widehat{\pi}_t^h + \alpha_t^k \widehat{\pi}_t^k \right) dt - (i_t - \delta + \theta \mathcal{I}_t) dt + (\sigma^2 - \sigma(\alpha_t^h \widehat{\sigma}_t^h + \alpha_t^k \widehat{\sigma}_t^k)) dt \\ & - \eta dt + d\psi_t + (\alpha_t^h \widehat{\sigma}_t^h + \alpha_t^k \widehat{\sigma}_t^k - \sigma) dZ_t \end{aligned} \quad (41)$$

$$\frac{d\mathcal{I}_t^S}{\mathcal{I}_t} = -\kappa dt \quad (42)$$

Equations (40) and (42) were derived in Appendix A. Equation (41) can be derived using Itô's lemma to expand $e_t = \frac{\varepsilon_t}{K_t}$ under the perceived processes $\frac{\widehat{d\varepsilon}_t}{\varepsilon_t} = \widehat{dR}_t - \eta dt + d\psi_t$ and $\frac{\widehat{dK}_t}{K_t} = (i_t - \delta)dt + \theta \mathcal{I}_t dt + \sigma dZ_t$. For simplicity, I rewrite the perceived evolution of e_t as:

$$\frac{\widehat{de}_t}{e_t} = \widehat{\mu}_t^e dt + \widehat{\sigma}_t^e dZ_t.$$

Price Processes. Let $q(e, \mathcal{I})$ and $p(e, \mathcal{I})$ denote the two price functions. Applying Itô's lemma using the perceived laws of motion for the two state variables gives:

$$\widehat{\mu}_t^q = \frac{q_e(e_t, \mathcal{I}_t)}{q_t} e_t \widehat{\mu}_t^e - \frac{q_{\mathcal{I}}(e_t, \mathcal{I}_t)}{q_t} \kappa \mathcal{I}_t + \frac{1}{2} \frac{q_{ee}(e_t, \mathcal{I}_t)}{q_t} (e_t \widehat{\sigma}_t^e)^2 \quad (43)$$

$$\widehat{\sigma}_t^q = \frac{q_e(e_t, \mathcal{I}_t)}{q_t} e_t \widehat{\sigma}_t^e \quad (44)$$

$$\widehat{\mu}_t^p = \frac{p_e(e_t, \mathcal{I}_t)}{p_t} e_t \widehat{\mu}_t^e - \frac{p_{\mathcal{I}}(e_t, \mathcal{I}_t)}{p_t} \kappa \mathcal{I}_t + \frac{1}{2} \frac{p_{ee}(e_t, \mathcal{I}_t)}{p_t} (e_t \widehat{\sigma}_t^e)^2 \quad (45)$$

$$\widehat{\sigma}_t^p = \frac{p_e(e_t, \mathcal{I}_t)}{p_t} e_t \widehat{\sigma}_t^e \quad (46)$$

These formulas will prove useful throughout. Equations (43) and (45) are second-order PDEs for the price functions, which I will solve numerically. To do so, I need to pin down $\widehat{\mu}_t^q, \widehat{\mu}_t^p, \widehat{\mu}_t^e$, and $\widehat{\sigma}_t^e$, leaving only the price functions undetermined. This is where I now turn.

Market Clearing and Returns. From goods market clearing equation (21):

$$\begin{aligned} Y_t &= C_t^y + \Phi(i_t, K_t) \\ A &= \frac{C_t^y}{K_t} + i_t + \frac{\xi}{2} (i_t - \delta)^2 \\ &= \frac{1 - \phi}{\phi} \frac{D_t}{K_t} + i_t + \frac{\xi}{2} (i_t - \delta)^2, \text{ using (10) and } C_t^h = 1 \\ \frac{D_t}{K_t} &= \frac{\phi}{1 - \phi} \left[A - i_t - \frac{\xi}{2} (i_t - \delta)^2 \right]. \end{aligned}$$

Since equation (12) gives $i_t = \delta + \frac{q_t - 1}{\xi}$, this pins down $\frac{D_t}{K_t}$ as a function of q_t .

D_t is the dividend paid on housing, and this expression can now be plugged into housing returns as follows:

$$\begin{aligned} \widehat{dR}_t^h &= \frac{\widehat{dP}_t + D_t dt}{P_t} \\ &= \frac{\widehat{d}(p_t K_t)}{p_t K_t} + \frac{D_t}{p_t K_t} dt \\ &= \frac{\widehat{d}(p_t K_t)}{p_t K_t} + \frac{\frac{\phi}{1 - \phi} [A - i_t - \frac{\xi}{2} (i_t - \delta)^2]}{p_t} dt. \end{aligned}$$

Applying Itô's lemma to the first term:

$$\begin{aligned}\widehat{dR}_t^h &= \left[\widehat{\mu}_t^p + i_t - \delta + \theta \mathcal{I}_t + \sigma \widehat{\sigma}_t^p + \frac{\phi}{1-\phi} \frac{A - i_t - \frac{\xi}{2}(i_t - \delta)^2}{p_t} \right] dt + (\sigma + \widehat{\sigma}_t^p) dZ_t \\ &= (\widehat{\pi}_t^h + r_t) dt + \widehat{\sigma}_t^h dZ_t.\end{aligned}$$

Equation (17) gives a similar process for capital returns. Repeating (17) here:

$$\begin{aligned}\widehat{dR}_t^k &= \left(\frac{\nu A}{q_t} + \widehat{\mu}_t^q - \delta + \theta \mathcal{I}_t + \sigma \widehat{\sigma}_t^q \right) dt + (\sigma + \widehat{\sigma}_t^q) dZ_t \\ &= (\widehat{\pi}_t^k + r_t) dt + \widehat{\sigma}_t^k dZ_t.\end{aligned}$$

The final return process to derive is the risk-free interest rate r_t . Starting again from market clearing:

$$\begin{aligned}C_t^y &= Y_t - \Phi(i_t, K_t) \\ &= Y_t - i_t K_t - \frac{\xi}{2} (i_t - \delta)^2 K_t \\ &= \left(A - \delta - \frac{q_t - 1}{\xi} - \frac{(q_t - 1)^2}{2\xi} \right) K_t, \text{ using (12).}\end{aligned}$$

Now deriving the perceived evolution of C_t^y using Itô's lemma:

$$\begin{aligned}\widehat{dC}_t^y &= \left(A - \delta - \frac{q_t - 1}{\xi} - \frac{(q_t - 1)^2}{2\xi} \right) K_t ((i_t - \delta + \theta \mathcal{I}_t) dt + \sigma dZ_t) \\ &\quad - \frac{q_t d\widehat{q}_t}{\xi} K_t - \frac{K_t}{2\xi} (q_t \widehat{\sigma}_t^q)^2 dt - \frac{q_t^2}{\xi} K_t \sigma \widehat{\sigma}_t^q dt \\ \frac{\widehat{dC}_t^y}{C_t^y} &= (i_t - \delta + \theta \mathcal{I}_t) dt - \frac{\frac{1}{\xi} q_t^2 (\widehat{\mu}_t^q + \frac{1}{2} \widehat{\sigma}_t^{q^2} + \sigma \widehat{\sigma}_t^q)}{A - \delta - \frac{q_t - 1}{\xi} - \frac{(q_t - 1)^2}{2\xi}} dt + \left(\sigma - \frac{\frac{1}{\xi} q_t^2 \widehat{\sigma}_t^q}{A - \delta - \frac{q_t - 1}{\xi} - \frac{(q_t - 1)^2}{2\xi}} \right) dZ_t\end{aligned}$$

Plugging this into the interest rate formula (14):

$$r_t = \rho + \zeta \left[i_t - \delta + \theta \mathcal{I}_t - \frac{\frac{1}{\xi} q_t^2 (\widehat{\mu}_t^q + \frac{1}{2} \widehat{\sigma}_t^{q^2} + \sigma \widehat{\sigma}_t^q)}{A - \delta - \frac{q_t - 1}{\xi} - \frac{(q_t - 1)^2}{2\xi}} \right] - \frac{\zeta(\zeta + 1)}{2} \left[\sigma - \frac{\frac{1}{\xi} q_t^2 \widehat{\sigma}_t^q}{A - \delta - \frac{q_t - 1}{\xi} - \frac{(q_t - 1)^2}{2\xi}} \right]^2 \quad (47)$$

Intermediary Optimality. From equation (41), it is the case that $\alpha_t^k \widehat{\sigma}_t^k + \alpha_t^h \widehat{\sigma}_t^h = \widehat{\sigma}_t^e + \sigma$. Using this in equation (20) gives:

$$\frac{\widehat{\pi}_t^h}{\widehat{\sigma}_t^h} = \frac{\widehat{\pi}_t^k}{\widehat{\sigma}_t^k} = \gamma(\widehat{\sigma}_t^e + \sigma).$$

Recall $\widehat{\sigma}_t^k = \sigma + \widehat{\sigma}_t^q$ and $\widehat{\sigma}_t^h = \sigma + \widehat{\sigma}_t^p$. Combining the banker's optimality condition with the perceived return on capital:

$$\begin{aligned} \gamma(\widehat{\sigma}_t^e + \sigma) &= \frac{\widehat{\pi}_t^k}{\widehat{\sigma}_t^k} \\ &= \frac{\left(\frac{\nu A}{q_t} + \widehat{\mu}_t^q - \delta + \theta \mathcal{I}_t + \sigma \widehat{\sigma}_t^q\right) - r_t}{\sigma + \widehat{\sigma}_t^q} \\ &= \frac{\left(\frac{\nu A}{q_t} + \widehat{\mu}_t^q - \delta + \theta \mathcal{I}_t + \sigma \frac{q_e(e_t, \mathcal{I}_t)}{q_t} e_t \widehat{\sigma}_t^e\right) - r_t}{\sigma + \frac{q_e(e_t, \mathcal{I}_t)}{q_t} e_t \widehat{\sigma}_t^e}, \text{ using equation (44)} \\ \gamma(\widehat{\sigma}_t^e + \sigma) \left(\sigma + \frac{q_e(e_t, \mathcal{I}_t)}{q_t} e_t \widehat{\sigma}_t^e\right) &= \left(\frac{\nu A}{q_t} + \widehat{\mu}_t^q - \delta + \theta \mathcal{I}_t + \sigma \frac{q_e(e_t, \mathcal{I}_t)}{q_t} e_t \widehat{\sigma}_t^e\right) - r_t. \end{aligned} \quad (48)$$

Proceeding similarly for housing returns:

$$\begin{aligned} \gamma(\widehat{\sigma}_t^e + \sigma) &= \frac{\widehat{\pi}_t^h}{\widehat{\sigma}_t^h} \\ &= \frac{\widehat{\mu}_t^p + i_t - \delta + \theta \mathcal{I}_t + \sigma \widehat{\sigma}_t^p + \frac{D_t}{p_t K_t} - r_t}{\sigma + \widehat{\sigma}_t^p} \\ &= \frac{\widehat{\mu}_t^p + i_t - \delta + \theta \mathcal{I}_t + \sigma \frac{p_e(e_t, \mathcal{I}_t)}{p_t} e_t \widehat{\sigma}_t^e + \frac{D_t}{p_t K_t} - r_t}{\sigma + \frac{p_e(e_t, \mathcal{I}_t)}{p_t} e_t \widehat{\sigma}_t^e}, \text{ using (46)} \\ \gamma(\widehat{\sigma}_t^e + \sigma) \left(\sigma + \frac{p_e(e_t, \mathcal{I}_t)}{p_t} e_t \widehat{\sigma}_t^e\right) &= \widehat{\mu}_t^p + i_t - \delta + \theta \mathcal{I}_t + \sigma \frac{p_e(e_t, \mathcal{I}_t)}{p_t} e_t \widehat{\sigma}_t^e + \frac{D_t}{p_t K_t} - r_t. \end{aligned} \quad (49)$$

Pinning Down $\widehat{\sigma}_t^e$. Equations (48) and (49) express $\widehat{\mu}_t^q$ and $\widehat{\mu}_t^p$ in terms of prices, state variables, and $\widehat{\sigma}_t^e$. The final step is to pin down $\widehat{\sigma}_t^e$:

$$\begin{aligned}
\widehat{\sigma}_t^e &= \alpha_t^h \widehat{\sigma}_t^h + \alpha_t^k \widehat{\sigma}_t^k - \sigma \\
&= \alpha_t^h (\sigma + \widehat{\sigma}_t^p) + \alpha_t^k (\sigma + \widehat{\sigma}_t^q) - \sigma \\
&= \frac{K_t}{E_t} \left[p_t (\sigma + \widehat{\sigma}_t^p) + q_t (\sigma + \widehat{\sigma}_t^q) \right] - \sigma, \text{ using (22) and (23)} \\
&= \frac{K_t}{E_t} \left[p_t \left(\sigma + \frac{p_e(e_t, \mathcal{I}_t)}{p_t} e_t \widehat{\sigma}_t^e \right) + q_t \left(\sigma + \frac{q_e(e_t, \mathcal{I}_t)}{q_t} e_t \widehat{\sigma}_t^e \right) \right] - \sigma \\
&= \frac{K_t}{E_t} \left[\left(p_t + q_t - \frac{E_t}{K_t} \right) \sigma + (p_e(e_t, \mathcal{I}_t) + q_e(e_t, \mathcal{I}_t)) e_t \widehat{\sigma}_t^e \right] \\
e_t \widehat{\sigma}_t^e \left(\frac{1}{e_t} - \frac{K_t}{E_t} (p_e(e_t, \mathcal{I}_t) + q_e(e_t, \mathcal{I}_t)) \right) &= \frac{K_t}{E_t} \left(p_t + q_t - \frac{E_t}{K_t} \right) \sigma \\
e_t \widehat{\sigma}_t^e &= \frac{K_t}{E_t} \frac{(p_t + q_t - \frac{E_t}{K_t}) \sigma}{\frac{1}{e_t} - \frac{K_t}{E_t} p_e(e_t, \mathcal{I}_t) - \frac{K_t}{E_t} q_e(e_t, \mathcal{I}_t)} \\
e_t \widehat{\sigma}_t^e &= \frac{(p_t + q_t - \frac{E_t}{K_t}) \sigma}{\frac{E_t}{K_t} \frac{1}{e_t} - p_e(e_t, \mathcal{I}_t) - q_e(e_t, \mathcal{I}_t)}. \tag{50}
\end{aligned}$$

Recall that $E_t = \min\{\mathcal{E}_t, (1-\lambda)(q_t K_t + p_t K_t)\}$, or equivalently $\frac{E_t}{K_t} = \min\{e_t, (1-\lambda)(q_t + p_t)\}$. Thus, equation (50) expresses $\widehat{\sigma}_t^e$ in terms of the two price functions and the two state variables e_t and \mathcal{I}_t .

Solving for Prices. I can now solve for price functions $q(e, \mathcal{I})$ and $p(e, \mathcal{I})$. Specifically, they are given by the following system of second-order PDEs:

$$\begin{aligned}
q_t \widehat{\mu}_t^q &= q_e(e_t, \mathcal{I}_t) e_t \widehat{\mu}_t^e - q_{\mathcal{I}}(e_t, \mathcal{I}_t) \kappa \mathcal{I}_t + \frac{1}{2} q_{ee}(e_t, \mathcal{I}_t) (e_t \widehat{\sigma}_t^e)^2 \\
p_t \widehat{\mu}_t^p &= p_e(e_t, \mathcal{I}_t) e_t \widehat{\mu}_t^e - p_{\mathcal{I}}(e_t, \mathcal{I}_t) \kappa \mathcal{I}_t + \frac{1}{2} p_{ee}(e_t, \mathcal{I}_t) (e_t \widehat{\sigma}_t^e)^2
\end{aligned}$$

All terms in this system of second-order PDEs have now been expressed in terms of state variables e_t and \mathcal{I}_t , exogenous parameters, and price functions. Specifically, r_t , $\widehat{\mu}_t^q$, and $\widehat{\mu}_t^p$ are given by equations (47), (48) and (49). $\widehat{\mu}_t^e$ is given by (41). Equations (44) and (46) give $\widehat{\sigma}_t^q$ and $\widehat{\sigma}_t^p$ in terms of the price functions and $\widehat{\sigma}_t^e$. Equation (50) closes the loop by solving for $\widehat{\sigma}_t^e$ in terms of the two price functions.

This system of PDEs is solved numerically. Details are in Appendix D.

C.2 True Laws of Motion

As with the perceived laws of motion, I begin by postulating that q_t and p_t truly evolve according to:

$$\frac{dq_t}{q_t} = \mu_t^q dt + \sigma_t^q dZ_t \quad (51)$$

$$\frac{dp_t}{p_t} = \mu_t^p dt + \sigma_t^p dZ_t. \quad (52)$$

The true evolution of the three state variables is:

$$\frac{dK_t}{K_t} = (i_t - \delta)dt + \sigma dZ_t, \quad (53)$$

$$\begin{aligned} \frac{de_t}{e_t} &= (r_t + \alpha_t^h \pi_t^h + \alpha_t^k \pi_t^k)dt - (i_t - \delta)dt + (\sigma^2 - \sigma(\alpha_t^h \sigma_t^h + \alpha_t^k \sigma_t^k))dt \\ &\quad - \eta dt + d\psi_t + (\alpha_t^h \sigma_t^h + \alpha_t^k \sigma_t^k - \sigma)dZ_t \end{aligned} \quad (54)$$

$$d\mathcal{I}_t = -\kappa \mathcal{I}_t dt + \sigma dZ_t \quad (55)$$

As above, equation (54) can be derived using Itô's lemma to expand $e_t = \frac{\mathcal{E}_t}{K_t}$ under the true processes $\frac{d\mathcal{E}_t}{\mathcal{E}_t} = d\tilde{R}_t - \eta dt + d\psi_t$ and $\frac{dK_t}{K_t} = (i_t - \delta)dt + \sigma dZ_t$. For simplicity, I rewrite the true evolution of e_t as:

$$\frac{de_t}{e_t} = \mu_t^e dt + \sigma_t^e dZ_t.$$

Price Processes. The methods developed above show how to solve for price functions $q(e, \mathcal{I})$ and $p(e, \mathcal{I})$. Applying Itô's lemma to these price functions using the true laws of

motion for the two state variables gives:

$$\mu_t^q = \frac{q_e(e_t, \mathcal{I}_t)}{q_t} e_t \mu_t^e - \frac{q_{\mathcal{I}}(e_t, \mathcal{I}_t)}{q_t} \kappa \mathcal{I}_t + \frac{q_{e\mathcal{I}}(e_t, \mathcal{I}_t)}{q_t} \sigma(e_t \sigma_t^e) + \frac{1}{2} \frac{q_{ee}(e_t, \mathcal{I}_t)}{q_t} (e_t \sigma_t^e)^2 + \frac{1}{2} \frac{q_{\mathcal{I}\mathcal{I}}(e_t, \mathcal{I}_t)}{q_t} \sigma^2 \quad (56)$$

$$\sigma_t^q = \frac{q_e(e_t, \mathcal{I}_t)}{q_t} e_t \sigma_t^e + \frac{q_{\mathcal{I}}(e_t, \mathcal{I}_t)}{q_t} \sigma \quad (57)$$

$$\mu_t^p = \frac{p_e(e_t, \mathcal{I}_t)}{p_t} e_t \mu_t^e - \frac{p_{\mathcal{I}}(e_t, \mathcal{I}_t)}{p_t} \kappa \mathcal{I}_t + \frac{p_{e\mathcal{I}}(e_t, \mathcal{I}_t)}{p_t} \sigma(e_t \sigma_t^e) + \frac{1}{2} \frac{p_{ee}(e_t, \mathcal{I}_t)}{p_t} (e_t \sigma_t^e)^2 + \frac{1}{2} \frac{p_{\mathcal{I}\mathcal{I}}(e_t, \mathcal{I}_t)}{p_t} \sigma^2 \quad (58)$$

$$\sigma_t^p = \frac{p_e(e_t, \mathcal{I}_t)}{p_t} e_t \sigma_t^e + \frac{p_{\mathcal{I}}(e_t, \mathcal{I}_t)}{p_t} \sigma \quad (59)$$

Market Clearing and Returns. Following similar steps as above, the true housing return process is given by:

$$\begin{aligned} dR_t^h &= \frac{dP_t + D_t dt}{P_t} \\ &= \frac{d(p_t K_t)}{p_t K_t} + \frac{D_t}{p_t K_t} dt \\ &= \left[\mu_t^p + i_t - \delta + \sigma \sigma_t^p + \frac{\phi}{1 - \phi} \frac{A - i_t - \frac{\xi}{2}(i_t - \delta)^2}{p_t} \right] dt + (\sigma + \sigma_t^p) dZ_t \\ &= (\pi_t^h + r_t) dt + \sigma_t^h dZ_t. \end{aligned}$$

The true process for capital returns is given by:

$$\begin{aligned} dR_t^k &= \left(\frac{\nu A}{q_t} + \mu_t^q - \delta + \sigma \sigma_t^q \right) dt + (\sigma + \sigma_t^q) dZ_t \\ &= (\pi_t^k + r_t) dt + \sigma_t^k dZ_t. \end{aligned}$$

Pinning Down σ_t^e . Solving for the true volatility of e_t :

$$\begin{aligned}
\sigma_t^e &= \alpha_t^h \sigma_t^h + \alpha_t^k \sigma_t^k - \sigma \\
&= \alpha_t^h (\sigma + \sigma_t^p) + \alpha_t^k (\sigma + \sigma_t^q) - \sigma \\
&= \frac{K_t}{E_t} [p_t (\sigma + \sigma_t^p) + q_t (\sigma + \sigma_t^q)] - \sigma, \text{ using (22) and (23)} \\
&= \frac{K_t}{E_t} \left[p_t \left(\sigma + \frac{p_e(e_t, \mathcal{I}_t)}{p_t} e_t \sigma_t^e + \frac{p_{\mathcal{I}}(e_t, \mathcal{I}_t)}{p_t} \sigma \right) + q_t \left(\sigma + \frac{q_e(e_t, \mathcal{I}_t)}{q_t} e_t \sigma_t^e + \frac{q_{\mathcal{I}}(e_t, \mathcal{I}_t)}{q_t} \sigma \right) \right] - \sigma \\
&= \frac{K_t}{E_t} \left[(p_t + q_t + p_{\mathcal{I}}(e_t, \mathcal{I}_t) + q_{\mathcal{I}}(e_t, \mathcal{I}_t) - \frac{E_t}{K_t}) \sigma + (p_e(e_t, \mathcal{I}_t) + q_e(e_t, \mathcal{I}_t)) e_t \sigma_t^e \right] \\
e_t \sigma_t^e \left[\frac{1}{e_t} - \frac{K_t}{E_t} p_e(e_t, \mathcal{I}_t) - \frac{K_t}{E_t} q_e(e_t, \mathcal{I}_t) \right] &= \frac{K_t}{E_t} (p_t + q_t + p_{\mathcal{I}}(e_t, \mathcal{I}_t) + q_{\mathcal{I}}(e_t, \mathcal{I}_t) - \frac{E_t}{K_t}) \sigma \\
e_t \sigma_t^e &= \frac{K_t}{E_t} \frac{(p_t + q_t + p_{\mathcal{I}}(e_t, \mathcal{I}_t) + q_{\mathcal{I}}(e_t, \mathcal{I}_t) - \frac{E_t}{K_t}) \sigma}{\frac{1}{e_t} - \frac{K_t}{E_t} p_e(e_t, \mathcal{I}_t) - \frac{K_t}{E_t} q_e(e_t, \mathcal{I}_t)} \\
e_t \sigma_t^e &= \frac{(p_t + q_t + p_{\mathcal{I}}(e_t, \mathcal{I}_t) + q_{\mathcal{I}}(e_t, \mathcal{I}_t) - \frac{E_t}{K_t}) \sigma}{\frac{E_t}{K_t} \frac{1}{e_t} - p_e(e_t, \mathcal{I}_t) - q_e(e_t, \mathcal{I}_t)}. \tag{60}
\end{aligned}$$

C.3 Verifying “Equity Member” Portfolio Choice

The main text assumes that the “equity member” will invest the maximal amount into the equity of the financial sector. This assumption must be verified ex-post given the resulting equilibrium.

The household maximizes the value function in equation (9), where $C_t = (c_t^y)^{1-\phi} (c_t^h)^\phi = (c_t^y)^{1-\phi}$, since $c^h = 1$ in equilibrium. From (9), the household accrues utility flow $\frac{(c_t^y)^{(1-\phi)(1-\gamma_h)}}{1-\gamma_h}$. Multiplying the utility function by $\frac{1}{1-\phi}$ (a positive affine transformation) shows that in equilibrium the household can be represented with power utility preferences, using relative risk aversion coefficient $\zeta = 1 - (1-\phi)(1-\gamma_h)$. Market clearing gives $c_t^y = AK_t - \Phi(i_t, K_t) = \left(A - \delta - \frac{q_t-1}{\xi} - \frac{(q_t-1)^2}{2\xi} \right) K_t$.

Let a be an arbitrary asset with perceived mean return $\widehat{\mu}^a$ and volatility $\widehat{\sigma}^a$. In equilibrium, CRRA utility implies:

$$\frac{\widehat{\mu}^a - r_t}{\widehat{\sigma}^a} = \zeta \widehat{\sigma}_t^{cy},$$

where $\widehat{\sigma}_t^{cy}$ is the perceived volatility of $\frac{dc_t^y}{c_t^y}$ (a formula is provided in Appendix C.1). Thus,

the household demands a perceived Sharpe ratio of $\zeta \widehat{\sigma}_t^{cy}$. Note that this equation need not hold with equality when there are portfolio restrictions placed on the household.

An investment in intermediary equity earns a perceived risk premium of $\alpha^k \widehat{\pi}^k + \alpha^h \widehat{\pi}^h$, with a perceived risk of $\alpha^k \widehat{\sigma}^k + \alpha^h \widehat{\sigma}^h$. From equation (20), intermediaries demand a risk premium of:

$$\begin{aligned}\widehat{\pi}_t^k &= \gamma(\alpha_t^k \widehat{\sigma}_t^k + \alpha_t^h \widehat{\sigma}_t^h) \widehat{\sigma}_t^k \\ \widehat{\pi}_t^h &= \gamma(\alpha_t^k \widehat{\sigma}_t^k + \alpha_t^h \widehat{\sigma}_t^h) \widehat{\sigma}_t^h\end{aligned}$$

For the portfolio as a whole, this implies:

$$\alpha_t^k \widehat{\pi}_t^k + \alpha_t^h \widehat{\pi}_t^h = \gamma(\alpha_t^k \widehat{\sigma}_t^k + \alpha_t^h \widehat{\sigma}_t^h)^2.$$

The equity member will invest all wealth in intermediary equity whenever the perceived Sharpe ratio on this investment is weakly greater than $\zeta \widehat{\sigma}_t^{cy}$:

$$\begin{aligned}\frac{\gamma(\alpha_t^k \widehat{\sigma}_t^k + \alpha_t^h \widehat{\sigma}_t^h)^2}{\alpha_t^k \widehat{\sigma}_t^k + \alpha_t^h \widehat{\sigma}_t^h} &\geq \zeta \widehat{\sigma}_t^{cy}, \text{ or equivalently} \\ \gamma(\alpha_t^k \widehat{\sigma}_t^k + \alpha_t^h \widehat{\sigma}_t^h) &\geq \zeta \widehat{\sigma}_t^{cy}.\end{aligned}$$

This condition is verified numerically over the entire state space.

D Numerical Methods

Before outlining the numerical methods, additional notation is required. The state variables $\{e, \mathcal{I}\}$ can be represented as a two-dimensional Itô process, denoted \mathcal{S} . Agents perceive that \mathcal{S} evolves according to:

$$\widehat{d\mathcal{S}}_t = \begin{bmatrix} \widehat{de}_t \\ d\mathcal{I}_t^S \end{bmatrix} = \begin{bmatrix} e_t \widehat{\mu}_t^e \\ -\kappa \mathcal{I}_t \end{bmatrix} dt + \begin{bmatrix} e_t \widehat{\sigma}_t^e \\ 0 \end{bmatrix} dZ_t, \quad (61)$$

where Z_t is a one-dimensional Brownian motion. The true evolution of \mathcal{S} is:

$$d\mathcal{S}_t = \begin{bmatrix} de_t \\ d\mathcal{I}_t \end{bmatrix} = \begin{bmatrix} e_t \mu_t^e \\ -\kappa \mathcal{I}_t \end{bmatrix} dt + \begin{bmatrix} e_t \sigma_t^e \\ \sigma \end{bmatrix} dZ_t. \quad (62)$$

The evolution of $\widehat{d\mathcal{S}}_t$ and $d\mathcal{S}_t$ is subject to a reflecting barrier in the e dimension at \underline{e} .

To simplify notation, let \mathcal{A} denote the infinitesimal generator of \mathcal{S}_t . Let $\widehat{\mathcal{A}}$ denote the infinitesimal generator of $\widehat{\mathcal{S}}_t$.

D.1 Solving for Price Functions

As shown in Appendix C, price functions $q(e, \mathcal{I})$ and $p(e, \mathcal{I})$ compose a system of second-order PDEs:

$$\begin{aligned} q_t \widehat{\mu}_t^q &= q_e(e_t, \mathcal{I}_t) e_t \widehat{\mu}_t^e - q_{\mathcal{I}}(e_t, \mathcal{I}_t) \kappa \mathcal{I}_t + \frac{1}{2} q_{ee}(e_t, \mathcal{I}_t) (e_t \widehat{\sigma}_t^e)^2 \\ &= \widehat{\mathcal{A}}q_t \end{aligned} \quad (63)$$

$$\begin{aligned} p_t \widehat{\mu}_t^p &= p_e(e_t, \mathcal{I}_t) e_t \widehat{\mu}_t^e - p_{\mathcal{I}}(e_t, \mathcal{I}_t) \kappa \mathcal{I}_t + \frac{1}{2} p_{ee}(e_t, \mathcal{I}_t) (e_t \widehat{\sigma}_t^e)^2 \\ &= \widehat{\mathcal{A}}p_t \end{aligned} \quad (64)$$

In order to solve for these price functions I use finite-difference methods. The numerical methods appendix of [Achdou et al. \(2022\)](#) provides an excellent reference. See also [d'Avernas and Vandeweyer \(2021\)](#). I assume knowledge of these methods here.

Algorithm. I solve for price functions using two nested while-loops. In the outer loop, I iterate over lower boundary \underline{e} . In the inner loop, I take \underline{e} as given and iterate over price functions p and q until convergence. Details for the inner loop are provided below. The outer loop continues to iterate over \underline{e} until the resulting Sharpe ratio at $e = \underline{e}$, $\mathcal{I} = 0$ is close to the calibration target in Table 1.

I create a discretized grid over state variables e and \mathcal{I} .⁶⁵ Let subscript i denote the gridpoints in the e -dimension, and let subscript j denote the gridpoints in the \mathcal{I} -dimension. The algorithm is as follows. Let $n = 1, 2, \dots$ track the current loop iteration.

1. Guess price functions $q_{i,j}^0$ and $p_{i,j}^0$ at each grid point $\{i, j\}$.
2. Solve for $\widehat{\mu}_{i,j}^q$, $\widehat{\mu}_{i,j}^p$, $\widehat{\mu}_{i,j}^e$, and $\widehat{\sigma}_{i,j}^e$ using the previous iteration's price functions of $q_{i,j}^{n-1}$ and $p_{i,j}^{n-1}$ (or the initial guess). To do so, use equation (50) to solve for $\widehat{\sigma}_{i,j}^e$, (48) to solve for $\widehat{\mu}_{i,j}^q$, (49) to solve for $\widehat{\mu}_{i,j}^p$, and (41) to solve for $\widehat{\mu}_{i,j}^e$. Next, construct the discretized infinitesimal generator, denoted $\widehat{\mathbf{A}}^{n-1}$, using $\widehat{\mu}_{i,j}^e$ and $\widehat{\sigma}_{i,j}^e$.⁶⁶ Note that $\widehat{\mathbf{A}}$ features a reflecting barrier at \underline{e} .⁶⁷
3. Use an implicit scheme to solve for price functions $q_{i,j}^n$ and $p_{i,j}^n$:

$$\frac{q_{i,j}^n - q_{i,j}^{n-1}}{\Delta} + \widehat{\mu}_{i,j}^q q_{i,j}^n = \widehat{\mathbf{A}}^{n-1} q_{i,j}^n, \text{ which implies}$$

$$q_{i,j}^n = \left(\frac{1}{\Delta} \mathbf{I} + \text{diag}(\widehat{\mu}_{i,j}^q) - \widehat{\mathbf{A}}^{n-1} \right)^{-1} \left(\frac{1}{\Delta} q_{i,j}^{n-1} \right).$$

Similarly,⁶⁸

$$p_{i,j}^n = \left(\frac{1}{\Delta} \mathbf{I} + \text{diag}(\widehat{\mu}_{i,j}^p) - \widehat{\mathbf{A}}^{n-1} \right)^{-1} \left(\frac{1}{\Delta} p_{i,j}^{n-1} \right).$$

⁶⁵The grid over e is non-uniform.

⁶⁶" $n - 1$ " notation is used because $\widehat{\mathbf{A}}$ is constructed using the price functions from iteration $n - 1$.

⁶⁷Implementation details are in Achdou et al. (2022).

⁶⁸Since $p_e(\underline{e}, \mathcal{I}) = \frac{p(\underline{e}, \mathcal{I})^\beta}{1 + \underline{e}\beta}$ (see Appendix B.3 for details), in the numerical solution for p the discretized matrix $\widehat{\mathbf{A}}$ is amended to ensure that $p_{1,j}^n = p_{2,j}^n - \frac{p_{1,j}^{n-1}\beta}{1 + \underline{e}\beta} \times \Delta e$, where Δe denotes the grid increment in the e -dimension.

These equations define $q_{i,j}^n$ and $p_{i,j}^n$ as functions of information from iteration $n - 1$. Parameter Δ is the step size, and governs how quickly the price functions are updated. Convergence is not guaranteed, so Δ should not be set too large.

4. If price functions have converged within a pre-specified tolerance, stop. If not, go to step 2 and repeat.

Once the algorithm has converged, I use the final values of $q_{i,j}$ and $p_{i,j}$ to solve for the realized evolution of state variables e_t and \mathcal{I}_t . The realized evolution of price functions p_t and q_t can also be derived (similar to step 2).

D.2 Kolmogorov Equations

Kolmogorov Forward Equation. Readers should refer to the numerical appendix of [Achdou et al. \(2022\)](#) for details. Let $g_t(e, \mathcal{I})$ denote a probability density function over e and \mathcal{I} . The Kolmogorov forward equation (KF) gives $\frac{\partial}{\partial t} g_t$. A stationary distribution is a distribution \bar{g} that solves $\frac{\partial}{\partial t} \bar{g} = 0$.

A benefit of finite-difference methods is that the KF equation comes “for free.” Let $g_{i,j}^t$ denote a discretized distribution over e and \mathcal{I} at time t . The perceived evolution of $g_{i,j}^t$ is given by:

$$\frac{\widehat{g_{i,j}^{t+\Delta t}} - g_{i,j}^t}{\Delta t} = (\widehat{\mathbf{A}})^T \widehat{g_{i,j}^{t+\Delta t}} \implies \widehat{g_{i,j}^{t+\Delta t}} = (\mathbf{I} - \Delta t (\widehat{\mathbf{A}})^T)^{-1} g_{i,j}^t.$$

The true evolution of $g_{i,j}^t$ is given by:

$$\frac{g_{i,j}^{t+\Delta t} - g_{i,j}^t}{\Delta t} = (\mathbf{A})^T g_{i,j}^{t+\Delta t} \implies g_{i,j}^{t+\Delta t} = (\mathbf{I} - \Delta t (\mathbf{A})^T)^{-1} g_{i,j}^t.$$

Kolmogorov Backward Equation. The Kolmogorov backward equation (KB) is used to derive the hitting probabilities in [Figure 5](#).

Let $\bar{e}_{crisis}(\mathcal{I})$ denote the upper boundary of the crisis region for sentiment level \mathcal{I} . For $s \in [0, T]$, let $f(e_s, \mathcal{I}_s, s)$ denote the true probability that the economy currently at $\{e_s, \mathcal{I}_s\}$ enters the crisis region between time s and T . Similarly, let $\widehat{f}(e_s, \mathcal{I}_s, s)$ denote the perceived probability. The goal is to solve for $f(e, \mathcal{I}, 0)$ and $\widehat{f}(e, \mathcal{I}, 0)$. Conditional probability function

$f(e, \mathcal{I}, s)$ is the solution to:

$$0 = \frac{\partial f(e, \mathcal{I}, s)}{\partial s} + \mathcal{A}f(e, \mathcal{I}, s), \text{ subject to boundary conditions}$$

(i) $f(e, \mathcal{I}, s) = 1$ if $e \leq \bar{e}_{crisis}(\mathcal{I})$, and

(ii) $f(e, \mathcal{I}, T) = 0$ if $e > \bar{e}_{crisis}(\mathcal{I})$.

This result is stated without proof. Informally, the differential equation $0 = \frac{\partial f(e, \mathcal{I}, s)}{\partial s} + \mathcal{A}f(e, \mathcal{I}, s)$ arises from applying Itô's lemma to $f(e, \mathcal{I}, s)$ and setting the drift of the resulting expression equal to 0. The drift is set to 0 in the non-crisis region due to the law of iterated expectations: $f(e_s, \mathcal{I}_s, s) = \mathbb{E}_s[f(e_{s+dt}, \mathcal{I}_{s+dt}, s + dt)]$ and therefore $\mathbb{E}_s[df(e_s, \mathcal{I}_s, s)] = 0$. The first boundary condition sets f equal to 1 whenever the crisis region is hit. The second boundary condition is a terminal condition which assigns $f(e, \mathcal{I}, T) = 0$ if the crisis region is not hit at terminal period T . f is solved backwards from this terminal condition.

Using the perceived generator $\widehat{\mathcal{A}}$, function $\widehat{f}(e, \mathcal{I}, s)$ is the solution to:

$$0 = \frac{\partial \widehat{f}(e, \mathcal{I}, s)}{\partial s} + \widehat{\mathcal{A}}\widehat{f}(e, \mathcal{I}, s), \text{ subject to boundary conditions}$$

(i) $\widehat{f}(e, \mathcal{I}, s) = 1$ if $e \leq \bar{e}_{crisis}(\mathcal{I})$, and

(ii) $\widehat{f}(e, \mathcal{I}, T) = 0$ if $e > \bar{e}_{crisis}(\mathcal{I})$.

Numerically, the discretized versions of both \mathcal{A} and $\widehat{\mathcal{A}}$ were already generated when solving for price functions and the stationary distribution. Finite-difference methods can then be used to solve backward for f and \widehat{f} starting from the terminal condition.

D.3 Feynman-Kac Equation

The Feynman-Kac equation is used to calculate the expected investment rate profile in Appendix Figure 14. A straightforward application of the formula implies that the conditional expectation:

$$u(e, \mathcal{I}, 0) = \mathbb{E}[i(e_\tau, \mathcal{I}_\tau) \mid e_0 = e, \mathcal{I}_0 = \mathcal{I}]$$

satisfies a partial differential equation:

$$0 = \frac{\partial u(e, \mathcal{I}, s)}{\partial s} + \mathcal{A}u(e, \mathcal{I}, s),$$

subject to the terminal condition that $u(e, \mathcal{I}, \tau) = i(e, \mathcal{I})$.

Numerically, the discretized version of \mathcal{A} was already generated when solving for price functions and the stationary distribution. Finite-difference methods can then be used to solve backward for $u(e, \mathcal{I}, 0)$ starting from the terminal condition.

E Diagnostic Expectations: Additional Details

E.1 Expectations of an AR(1): Equivalence to [Bordalo et al. \(2018\)](#)

Here I show how the discrete-time analogue of this paper’s formulation of diagnostic expectations relates to the model of [Bordalo et al. \(2018\)](#) when applied to exogenous AR(1) processes. In particular, I show that this paper’s specification of diagnostic expectations generalizes the original BGS specification, which can be recovered under a specific calibration of the current model.

Discrete-Time Setup. Following similar notation to BGS, let ω_t be an AR(1) process $\omega_t = b\omega_{t-1} + \epsilon_t$, where $\epsilon_t \sim \mathcal{N}(0, \sigma^2)$.

In discrete time, information measure \mathcal{I}_t is given by:

$$\mathcal{I}_t = \sum_{j=0}^{\infty} \mathcal{K}^j \epsilon_{t-j},$$

where \mathcal{K} is the discount factor governing the speed of information decay.⁶⁹ Proceeding as in [Appendix A.1](#), the background context is:

$$G_t^- = \omega_t - \mathcal{I}_t.$$

As the agent simulates the economy forward from period t , the internal representativeness parameter at simulated future time $t + \tau$ is given by:

$$\mathcal{I}_{t+\tau}^S = \sum_{j=0}^{\infty} \mathcal{K}^{j+\tau} \epsilon_{t-j}.$$

For any future value $\omega'_{t+\tau}$, the simulated future background context is:

$$G'_{t+\tau} = \omega'_{t+\tau} - \mathcal{I}_{t+\tau}^S.$$

⁶⁹If the discrete-time model is written with a period frequency of Δ years, then $\mathcal{K} = e^{-\kappa\Delta}$.

Expectations of $\omega_{t+\tau}$. As in BGS and Appendix A.1, the diagnostic agent evaluates the distribution of ω_{t+1} according to the distorted density

$$h_t^\theta(\omega'_{t+1}|\omega_t, \mathcal{I}_t) = h(\omega'_{t+1}|\omega_t) \cdot \left[\frac{h(\omega'_{t+1}|\omega_t)}{h(\omega'_{t+1}|G_t^-)} \right]^\theta \frac{1}{Z}, \quad (65)$$

where G_t^- should be interpreted as a counterfactual level of ω at time t . This implies that the diagnostic agent perceives that

$$\begin{aligned} h_t^\theta(\omega'_{t+1}|\omega_t, \mathcal{I}_t) &= \mathcal{N}(b\omega_t + \theta(b\omega_t - bG_t^-), \sigma^2) \\ &= \mathcal{N}(b\omega_t + \theta b\mathcal{I}_t, \sigma^2). \end{aligned}$$

Simulating forward, for any $\omega'_{t+\tau}$ the perceived evolution from $t + \tau$ to $t + \tau + 1$ is:

$$\begin{aligned} h_t^\theta(\omega'_{t+\tau+1}|\omega'_{t+\tau}, \mathcal{I}_{t+\tau}^S) &= \mathcal{N}(b\omega'_{t+\tau} + \theta b\mathcal{I}_{t+\tau}^S, \sigma^2) \\ &= \mathcal{N}(b\omega'_{t+\tau} + \theta b\mathcal{K}^\tau \mathcal{I}_t, \sigma^2). \end{aligned}$$

Generally, in this AR(1) context the diagnostic agent will have the following perceptions about the distribution of $\omega_{t+\tau}$:

$$\begin{aligned} h_t^\theta(\omega'_{t+1}|\omega_t, \mathcal{I}_t) &= \mathcal{N}(b\omega_t + \theta b\mathcal{I}_t, \sigma^2) \\ h_t^\theta(\omega'_{t+2}|\omega_t, \mathcal{I}_t) &= \mathcal{N}(b(b\omega_t + \theta b\mathcal{I}_t) + \theta b\mathcal{K}\mathcal{I}_t, \sigma^2 + b^2\sigma^2) \\ h_t^\theta(\omega'_{t+3}|\omega_t, \mathcal{I}_t) &= \mathcal{N}(b^2(b\omega_t + \theta b\mathcal{I}_t) + b(\theta b\mathcal{K}\mathcal{I}_t) + \theta b\mathcal{K}^2\mathcal{I}_t, \sigma^2 + b^2\sigma^2 + b^4\sigma^2) \\ &\vdots \\ h_t^\theta(\omega'_{t+\tau}|\omega_t, \mathcal{I}_t) &= \mathcal{N}\left(b^\tau\omega_t + \theta\mathcal{I}_t \left(\sum_{i=1}^{\tau} b^i \mathcal{K}^{\tau-i}\right), \sigma^2 \sum_{i=0}^{\tau-1} b^{2i}\right), \text{ or equivalently} \\ h_t^\theta(\omega'_{t+\tau}|\omega_t, \mathcal{I}_t) &= \mathcal{N}\left(b^\tau\omega_t + \theta b\mathcal{I}_t \left(\frac{b^\tau - \mathcal{K}^\tau}{b - \mathcal{K}}\right), \sigma^2 \sum_{i=0}^{\tau-1} b^{2i}\right). \end{aligned}$$

BGS Equivalence. To reproduce the AR(1) framework of BGS, take $\mathcal{K} \rightarrow 0$. In the limit, $\mathcal{I}_t = \epsilon_t$ and $G_t^- = \omega_t - \epsilon_t = b\omega_{t-1}$. In other words, background context G_t^- does not incorporate the most recent shock but fully incorporates all shocks of further lags.

Consider this paper’s iterative framework for characterizing expectations. From t to $t + 1$, expectations are biased by $\theta b\mathcal{I}_t = \theta b\epsilon_t$. So, the diagnostic distribution at time $t + 1$ is $\mathcal{N}(b\omega_t + \theta b\epsilon_t, \sigma^2)$. Because taking $\mathcal{K} \rightarrow 0$ implies that $\mathcal{I}_{t+\tau}^S = 0$ for all $\tau \geq 1$, the diagnostic distribution at time $t + 2$ is $\mathcal{N}(b(b\omega_t + \theta b\epsilon_t), \sigma^2 + b^2\sigma^2)$. The diagnostic distribution at time $t + 3$ is $\mathcal{N}(b^2(b\omega_t + \theta b\epsilon_t), \sigma^2 + b^2\sigma^2 + b^4\sigma^2)$, and so on. Using the formula above as $\mathcal{K} \rightarrow 0$, the diagnostic distribution at time $t + \tau$ is $\mathcal{N}(b^\tau(\omega_t + \theta\epsilon_t), \sigma^2 \sum_{i=0}^{\tau-1} b^{2i})$. This is identical to diagnostic expectations in BGS (see the full proof of Proposition 1 in the BGS Internet Appendix).

Moving from Discrete to Continuous Time. To pass from discrete to continuous time, one needs to set $\mathcal{K} > 0$. When $\mathcal{K} \rightarrow 0$ only the most recent shock matters. But, the concept of “only the most recent shock” varies with the length of the period. This is especially important when passing to continuous time, where the most recent shock is an instantaneous Brownian increment. Thus, in this paper I instead adopt a sentiment function \mathcal{I}_t that is based on multiple lags of past shocks (i.e., $\mathcal{K} > 0$).

E.2 Diagnostic Expectations of an Ornstein-Uhlenbeck Process

For further comparison to [Bordalo et al. \(2018\)](#), I now apply diagnostic expectations to an Ornstein-Uhlenbeck process. Ornstein-Uhlenbeck processes are the continuous-time analogue of the AR(1) processes studied in BGS. The main result of this section is that, exactly as in BGS, the extent of extrapolation depends on the true persistence of the underlying Ornstein-Uhlenbeck process. BGS argue that this is a key property of diagnostic expectations that differentiates them from mechanical extrapolation.

I consider a mean-zero Ornstein-Uhlenbeck (OU) process:

$$\omega_t = \int_0^t e^{-\alpha(t-s)} \sigma dZ_s, \tag{66}$$

which can be expressed as

$$d\omega_t = -\alpha\omega_t dt + \sigma dZ_t.$$

Parameter α controls the speed of mean reversion.

Using equation (66), the conditional distribution of $\omega_{t+\tau}$ given ω_t can be characterized as follows:

$$\begin{aligned}\omega_{t+\tau} &= \int_0^{t+\tau} e^{-\alpha(t+\tau-s)} \sigma dZ_s \\ &= e^{-\alpha\tau} \omega_t + \int_t^{t+\tau} e^{-\alpha(t+\tau-s)} \sigma dZ_s.\end{aligned}$$

Since $\{Z_t\}$ is a standard Brownian motion, the conditional mean of $\omega_{t+\tau}$ is $e^{-\alpha\tau} \omega_t$ and the conditional variance is $\frac{\sigma^2}{2\alpha}(1 - e^{-2\alpha\tau})$.⁷⁰ Therefore:

$$h(\omega'_{t+\tau}|\omega_t) = \mathcal{N}\left(e^{-\alpha\tau} \omega_t, \frac{\sigma^2}{2\alpha}(1 - e^{-2\alpha\tau})\right). \quad (67)$$

Now I model the beliefs of the diagnostic agent. Because the evolution of ω_t is exogenous, it is possible to characterize the diagnostic agent's beliefs about the distribution of $\omega_{t+\tau}$ in closed form. Given current sentiment of \mathcal{I}_t , the diagnostic agent believes that the evolution of $\omega_{t+\tau}$ in any future period $t + \tau$ is:

$$\widehat{d\omega}_{t+\tau} = -\alpha\omega_{t+\tau}dt + \theta\mathcal{I}_t e^{-\kappa\tau} dt + \sigma dZ_{t+\tau}.$$

Using this perceived law of motion, the diagnostic agent's expectations are as follows:

Proposition 4. *Let $\mathcal{D}_\tau = \left(\frac{e^{-\alpha\tau} - e^{-\kappa\tau}}{\kappa - \alpha}\right)$. When ω_t is an Ornstein-Uhlenbeck process, a diagnostic agent perceives that the distribution of $\omega_{t+\tau}$ is:*

$$h_t^\theta(\omega'_{t+\tau}|\omega_t, \mathcal{I}_t) = \mathcal{N}\left(e^{-\alpha\tau} \omega_t + \theta\mathcal{I}_t \mathcal{D}_\tau, \frac{\sigma^2}{2\alpha}(1 - e^{-2\alpha\tau})\right). \quad (68)$$

Proof. See Appendix E.2.1. □

Comparing the true distribution in equation (67) to the perceived distribution in (68) shows that diagnostic expectations bias the perceived mean of $\omega_{t+\tau}$ by $\theta\mathcal{I}_t \mathcal{D}_\tau$. Proposition 4 can be viewed as a continuous-time parallel to Proposition 1 and Corollary 1 of BGS.

⁷⁰The conditional variance can be proven using Itô isometry.

Critically, \mathcal{D}_τ has the property that the extent to which the diagnostic agent overreacts depends on the persistence α of the true OU process.

Appendix Figure 17 provides an illustration of the diagnostic expectations in equation (68). The top four panels provide four different calibrations of α , corresponding to a half-life of $\frac{1}{4}$, $\frac{1}{2}$, 1, and 2 years. The blue curve plots a realized sample path of the OU process from $t = -2$ to $t = 0$, the dashed black curve plots the rational prediction at $t = 0$, and the solid red curve plots the diagnostic prediction. The bottom panel of Appendix Figure 17 plots the difference between the diagnostic prediction and the rational prediction, which is given by $\theta \mathcal{I}_t \mathcal{D}_\tau$.

Importantly, the OU persistence parameter α is the only source of variation across these four experiments. Each simulation starts at $\omega_{-2} = 0$ and uses the same sequence of shocks from $t = -2$ to $t = 0$. The calibration of sentiment parameters κ and θ is identical in all four panels.

Appendix Figure 17 highlights how this paper’s model of diagnostic expectations differs from mechanical extrapolation: the extent of diagnosticity depends on the informativeness of past news for future events, as captured by the persistence (α) of the underlying OU process. This continuous-time result parallels a similar conclusion in BGS for AR(1) processes.

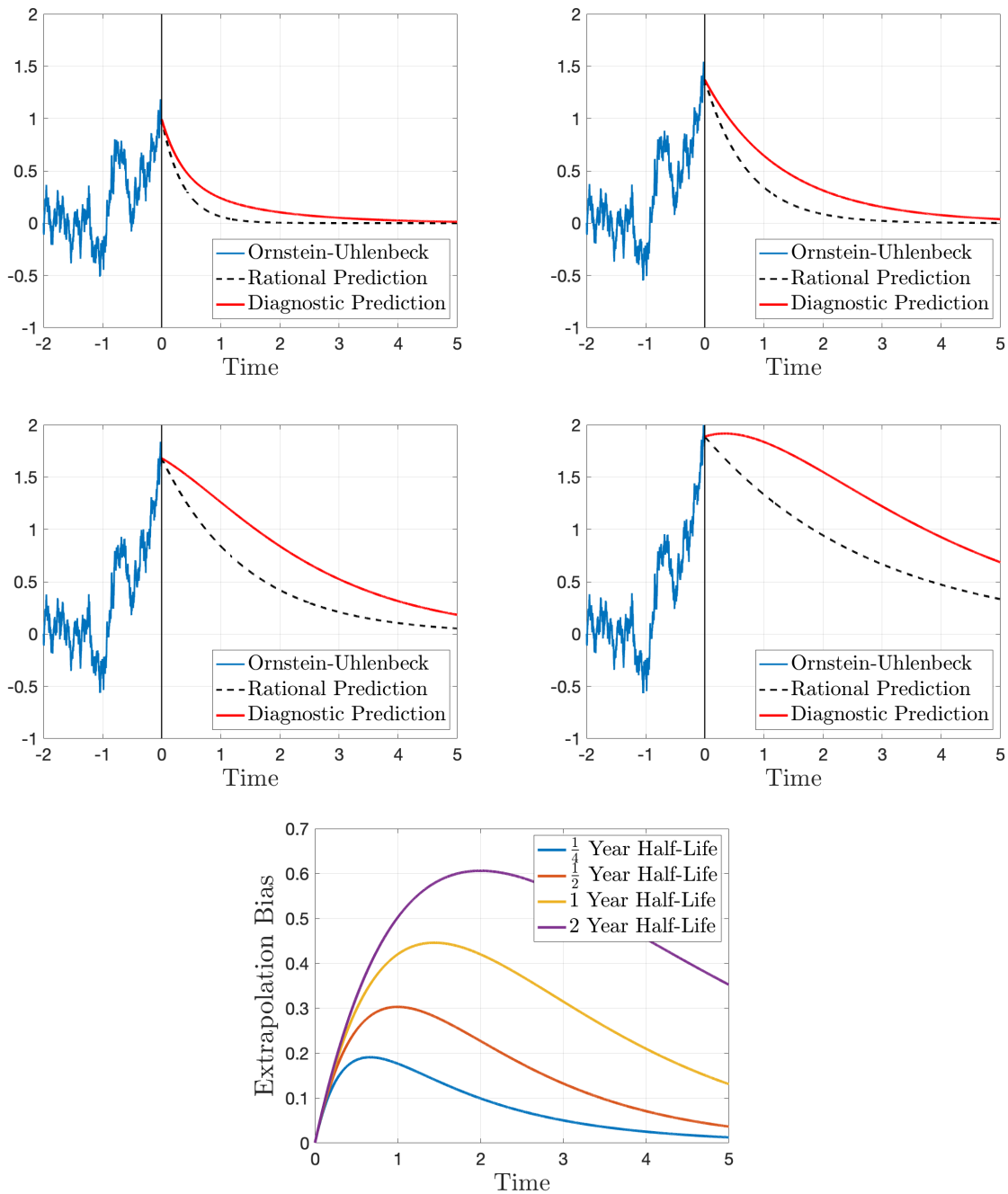


Figure 17: **Diagnostic expectations of an OU process.** From left to right, top to bottom, the half-life of the OU process is $\frac{1}{4}$, $\frac{1}{2}$, 1, and 2 years. The blue line plots the sample path of the OU process. The solid red line plots diagnostic expectations of the OU process' future evolution, and the dashed black line plots rational expectations. The bottom panel plots the bias caused by diagnostic expectations in all four calibrations. The level of extrapolation depends on the persistence of the underlying OU process.

E.2.1 Proof of Proposition 4

To characterize the diagnostic agent's beliefs about ω , let $\widehat{f}_t(\omega_{t+\tau}, \tau) = \omega_{t+\tau}e^{\alpha\tau}$ such that

$$\begin{aligned} d\widehat{f}_t(\omega_{t+\tau}, \tau) &= e^{\alpha\tau}d\widehat{\omega}_{t+\tau} + \alpha\omega_{t+\tau}e^{\alpha\tau}dt \\ &= \theta\mathcal{I}_te^{(\alpha-\kappa)\tau}dt + e^{\alpha\tau}\sigma dZ_{t+\tau}. \end{aligned}$$

Starting from an initial condition of $\widehat{f}_t(\omega_t, t) = \omega_t$:

$$\begin{aligned} \omega_{t+\tau}e^{\alpha\tau} &= \widehat{f}_t(\omega_{t+\tau}, \tau) = \widehat{f}_t(\omega_t, t) + \int_t^{t+\tau} d\widehat{f}_t(\omega_{t+s}, s) \\ &= \omega_t + \int_t^{t+\tau} \theta\mathcal{I}_te^{(\alpha-\kappa)(s-t)}ds + \int_t^{t+\tau} e^{\alpha(s-t)}\sigma dZ_s. \end{aligned}$$

Dividing through by $e^{\alpha\tau}$ recovers:

$$\omega_{t+\tau} = e^{-\alpha\tau}\omega_t + \theta\mathcal{I}_t\left(\frac{e^{-\alpha\tau} - e^{-\kappa\tau}}{\kappa - \alpha}\right) + \int_t^{t+\tau} e^{-\alpha(t+\tau-s)}\sigma dZ_s.$$

Since $\{Z_t\}$ is a standard Brownian motion, this completes the proof.

E.3 Extensions of the Baseline Model

Objective versus Subjective Shocks. Information measure $\mathcal{I}_t \equiv \int_0^t e^{-\kappa(t-s)}\sigma dZ_s$ is based on objective shocks, σdZ_t . This choice is consistent with BGS, who argue that over-reaction to objective news is more consistent with the psychology of diagnostic expectations (see the discussion in footnote 9).

However, it is also tractable to define \mathcal{I}_t based on subjective capital quality shocks. A diagnostic agent with a bias of $\theta\mathcal{I}_t$ will perceive a subjective shock at time t of $\sigma d\widehat{Z}_t = -\theta\mathcal{I}_tdt + \sigma dZ_t$. In this case, the measure of subjective recent information can be defined as

$$\mathcal{I}_t = \int_0^t e^{-\kappa(t-s)}\sigma d\widehat{Z}_s. \quad (69)$$

The key difference between subjective information measure (69) and objective information measure (3) is that, for any given κ , sentiment \mathcal{I}_t is less persistent when defined in terms

of subjective shocks. The evolution of sentiment in equation (69) is

$$\begin{aligned} d\mathcal{I}_t &= -\kappa\mathcal{I}_t dt + \sigma d\widehat{Z}_t \\ &= -(\kappa + \theta)\mathcal{I}_t dt + \sigma dZ_t, \end{aligned}$$

whereas the evolution of the baseline measure of sentiment in equation (3) is

$$d\mathcal{I}_t = -\kappa\mathcal{I}_t dt + \sigma dZ_t.$$

Comparing these two equations shows that \mathcal{I}_t decays more quickly when defined in terms of subjective shocks. This is because an overoptimistic agent will interpret incoming shocks with a negative bias (and vice-versa for an overpessimistic agent), leading to a faster unwinding of sentiment.

Multiple Frequencies of Extrapolation. The main text assumes that sentiment evolves at a single frequency, with shocks fading from \mathcal{I}_t at rate κ . However, it is likely more psychologically realistic to have sentiment operate over multiple frequencies. The empirical literature on extrapolative expectations has documented extrapolation over a variety of horizons. At a low frequency, [Malmendier and Nagel \(2011\)](#) find that long-term risk attitudes are shaped by lifetime macroeconomic experiences. Alternatively, [Greenwood and Shleifer \(2014\)](#) find that stock market expectations depend strongly on returns experienced in the past quarter.

The expectations model can be modified to capture multiple frequencies of extrapolation. For illustration, consider an agent whose sentiment is a function of a slow-moving component and a fast-moving component. The agent has a low-frequency measure of new information:

$$\mathcal{I}_t^L = \int_0^t e^{-\kappa^L(t-s)} \sigma dZ_s,$$

and a high-frequency measure of new information:

$$\mathcal{I}_t^H = \int_0^t e^{-\kappa^H(t-s)} \sigma dZ_s,$$

with $\kappa^L < \kappa^H$. The overall measure of new information can be defined as:

$$\mathcal{I}_t = \theta^L \mathcal{I}_t^L + \theta^H \mathcal{I}_t^H.$$

Parameters θ^L and θ^H determine the relative strength of low-frequency and high-frequency sentiment.

The downside of including multiple sentiment frequencies is that each frequency requires its own state variable. The main text uses a single frequency for parsimony.

Appendix References

- Achdou, Yves, Jiequn Han, Jean-Michel Lasry, Pierre-Louis Lions, and Benjamin Moll**, “Income and Wealth Distribution in Macroeconomics: A Continuous-Time Approach,” *The Review of Economic Studies*, 2022, 89 (1), 45–86.
- Aghion, Philippe and Peter W. Howitt**, *The Economics of Growth*, MIT Press, 2008.
- Bansal, Ravi and Amir Yaron**, “Risks for the Long Run: A Potential Resolution of Asset Pricing Puzzles,” *The Journal of Finance*, 2004, 59 (4), 1481–1509.
- Baron, Matthew, Emil Verner, and Wei Xiong**, “Banking Crises Without Panics,” *The Quarterly Journal of Economics*, 2021, 136 (1), 51–113.
- Bordalo, Pedro, Nicola Gennaioli, and Andrei Shleifer**, “Diagnostic Expectations and Credit Cycles,” *The Journal of Finance*, 2018, 73 (1), 199–227.
- , – , – , and **Stephen J. Terry**, “Real Credit Cycles,” *NBER w28416*, 2021.
- , – , **Rafael La Porta, and Andrei Shleifer**, “Diagnostic Expectations and Stock Returns,” *The Journal of Finance*, 2019, 74 (6), 2839–2874.
- , – , **Yueran Ma, and Andrei Shleifer**, “Overreaction in Macroeconomic Expectations,” *American Economic Review*, 2020, 110 (9), 2748–82.
- Brunnermeier, Markus K. and Yuliy Sannikov**, “Macro, Money, and Finance: A Continuous-Time Approach,” in “Handbook of Macroeconomics,” Vol. 2, Elsevier, 2016, pp. 1497–1545.
- Campbell, John Y.**, *Financial Decisions and Markets: A Course in Asset Pricing*, Princeton University Press, 2017.
- d’Arienzo, Daniele**, “Maturity Increasing Over-reaction and Bond Market Puzzles,” *SSRN 3733056*, 2020.

- Davis, Morris A. and Stijn Van Nieuwerburgh**, “Housing, Finance, and the Macroeconomy,” *Handbook of Regional and Urban Economics*, 2015, 5, 753–811.
- d’Avernas, Adrien and Quentin Vandeweyer**, “A Solution Method for Continuous-Time Models,” *Mimeo*, 2021.
- Frankel, Marvin**, “The Production Function in Allocation and Growth: A Synthesis,” *The American Economic Review*, 1962, 52 (5), 996–1022.
- Gennaioli, Nicola and Andrei Shleifer**, “What Comes to Mind,” *The Quarterly Journal of Economics*, 2010, 125 (4), 1399–1433.
- Greenwood, Robin and Andrei Shleifer**, “Expectations of Returns and Expected Returns,” *The Review of Financial Studies*, 2014, 27 (3), 714–746.
- He, Zhiguo and Arvind Krishnamurthy**, “A Macroeconomic Framework for Quantifying Systemic Risk,” *American Economic Journal: Macroeconomics*, October 2019, 11 (4), 1–37.
- , **Bryan Kelly, and Asaf Manela**, “Intermediary Asset Pricing: New Evidence from Many Asset Classes,” *Journal of Financial Economics*, 2017, 126 (1), 1–35.
- Long, J. Bradford De, Andrei Shleifer, Lawrence H. Summers, and Robert J. Waldmann**, “Noise Trader Risk In Financial Markets,” *Journal of Political Economy*, 1990, 98 (4), 703–738.
- Malmendier, Ulrike and Stefan Nagel**, “Depression Babies: Do Macroeconomic Experiences Affect Risk Taking?,” *The Quarterly Journal of Economics*, 2011, 126 (1), 373–416.
- Rabin, Matthew**, “An Approach to Incorporating Psychology into Economics,” *American Economic Review*, 2013, 103 (3), 617–22.
- Romer, Christina D. and David H. Romer**, “New Evidence on the Aftermath of Financial Crises in Advanced Countries,” *American Economic Review*, 2017, 107 (10), 3072–3118.